IMPROVED ROUTING ON THE DELAUNAY TRIANGULATION[*]

NICOLAS BONICHON[†], PROSENJIT BOSE[‡], JEAN-LOU DE CARUFEL[§], VINCENT DESPRÉ[¶], DARRYL HILL[‡], AND MICHIEL SMID[‡]

Abstract. A geometric graph $G = (P, E)$ is a set of points P in the plane and a set E of edges between pairs of points, where the weight of an edge is equal to the Euclidean distance between its two endpoints. In local routing we find a path in G from a source vertex s to a destination vertex t, using only knowledge of the current vertex, its incident edges, and the locations of s and t. We present an algorithm for local routing on the Delaunay triangulation, and show that it finds a path between a source vertex s and a target vertex t that is not longer than $3.56|st|$, improving the previous bound of $5.9|st|$.

1. Introduction. A Euclidean geometric graph $G = (P, E)$ is a set P of points embedded in the plane, and a set E of edges, where each $e \in E$ is segment joining a pair of points (u, v) in P, and the weight of e is the Euclidean distance $|uv|$.

A *local routing algorithm* A is an algorithm that routes a packet in the geometric graph G from a source vertex s to a target vertex t using only knowledge of the locations of s and t, as well as the location of the current vertex and its adjacent vertices. Let $\mathcal{P}\langle s,t\rangle$ be the path found in G from s to t using A. The *routing ratio* of A for any two points s and t in the geometric graph G is the ratio of the length of $\mathcal{P}\langle s,t\rangle$ to the Euclidean distance from s to t. An algorithm A has a routing ratio μ for a class of geometric graphs $\mathcal{G}$, if, for any two vertices s and t in $G \in \mathcal{G}$, $|\mathcal{P}\langle s,t\rangle| \leq \mu \cdot |st|$.

A graph $G = (P, E)$ is a c-spanner if for any pair of points u and v in P, the shortest path in G not longer than $c|uv|$. The value c is referred to as the *stretch factor* or *spanning ratio* of G. The stretch factor of G is thus a lower bound on the routing ratio of G for any routing algorithm A, and the routing ratio is an upper bound on the spanning ratio of G. Geometric spanners are described in detail in the book by Narasimhan and Smid [14].

A notable geometric graph is the *Delaunay triangulation*. Given a set P of points in the plane, we construct the Delaunay triangulation of P as follows. For each triple (p, q, r) of points in P, let C be the unique circle through p, q, and r. If there are no points of P in the interior of C, then we connect p, q, and r by edges to form a triangle. In this paper we assume that P is in general position: no 3 points are colinar and no 4 points are cocircular.

The Delaunay triangulation was first proven to be a spanner by Dobkin et al. [12], who showed an upper bound of 5.08 on the spanning ratio. This was subsequently improved to 2.42 by Keil and Gutwin [13], and then to 1.998 by Xia [15]. Bose et. al [6] initially showed that nearly all Delaunay triangulations have spanning ratio greater than $\pi/2$. Xia and Zhang then proved that there exist Delaunay triangulations with spanning ratio greater than 1.59 [16].

[*]THIS WORK WAS SUPPORTED BY THE NATIONAL SCIENCES AND ENGINEERING RESEARCH COUNCIL OF CANADA (NSERC) AND BY THE FRENCH ANR GRANT ASPAG (ANR-17-CE40-0017)

[†]Université de Bordeaux, LaBRI, UMR 5800, F-33400 Talence, France
[‡]Carleton University, 1125 Colonel By Dr, Ottawa, ON, Canada
[§]University of Ottawa, 800 King Edward Ave, Ottawa, ON, Canada
[¶]Université de Lorraine, Loria, UMR 7503, Nancy, France

Bose and Morin [8] explored some of the theoretical limitations of routing, and provided some of the first deterministic routing algorithms with constant routing ratio on the Delaunay triangulation. They denoted the spanning ratio found by Dobkin et al. [12] as $c_{dfs} \approx 5.08$. They showed that it is possible to locally route on the Delaunay triangulation with a routing ratio of $9 \cdot c_{dfs} \approx 45.749$. Bose et al. [5] further improved this bound to ≈ 15.479. Then, Bonichon et al. [3] showed that we can locally route on the Delaunay triangulation with a routing ratio of at most 5.9. In the same paper it was shown that the routing ratio of any deterministic local algorithm is at least 1.70 for the Delaunay triangulation.

Efforts to evaluate the spanning ratio and routing ratio have been made for Delaunay triangulations defined on other metrics. We can define these metrics by taking a convex shape and translating and scaling it until it intersects three vertices but contains no points of P in its interior. When we use a circle we obtain the L_2, or classical Delaunay triangulation. When the metric is not specified (as in the rest of this paper), then we are referring to the L_2-Delaunay triangulation. The L_1-Delaunay triangulation uses an axis aligned square, while the L_∞-Delaunay triangulation uses a square tipped at 45 degrees. By rotating the point set 45 degrees, it is easy to show the L_1 and L_∞ triangulations are equivalent. Bonichon et al. [4] showed that the L_1 and L_∞ Delaunay triangulations are $\sqrt{4+2\sqrt{2}} \approx 2.61$-spanners, and they showed that this bound was tight. On this triangulation, Chew [9] proposed a routing algorithm with routing ratio at most $\sqrt{10}$. Moreover, the routing ratio of any deterministic local algorithm is at least 2.70 for this class of graphs [1]. The TD-Delaunay triangulation is constructed using an equilateral triangle. Chew [10] showed that they are 2-spanners and Bose et al. [7] proposed a routing algorithm with routing ratio $\sqrt{5/3} \approx 2.89$ and they show that this ratio is the best possible. Recently Dennis, Perkovic and Duru [11] showed that the stretch factor of the Delaunay triangulation where the empty circle is a hexagon is 2 and this is tight.

Table 1.1: Spanning and Routing Ratios of Delaunay Triangulations. Tight results are shown in bold.

Graph	Spanning Ratio	Routing Ratio
TD-Delaunay	$\mathbf{2}$ [10]	$\mathbf{5/\sqrt{3} \approx 2.89}$ [7]
L_1 and L_∞-Delaunay	$\mathbf{\sqrt{4+2\sqrt{2}} \approx 2.61}$ [4]	$\sqrt{10} \approx 3.16$ [9]
$Hexagon$-Delaunay	$\mathbf{2}$ [11]	
L_2-Delaunay	1.998 [15]	3.56 (this paper)

In this paper we present a local routing algorithm, called *MixedChordArc*, for the L_2-Delaunay triangulation, with a routing ratio of 3.56. This improves the current best routing ratio of 5.9 [1]. Table 1.1 shows our result in the context of spanning and routing ratios of other Delaunay triangulations.

In Section 2 we define a local algorithm that achieves this routing ratio. In Section 3 we first prove the result for a special case, called *balanced configurations*. In Section 4 we extend the technique presented in Section 3 to prove the main result for the general case. In Section 5 we present our conclusions and our ideas for future directions.

2. The MixedChordArc Algorithm. Let P be a finite set of points in the plane, and let $DT(P)$ be the Delaunay triangulation of P. We want to route a packet between two vertices of P along edges of $DT(P)$ using only local knowledge and knowledge of the location of our start and destination vertices.

Let s and t be the start and destination vertices respectively, and assume, without loss of generality, that s and t are on the x-axis with s to the left of t. Consider two triangles T and T' that have non-empty intersections with st. We say that T is to the left of T', and T' is to the right of T, if a walk from s to t along st intersects T before T'.

Let C be a circle that intersects st. We denote by t_C the rightmost point of C on st. Let u and v be two points on C. We denote by $\mathcal{A}_C(u, v)$ the clockwise arc of C from u to v, and by $\mathcal{B}_C(u, v)$ the counter-clockwise arc of C from u to v. We denote the length of a geometric structure S by $|S|$.

Let $p \neq t$ be the vertex representing the current location of the packet. Let T be the rightmost triangle with p as a vertex that has a non-empty intersection with st. Let $a \neq p$ be the vertex of T that is above st, and let $b \neq p$ be the vertex of T that is below st. Let C be the circumcircle of T. We assume s to be above st, and we assume t to be on the opposite side of st from the current vertex. This ensures that when t is a neighbour of the current vertex, the algorithm will forward the packet directly to t.

Here is the algorithm MixedChordArc. First assume that $p = s$. If $|\mathcal{A}_C(s, t_C)| \leq |\mathcal{B}_C(s, t_C)|$, set $p = a$, otherwise set $p = b$. See Fig. 2.1a. If $p \neq s$, we repeat the following until $p = t$.

1. If p is above st:
   (a) If $|\mathcal{A}_C(p, t_C)| \leq |pb| + |\mathcal{B}_C(b, t_C)|$, set $p = a$
   (b) Else set $p = b$.
2. If p is below st:
   (a) If $|\mathcal{B}_C(p, t_C)| \leq |pa| + |\mathcal{A}_C(a, t_C)|$, set $p = b$
   (b) Else set $p = a$.

The possible choices are illustrated in Fig. 2.1. Let $\mathcal{P}\langle s, t\rangle = (s = p_0, p_1, ..., p_n = t)$ be the sequence of vertices produced by the algorithm. In this paper we prove the following theorem.

THEOREM 2.1. *The MixedChordArc Algorithm finds a path $\mathcal{P}\langle s, t\rangle$ from s to t whose length $|\mathcal{P}\langle s, t\rangle|$ is not more than $\mu|st|$, where $\mu = \sqrt{\frac{2}{1-\sin(1)}} < 3.56$.*

We present a complete trace of the algorithm in Fig. A.1a of Appendix A. In the remaining figures of Appendix A, we illustrate the proof of Theorem 2.1 on a complete example.

In some cases, the path produced by our algorithm is a *balanced configuration*. In such cases, the analysis of the length of $\mathcal{P}\langle s, t\rangle$ is much easier. In Section 3 we define what a balanced configuration is, and analyze the length of $\mathcal{P}\langle s, t\rangle$ for this specific case. Then, in Section 4, we analyze the length of $\mathcal{P}\langle s, t\rangle$ for the general case.

3. Bounding $|\mathcal{P}\langle s, t\rangle|$ in a Balanced Configuration. Let us consider a path $\mathcal{P}\langle s, t\rangle$ of vertices such that $p_0 = s, p_n = t$ and $p_{i-1}p_i$ is an edge of the rightmost triangle T_i of p_{i-1} that has a non-empty intersection with st. Let a_i and b_i be the other two vertices of T_i, where a_i is above st, and b_i is below st. Thus $p_i = a_i$ or $p_i = b_i$, for all $1 \leq i \leq n$. Let $s = p_0 = a_0 = b_0$ and let $t = p_n$. Let C_i be the circumcircle of

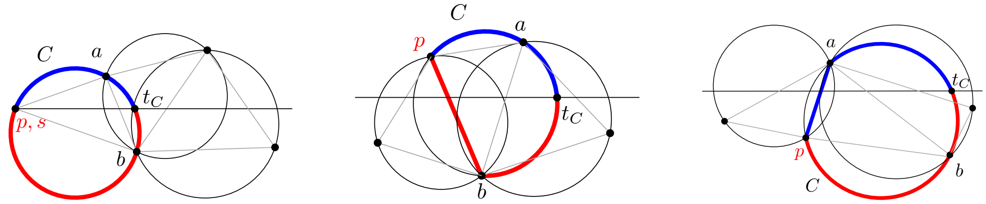

(a) From $p = s$, the blue arc is shorter than the red arc, so we forward to a.

(b) From p, the blue path is shorter than the red path, so we forward to a.

(c) From p, the blue path is shorter than the red path, so we forward to a.

Figure 2.1: Illustrating one step of the algorithm.

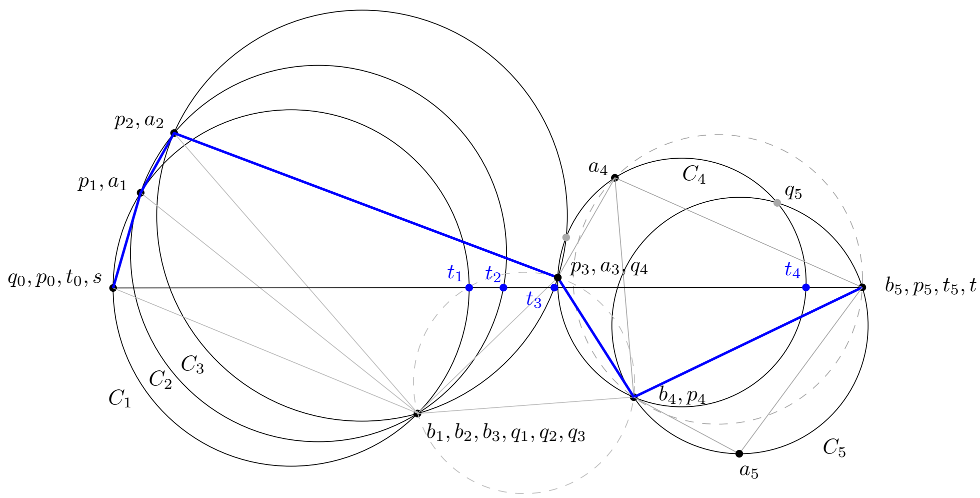

Figure 3.1: Sequence of circles in a balanced configuration and the path in blue. The dotted circles are circumcircles of triangles intersected by st but not in $\mathcal{T}$.

T_i, let r_i be its radius and let c_i be its center. Let C_0 be the circle centered at s with radius $r_0 = 0$. Let $\mathcal{T} = (T_1, T_2, ..., T_n)$, and let $\mathcal{C} = (C_0, C_1, ..., C_n)$ be the sequence of circles starting at C_0, followed by the circumcircles of $\mathcal{T}$. Note that the vertex of T_i that is on the opposite side of st to p_{i-1} may not be at the intersection of C_{i-1} and C_i because we always consider the rightmost triangle at each step. Thus we define a second intersection point of C_{i-1} and C_i as follows (p_{i-1} being one intersection point). If p_{i-1} is above st, then q_i is the lowest intersection of C_i and C_{i-1}. If p_{i-1} is below st, let q_i be the highest intersection of C_{i-1} and C_i. Observe that if T_i and T_{i-1} share an edge, then q_i is the vertex of T_i on the opposite side of st from p_{i-1}. See Fig. 3.1. To simplify the notation, we write t_i instead of t_{C_i}, and we write $\mathcal{A}_i(u, v)$ and $\mathcal{B}_i(u, v)$ instead of $\mathcal{A}_{C_i}(u, v)$ and $\mathcal{B}_{C_i}(u, v)$, respectively.

We say that a pair of consecutive circles C_{i-1} and C_i is *balanced* if $|\mathcal{A}_i(p_{i-1}, t_i)| = |p_{i-1}q_i| + |\mathcal{B}_i(q_i, t_i)|$ when p_{i-1} is above st, and if $|\mathcal{B}_i(p_{i-1}, t_i)| = |p_{i-1}q_i| + |\mathcal{A}_i(q_i, t_i)|$ when p_{i-1} is below st. A path $\mathcal{P}\langle s, t\rangle$ on a point set P is a *balanced configuration* when C_{i-1} and C_i are balanced for all $1 \leq i \leq n$.

3.1. Analysis Technique.

LEMMA 3.1. *Let C_{i-1} and C_i be arbitrary circles of $\mathcal{C}$, where $1 \le i \le n$. Then*

1. $|p_{i-1}b_i| + |\mathcal{B}_i(b_i, t_i)| \le |p_{i-1}q_i| + |\mathcal{B}_i(q_i, t_i)|$ *when p_{i-1} is above st, and*
2. $|p_{i-1}a_i| + |\mathcal{A}_i(a_i, t_i)| \le |p_{i-1}q_i| + |\mathcal{A}_i(q_i, t_i)|$ *when p_{i-1} is below st.*

Proof. By the triangle inequality we have $|p_{i-1}b_i| \le |p_{i-1}q_i| + |\mathcal{B}_i(q_i, b_i)|$, from which 1 follows. Case 2 is symmetric. ☐

For the rest of this section, we assume that $\mathcal{P}\langle s,t\rangle$ is a balanced configuration. Consider the case when p_{i-1} is above st (the case when p_{i-1} is below st is symmetric). If $q_i = b_i$ then $|\mathcal{A}_i(p_{i-1}, t_i)| = |p_{i-1}b_i| + |\mathcal{B}_i(b_i, t_i)|$, and the algorithm proceeds to a_i. If $q_i \ne b_i$, observe that $|p_{i-1}b_i| \le |p_{i-1}q_i| + |\mathcal{B}_i(q_i, b_i)|$ by the triangle inequality (see circles C_4 and C_5 in Fig. 3.1). Thus we have $|p_{i-1}b_i| + |\mathcal{B}_i(b_i, t_i)| < |p_{i-1}q_i| + |\mathcal{B}_i(q_i, t_i)| = |\mathcal{A}_i(p_{i-1}, t_i)|$, and the algorithm proceeds to b_i. Thus a balanced configuration allows for steps that cross st and steps that do not cross st. It also allows us to use $|\mathcal{A}_i(p_{i-1}, t_i)|$ as an upper bound on $|p_{i-1}b_i| + |\mathcal{B}_i(b_i, t_i)|$ in the case where $p_{i-1}p_i$ crosses st.

Let $x(v)$ and $y(v)$ be the x and y-coordinates of a point v, respectively. Let s_i be a point on st such that $x(s_i) = x(t_i) - 2r_i$. We define the following potential function that we use to bound the length of $\mathcal{P}\langle s,t\rangle$.

DEFINITION 3.2. *If p_{i-1} is above st, then*

$$\Phi(C_{i-1}, C_i) = |\mathcal{A}_i(p_{i-1}, t_i)| - |\mathcal{A}_{i-1}(p_{i-1}t_{i-1})| - \lambda|s_{i-1}s_i| - (\mu - \lambda)|t_{i-1}t_i|.$$

Otherwise, if p_{i-1} is below st, then

$$\Phi(C_{i-1}, C_i) = |\mathcal{B}_i(p_{i-1}, t_i)| - |\mathcal{B}_{i-1}(p_{i-1}t_{i-1})| - \lambda|s_{i-1}s_i| - (\mu - \lambda)|t_{i-1}t_i|,$$

where $\lambda = \left(\frac{1+\sin(1)}{\cos(1)} - \pi/2 - 1\right)/2 \approx 0.42$ (see (C.11) in Lemma C.4, Appendix C.2.3) and $\mu = \sqrt{\frac{2}{1-\sin(1)}} < 3.56$ (see (C.10) in Lemma C.3, Appendix C.2.3).

See Fig. 3.1 and 3.2 for a complete example and an illustration of the potential functions. See Fig. 3.3 for an illustration of $\Phi(C_{i-1}, C_i)$. Three lemmas are used to prove Theorem 2.1 for balanced configurations. The proof of Lemma 3.3 is found in Section 3.3 while the proof of Lemma 3.4 is in Section 3.2.

LEMMA 3.3. *Given a pair of balanced circles C_{i-1} and C_i,*

$$\Phi(C_{i-1}, C_i) \le 0.$$

LEMMA 3.4. *For any balanced configuration $\mathcal{P}\langle s,t\rangle$, $\sum_{i=1}^{n} |s_{i-1}s_i| \le |st|$.*

LEMMA 3.5. *For any $\mathcal{C}$, $\sum_{i=1}^{n} |t_{i-1}t_i| \le |st|$.*

Proof. We have $t_0 = s$ and $t_n = t$. We claim that $x(t_{i-1}) < x(t_i)$ for all $1 \le i \le n$. If this is true, the lemma follows. We prove the claim by contradiction. Assume that $x(t_{i-1}) \ge x(t_i)$. If q_i is to the same side of st as p_{i-1}, then C_{i-1} must contain the vertex of T_i on the opposite side of st. If q_i is on the opposite side of st as p_{i-1}, then C_{i-1} contains the vertex of T_i on the same side of st as p_{i-1}. Both cases contradict the construction of a Delaunay triangulation. ☐

LEMMA 3.6. *For $1 \le i \le n$, if p_{i-1} is above st, then*

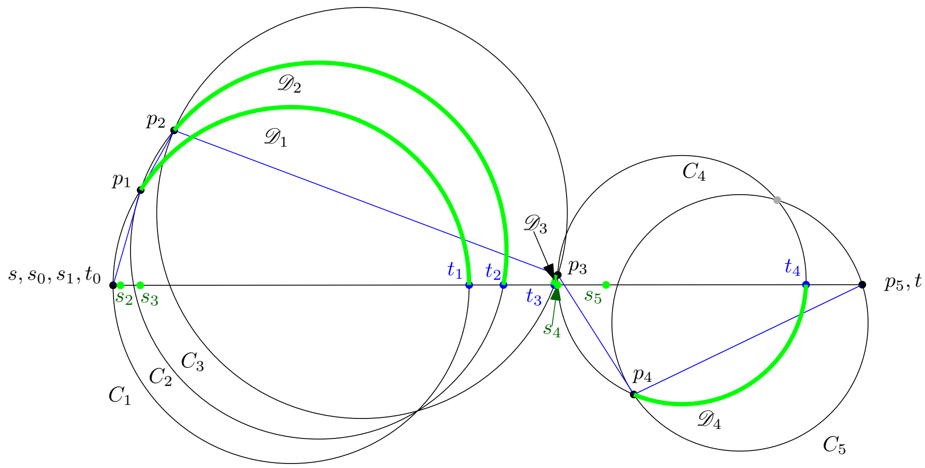

Figure 3.2: Potential functions of a balanced configuration.

1. (a) $|\mathcal{A}_i(p_{i-1}, t_i)| > |p_{i-1}p_i| + |\mathcal{A}_i(p_i, t_i)|$ *if* p_i *is above* st*, and*
   (b) $|\mathcal{A}_i(p_{i-1}, t_i)| > |p_{i-1}p_i| + |\mathcal{B}_i(p_i, t_i)|$ *if* p_i *is below* st

   otherwise p_{i-1} *is below* st *and*
2. (a) $|\mathcal{B}_i(p_{i-1}, t_i)| > |p_{i-1}p_i| + |\mathcal{B}_i(p_i, t_i)|$ *if* p_i *is below* st*, and*
   (b) $|\mathcal{B}_i(p_{i-1}, t_i)| > |p_{i-1}p_i| + |\mathcal{A}_i(p_i, t_i)|$ *if* p_i *is above* st*.*

Proof. Case 1a is because $|\mathcal{A}_i(p_{i-1}, p_i)| > |p_{i-1}p_i|$, and Case 1b is because if p_i is below st, then the algorithm chose to cross st, which implies 1b. Case 2 is symmetric. ∎

Theorem 2.1 follows from Lemmas 3.3, 3.4, 3.5, and 3.6:

Proof. We first analyze the case when p_{i-1} is above st. Recall that in this case, $\Phi(C_{i-1}, C_i)$ is defined as

$$\Phi(C_{i-1}, C_i) = |\mathcal{A}_i(p_{i-1}, t_i)| - |\mathcal{A}_{i-1}(p_{i-1}t_{i-1})| - \lambda|s_{i-1}s_i| - (\mu - \lambda)|t_{i-1}t_i|.$$

If p_i is above st (same side of st as p_{i-1}), then $|\mathcal{A}_i(p_{i-1}, t_i)| > |p_{i-1}p_i| + |\mathcal{A}_i(p_i, t_i)|$ by Lemma 3.6. In this case, let $\mathscr{D}_i = \mathcal{A}_i(p_i, t_i)$. If p_i is below st, then $|\mathcal{A}_i(p_{i-1}, t_i)| > |p_{i-1}p_i| + |\mathcal{B}_i(p_i, t_i)|$ by Lemma 3.6. In this case,l et $\mathscr{D}_i = \mathcal{B}_i(p_i, t_i)$. In both cases we have $|\mathcal{A}_i(p_{i-1}, t_i)| > |p_{i-1}p_i| + |\mathscr{D}_i|$.

Let $\Phi'(C_{i-1}, C_i)$ be the function defined by

$$\Phi'(C_{i-1}, C_i) = |p_{i-1}p_i| + |\mathscr{D}_i| - |\mathscr{D}_{i-1}| - \lambda|s_{i-1}s_i| - (\mu - \lambda)|t_{i-1}t_i|.$$

Observe that $\Phi'(C_{i-1}, C_i) \leq \Phi(C_{i-1}, C_i)$. Lemma 3.3 tells us that $\Phi(C_{i-1}, C_i) \leq 0$, thus $\Phi'(C_{i-1}, C_i) \leq 0$. When p_{i-1} is below st, a symmetric proof again shows us that $\Phi'(C_{i-1}, C_i) \leq 0$. Recall that $p_0 = t_0 = s$, and $p_n = t_n = t$, which means

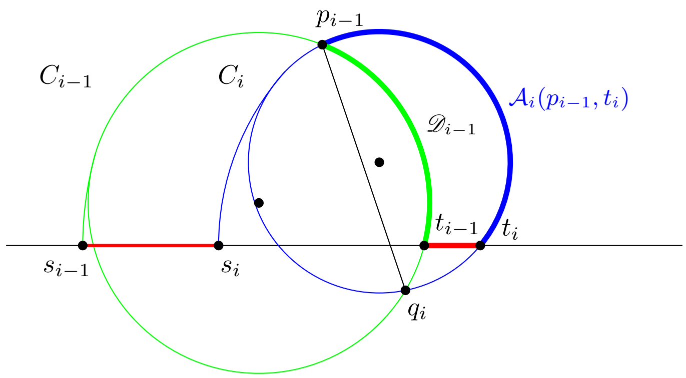

Figure 3.3: $\Phi(C_{i-1}, C_i)$.

$|\mathscr{D}_0| = |\mathscr{D}_n| = 0$. Therefore we have

$$\sum_{i=1}^{n} \Phi'(C_{i-1}, C_i) \leq 0$$

from which we get:

$$\sum_{i=1}^{n} (|p_{i-1}p_i| + |\mathscr{D}_i| - |\mathscr{D}_{i-1}|) \leq \sum_{i=1}^{n} (\lambda |s_{i-1}s_i| + (\mu - \lambda)|t_{i-1}t_i|)$$

$$|\mathcal{P}\langle s, t\rangle| - |\mathscr{D}_0| + |\mathscr{D}_n| \leq (\lambda + \mu - \lambda)|st| \tag{3.1}$$

$$|\mathcal{P}\langle s, t\rangle| \leq \mu|st|.$$

The right hand side of (3.1) is due to Lemmas 3.4 and 3.5. ∎

Lemma 3.4 is discussed in the next section. Lemma 3.3 is discussed in Section 3.3.

3.2. Proof of Lemma 3.4. Lemma 3.4 uses the following supporting result:

LEMMA 3.7. *Let C_{i-1} and C_i be balanced. Let s_{i-1} be the point on st where $x(s_{i-1}) = x(t_{i-1}) - 2r_{i-1}$ and let s_i be the point on st where $x(s_i) = x(t_i) - 2r_i$. Then $x(s_{i-1}) \leq x(s_i)$.*

Proof. See Fig. 3.4. Let u_{i-1} be the point on C_{i-1} that is diametrically opposed to t_{i-1} and let u_i be the point on C_i that is diametrically opposed to t_i. We will show the case when p_{i-1} is above st; the case when it is below st is symmetric. Since C_{i-1} and C_i are balanced, we have that $|\mathcal{A}_i(p_{i-1}, t_i)| = |p_{i-1}q_i| + |\mathcal{B}_i(q_i, t_i)|$ which implies that $|\mathcal{A}_i(p_{i-1}, t_i)| \leq \pi r_i$ and $|\mathcal{B}_i(q_i, t_i)| \leq \pi r_i$. Since $|\mathcal{A}_i(u_i, t_i)| = |\mathcal{B}_i(u_i, t_i)| = \pi r_i$, u_i is not on the open interval $\mathcal{A}_i(p_{i-1}, t_i)$ or $\mathcal{B}_i(q_i, t_i)$, which implies that either u_i is to the left of $p_{i-1}q_i$, or $u_i = p_{i-1} = q_i$, which implies that u_i is on or inside C_{i-1}.

Let O_i be the circle centered at t_i with radius $|t_iu_i| = 2r_i$. Thus O_i and C_i are tangent at u_i, and O_i intersects st at s_i. Let O_{i-1} be the circle centered at t_{i-1} with radius $2r_{i-1}$. Thus O_{i-1} and C_{i-1} are tangent at u_{i-1}, and O_{i-1} intersects st at s_{i-1}.

We prove the lemma by contradiction, thus assume that $x(s_i) < x(s_{i-1})$. In the proof of Lemma 3.5, we showed that $x(t_i) > x(t_{i-1})$. Therefore, it must be that O_{i-1} is in the interior of O_i, and thus they do not intersect. Since u_i is on or inside C_{i-1},

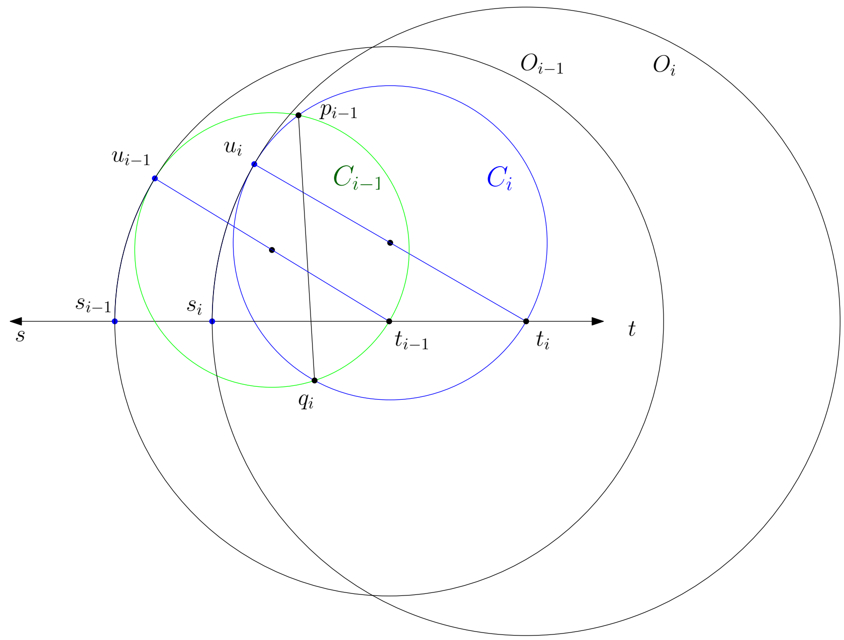

Figure 3.4: O_i must intersect O_{i-1} if C_{i-1} and C_i are path balanced, which implies that $x(s_{i-1}) \leq x(s_i)$.

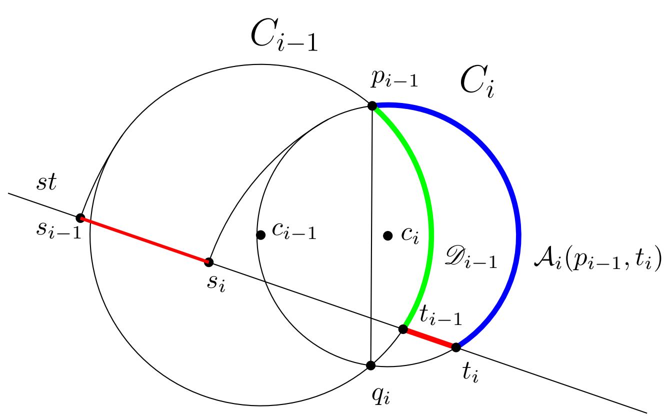

Figure 3.5: Coordinate system for analyzing $\Phi(C_{i-1}, C_i)$.

and O_i intersects u_i, O_i must intersect C_{i-1}. But C_{i-1} is contained in O_{i-1} except for the point u_{i-1}, and O_{i-1} is contained in O_i, and thus O_i cannot intersect C_{i-1}, which is a contradiction. See Fig. 3.4. ∎

We can now prove Lemma 3.4:

Proof of Lemma 3.4. Follows from Lemma 3.7 and the fact that $x(s_0) = x(s)$ and $x(s_n) < x(t)$. ∎

3.3. Proof of Lemma 3.3. To show that $\Phi(C_{i-1}, C_i) \leq 0$ when C_{i-1} and C_i are balanced, we set up the following coordinate system. We show the proof for the case when p_{i-1} is above st; the case when p_{i-1} is below st is symmetric. Let c_{i-1} and c_i lie along the x-axis, and let p_{i-1} and q_i lie along the y-axis. See Fig. 3.5. Lemma 3.3 follows from the following two lemmas:

Lemma 3.8. *When C_{i-1} and C_i are balanced, if $y(t_{i-1}) \leq 0$, then $\Phi(C_{i-1}, C_i) \leq 0$.*

Lemma 3.9. *When C_{i-1} and C_i are balanced, if $y(t_{i-1}) > 0$, then $\Phi(C_{i-1}, C_i) \leq 0$.*

The main tool to prove these two lemmas is the following transformation, which is similar to a transformation used by Xia [15].

Transformation 3.10. *Fix p_{i-1} and q_i, and translate c_i to the left along the x-axis until $c_i = c_{i-1}$. Moreover keep C_{i-1} unchanged and maintain C_i as the circle with center c_i with p_{i-1} on its boundary.*

Observe that, after we have completed Transformation 3.10, we have $C_i = C_{i-1}$ and thus $\Phi(C_{i-1}, C_i) = 0$. If we can show that $\Phi(C_{i-1}, C_i)$ is increasing while $x(c_i)$ decreases, then it must be that $\Phi(C_{i-1}, C_i) \leq 0$ before Transformation 3.10. Thus we wish to find the change in $\Phi(C_{i-1}, C_i)$ with respect to the change in $x(c_i)$ during Transformation 3.10. Formally:

Lemma 3.11. *If $\frac{d\Phi(C_{i-1},C_i)}{dx(c_i)} \leq 0$ during Transformation 3.10, then $\Phi(C_{i-1}, C_i) \leq 0$.*

Proof. At the end of Transformation 3.10 we have that $\Phi(C_{i-1}, C_i) = 0$. If $\frac{d\Phi(C_{i-1},C_i)}{dx(c_i)} \leq 0$ then $\Phi(C_{i-1}, C_i)$ is not decreasing during Transformation 3.10, and thus $\Phi(C_{i-1}, C_i) \leq 0$ before Transformation 3.10. ∎

The analysis of this function is similar to Xia's approach[15]. Full details of this analysis and the proofs for Lemmas 3.8 and 3.9 can be found in Appendix C.

4. Bounding $\mathcal{P}\langle s, t\rangle$ in the General Case. In Section 3, we proved Theorem 2.1 for the case when the path produced by our algorithm results in a balanced configuration. In this section, we prove Theorem 2.1 for the general case. Given a sequence $\mathcal{C}$ of circles that intersect st, no series of transformations were found that could achieve a balanced configuration, while simultaneously providing a provable upper bound on the length of $|p_{i-1}, p_i|$. However, we were able to find *two* sequences of circles to substitute for $\mathcal{C}$. To represent each C_i in $\mathcal{C}$, we have a *potential circle* C_i^P and a *bounding circle* C_i^B. Like C_i, both C_i^P and C_i^B have t_i as their rightmost intersection with st. However, C_i intersects both p_i and p_{i-1}, while C_i^B is only required to intersect p_{i-1}, and C_i^P is only required to intersect p_i. If we look at a bounding circle C_i^B and the previous potential circle C_{i-1}^P, which intersect at p_{i-1}, they are balanced, and we can thus apply the function $\Phi(C_{i-1}^P, C_i^B)$ to relate the lengths of the arcs of these circles to $|st|$. Finally, when analyzed properly, they provide an upper bound on the length $|p_i p_{i-1}|$.

Formally, let C_0^P be the circle centered at $s = p_0$ with radius $r_0^P = 0$, and let C_n^P be the circle centered at t with radius $r_n^P = 0$. Assuming we have defined C_{i-1}^P, we will define C_i^B and C_i^P. If p_{i-1} is above st, let C_i^B be the circle through p_{i-1} and t_i for which $|\mathcal{A}_{C_i^B}(p_{i-1}, t_i)| = |p_{i-1}q_i'| + |\mathcal{B}_{C_i^B}(q_i', t_i)|$, where q_i' is the bottommost intersection of C_{i-1}^P and C_i^B. If p_{i-1} is below st, let C_i^B be the circle through p_{i-1} and t_i for which $|\mathcal{B}_{C_i^B}(p_{i-1}, t_i)| = |p_{i-1}q_i'| + |\mathcal{A}_{C_i^B}(q_i', t_i)|$, where q_i' is the topmost

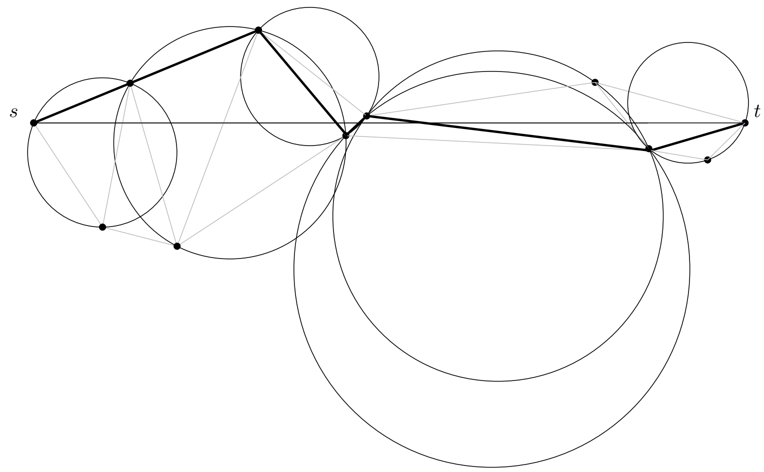

(a) The triangles and the respective circumcircles of a Delaunay triangulation intersected by st, as well as the path $\mathcal{P}\langle s, t\rangle$ found by the algorithm.

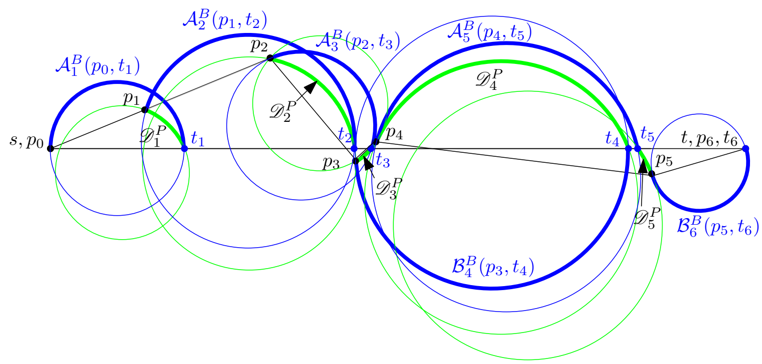

(b) The complete set of bounding arcs and potential arcs.

Figure 4.1: The construction of the potential circles and bounding circles in the general case.

intersection of C_{i-1}^P and C_i^B. That is, C_{i-1}^P and C_i^B are balanced. Let r_i^B be the radius of C_i^B. The potential circle C_i^P is the circle through p_i, whose rightmost intersection with st is t_i, and whose radius is given by $r_i^P = \min\{r_i, r_i^B\}$ (with the exception of $r_n^P = 0$). Let s_i^P be the point on st with $x(s_i^P) = x(t_i) - 2r_i^P$, and let s_i^B be the point on st with $x(s_i^B) = x(t_i) - 2r_i^B$.

To simplify notation, for points u and v on C_i^P, instead of writing $\mathcal{A}_{C_i^P}(u, v)$ and $\mathcal{B}_{C_i^P}(u, v)$ to indicate clockwise and counter-clockwise arcs of C_i^P from u to v, respectively, we write $\mathcal{A}_i^P(u, v)$ and $\mathcal{B}_i^P(u, v)$. Likewise, for points u and v on C_i^B, instead of writing $\mathcal{A}_{C_i^B}(u, v)$ and $\mathcal{B}_{C_i^B}(u, v)$, we write $\mathcal{A}_i^B(u, v)$ and $\mathcal{B}_i^B(u, v)$.

See Figs. 4.1a and 4.1 for an example of the initial sequences $\mathcal{T}$ and $\mathcal{C}$ and the resulting bounding and potential arcs that we are interested in. See Appendix A for a series of diagrams walking through a complete example.

Since C_{i-1}^P and C_i^B are balanced, Φ can be extended to C_{i-1}^P and C_i^B, and thus we have

$$\Phi(C_{i-1}^P, C_i^B) = |\mathcal{A}_i^B(p_{i-1}, t_i)| - |\mathcal{A}_{i-1}^P(p_{i-1}, t_{i-1})| - \lambda|s_{i-1}^P s_i^B| - \mu|t_{i-1}t_i|$$

when p_{i-1} is above st and

$$\Phi(C_{i-1}^P, C_i^B) = |\mathcal{B}_i^B(p_{i-1}, t_i)| - |\mathcal{B}_{i-1}^P(p_{i-1}, t_{i-1})| - \lambda|s_{i-1}^P s_i^B| - \mu|t_{i-1}t_i|$$

when p_{i-1} is below st. Lemma 3.3 tells us that $\Phi(C_{i-1}^P, C_i^B) \leq 0$. To prove Theorem 2.1 in the general case, it is sufficient to prove the following two lemmas. Lemma 4.1 is a generalization of Lemma 3.4, whereas Lemma 4.2 is a generalization of Lemma 3.6.

Lemma 4.1. $\sum_{i=1}^n |s_{i-1}^P s_i^B| \leq |st|$.

Proof. Since C_{i-1}^P and C_i^B are balanced, Lemma 3.7 tells us that $x(s_{i-1}^P) \leq x(s_i^B)$. We know that $x(s_i^P) = x(t_i) - 2r_i^P$ and $x(s_i^B) = x(t_i) - 2r_i^B$, thus the fact that $r_i^P = \min\{r_i, r_i^B\}$ implies that $x(s_i^B) \leq x(s_i^P)$. Thus $|s_{i-1}^P s_i^B| \leq |s_{i-1}^P s_i^P|$, and it is sufficient to show that $\sum_{i=1}^n |s_{i-1}^P s_i^P| \leq |st|$. The fact that $x(s_{i-1}^P) \leq x(s_i^B)$ implies that $x(s_{i-1}^P) \leq x(s_i^P)$, and C_0^P is the circle centered at s with radius 0, and thus $s_0^P = s$. Since $x(s_n^P) \leq x(t)$, this completes the proof. ∎

Due to space constraints, the following lemma will be proved in Appendix B.

Lemma 4.2. *For $1 \leq i \leq n$, if p_{i-1} is above st, then*

1. (a) $|\mathcal{A}_i^B(p_{i-1}, t_i)| \geq |p_{i-1}p_i| + |\mathcal{A}_i^P(p_i, t_i)|$ *if p_i is above st, and*
   (b) $|\mathcal{A}_i^B(p_{i-1}, t_i)| \geq |p_{i-1}p_i| + |\mathcal{B}_i^P(p_i, t_i)|$ *if p_i is below st*

   otherwise p_{i-1} is below st and
2. (a) $|\mathcal{B}_i^B(p_{i-1}, t_i)| \geq |p_{i-1}p_i| + |\mathcal{B}_i^P(p_i, t_i)|$ *if p_i is below st, and*
   (b) $|\mathcal{B}_i^B(p_{i-1}, t_i)| \geq |p_{i-1}p_i| + |\mathcal{A}_i^P(p_i, t_i)|$ *if p_i is above st.*

Theorem 2.1 follows from Lemmas 3.3, 3.5, 4.1, and 4.2.

Proof of Theorem 2.1. If p_i is above st, let $\mathscr{D}_i^P = \mathcal{A}_i^P(p_i, t_i)$. If p_i is below st, let $\mathscr{D}_i^P = \mathcal{B}_i^P(p_i, t_i)$. Let $\Phi'(C_{i-1}^P, C_i^B) = |p_{i-1}p_i| + |\mathscr{D}_i^P| - |\mathscr{D}_{i-1}^P| - \lambda|s_{i-1}^P s_i^B| - (\mu - \lambda)|t_{i-1}t_i|$. Lemmas 4.2 and 3.3 imply that $\Phi'(C_{i-1}^P, C_i^B) \leq \Phi(C_{i-1}^P, C_i^B) \leq 0$. Using $\Phi'(C_{i-1}^P, C_i^B)$ we get:

$$\sum_{i=1}^n \Phi'(C_{i-1}, C_i) \leq 0$$

$$\sum_{i=1}^n \left(|p_{i-1}p_i| + |\mathscr{D}_i^P| - |\mathscr{D}_{i-1}^P|\right) \leq \sum_{i=1}^n (\lambda|s_{i-1}^P s_i^B| + (\mu - \lambda)|t_{i-1}t_i|)$$

$$|\mathcal{P}\langle s,t\rangle| - |\mathscr{D}_0^P| + |\mathscr{D}_n^P| \leq (\lambda + \mu - \lambda)|st| \tag{4.1}$$

$$|\mathcal{P}\langle s,t\rangle| \leq \mu|st|.$$

Line (4.1) follows from Lemmas 3.5 and 4.1. ∎

We give some insight into the selection of r_i^P. Assume that p_{i-1} is above st (when p_{i-1} is below st the explanation is symmetric).

The purpose of $|\mathcal{A}_i^B(p_{i-1}, t_i)|$ is to bound $|p_{i-1}p_i| + |\mathcal{A}_i^P(p_i, t_i)|$, as expressed in Lemma 4.2. This lemma is also the reason for selecting the radius of C_i^P as $r_i^P = \min\{r_i, r_i^B\}$. It would be simpler to let $r_i^P = r_i^B$, since then we would have

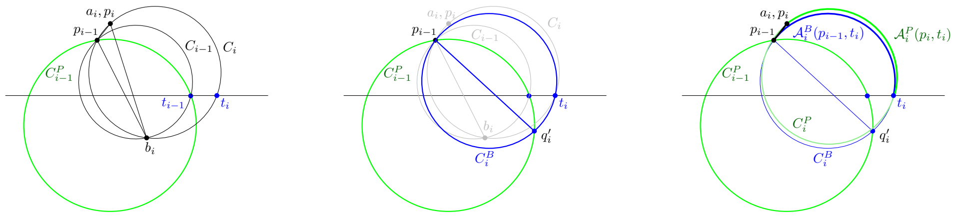

(a) C_{i-1}, C_i, and C^P_{i-1}. Notice that $r^P_{i-1} > r_{i-1}$.

(b) C^B_i and its intersection with C^P_{i-1}.

(c) $|\mathcal{A}^B_i(p_{i-1}, t_i)| < |p_{i-1}, p_i| + |\mathcal{A}^P_i(p_i, t_i)|$.

Figure 4.2: The reasoning behind $r^P_i = \min\{r_i, r^B_i\}$. In this diagram, $r^P_i > r_i$, and we show why it is detrimental to our analysis. Notice that $|\mathcal{A}^B_i(p_{i-1}, t_i)| < |p_{i-1}, p_i| + |\mathcal{A}^P_i(p_i, t_i)|$. Thus the arc $\mathcal{A}^B_i(p_{i-1}, t_i)$ of the bounding circle is not long enough to pay for $|p_{i-1}, p_i| + |\mathcal{A}^P_i(p_i, t_i)|$.

$s^P_i = s^B_i$. However, if we allow $r^P_i > r_i$, it can happen that the arc $|\mathcal{A}^B_{i+1}(p_i, t_{i+1})|$ on the next bounding circle is not large enough to cover $|p_i p_{i+1}| + |\mathcal{A}^P_{i+1}(p_{i+1}, t_{i+1})|$. See Fig. 4.2. Thus Lemma 4.2 would not hold. To account for this, we ensure that C^P_i has radius at most r_i.

5. Conclusion and Future Work. Consider the algorithm presented in Section 2, along with two variations. To keep the algorithms simple, assume we are at a vertex p above st. Otherwise all assumptions are the same as in Section 2.

- **BestChord:** If $|pa| + |\mathcal{A}_C(a, t_C)| \leq |pb| + |\mathcal{A}_C(b, t_C)|$ then $p = a$ else $p = b$.
- **MixedChordArc:** If $|\mathcal{A}_C(p, t_C)| \leq |pb| + |\mathcal{A}_C(b, t_C)|$ then $p = a$ else $p = b$.
- **MinArc:** If $|\mathcal{A}_C(p, t_C)| \leq \pi r$ then $p = a$ else $p = b$.

The algorithm presented in this paper is *MixedChordArc*. Following the techniques used in [1] we show that the routing ratio of *MinArc* is between 3.20 and 3.96. Since the routing ratio of 3.56 of *MixedChordArc* is better the details of *MinArc* analysis are left in Appendix D.

We suspect that *BestChord* is an improvement on *MixedChordArc*. It seems plausible that we can modify the proofs presented in this paper to obtain the same upper bound for *BestChord* as for *MixedChordArc*, but for now that remains unverified. Whether or not *BestChord* is asymptotically superior to *MixedChordArc*, or whether they are asymptotically the same is still unknown.

Although we have improved the upper bound of the routing ratio on the L_2-Delaunay triangulation, it is not clear how tight our analysis is. The upper bound on the analysis is where our potential function is the weakest. A more clever potential function could lower the routing ratio using a comparable analysis. Or perhaps one of the algorithms above would respond to a completely different style of analysis.

Furthermore, the lower bound on *MixedChordArc* is still the same as the lower bound on routing on the L_2-Delaunay triangulation in general, which is approximately 1.70 [1]. So it seems there is still much room for improvement. The question remains, what other algorithms or analysis can we use to improve the routing ratio of the Delaunay triangulation? And given that the upper and lower bounds on the spanning ratio of the L_2-Delaunay triangulation are 1.998 [15] and 1.5932 [16] respectively, is there a separation of the spanning and routing ratios of the Delaunay triangulation?

REFERENCES

[1] Nicolas Bonichon, Prosenjit Bose, Jean-Lou De Carufel, Ljubomir Perković, and André van Renssen. Upper and lower bounds for online routing on Delaunay triangulations. In Nikhil Bansal and Irene Finocchi, editors, *Algorithms - ESA 2015*, volume 9294 of *Lecture Notes in Computer Science*, pages 203–214. Springer Berlin Heidelberg, 2015. URL: http://dx.doi.org/10.1007/978-3-662-48350-3_18, doi:10.1007/978-3-662-48350-3_18.

[2] Nicolas Bonichon, Prosenjit Bose, Jean-Lou De Carufel, Ljubomir Perković, and André van Renssen. Upper and lower bounds for online routing on delaunay triangulations. *Discrete & Computational Geometry*, pages 1–23, 2016. URL: http://dx.doi.org/10.1007/s00454-016-9842-y, doi:10.1007/s00454-016-9842-y.

[3] Nicolas Bonichon, Prosenjit Bose, Jean-Lou De Carufel, Ljubomir Perković, and André van Renssen. Upper and lower bounds for online routing on Delaunay triangulations. *Discrete & Computational Geometry*, 58(2):482–504, Sep 2017. URL: https://doi.org/10.1007/s00454-016-9842-y, doi:10.1007/s00454-016-9842-y.

[4] Nicolas Bonichon, Cyril Gavoille, Nicolas Hanusse, and Ljubomir Perković. Tight stretch factors for L_1 and L_∞ Delaunay triangulations. *Computational Geometry*, 48(3):237 – 250, 2015. URL: http://www.sciencedirect.com/science/article/pii/S0925772114001126, doi:https://doi.org/10.1016/j.comgeo.2014.10.005.

[5] Prosenjit Bose, Jean-Lou De Carufel, Stephane Durocher, and Perouz Taslakian. Competitive online routing on Delaunay triangulations. In R. Ravi and Inge Li Gørtz, editors, *Algorithm Theory - SWAT 2014 - 14th Scandinavian Symposium and Workshops, Copenhagen, Denmark, July 2-4, 2014. Proceedings*, volume 8503 of *Lecture Notes in Computer Science*, pages 98–109. Springer, 2014. URL: http://dx.doi.org/10.1007/978-3-319-08404-6_9, doi:10.1007/978-3-319-08404-6_9.

[6] Prosenjit Bose, Luc Devroye, Maarten Löffler, Jack Snoeyink, and Vishal Verma. Almost all Delaunay triangulations have stretch factor greater than pi/2. *Comput. Geom.*, 44(2):121–127, 2011.

[7] Prosenjit Bose, Rolf Fagerberg, André van Renssen, and Sander Verdonschot. Competitive routing in the half-Theta-6-graph. In *Proceedings of the Twenty-third Annual ACM-SIAM Symposium on Discrete Algorithms*, SODA '12, pages 1319–1328. SIAM, 2012. URL: http://dl.acm.org/citation.cfm?id=2095116.2095220.

[8] Prosenjit Bose and Pat Morin. Online routing in triangulations. In *Algorithms and Computation*, volume 1741 of *Lecture Notes in Computer Science*, pages 113–122. Springer Berlin Heidelberg, 1999. URL: http://dx.doi.org/10.1007/3-540-46632-0_12, doi:10.1007/3-540-46632-0_12.

[9] L. Paul Chew. There is a planar graph almost as good as the complete graph. In *Proceedings of the Second Annual Symposium on Computational Geometry*, SCG '86, pages 169–177, New York, NY, USA, 1986. ACM. URL: http://doi.acm.org/10.1145/10515.10534, doi:10.1145/10515.10534.

[10] L. Paul Chew. There are planar graphs almost as good as the complete graph. *Journal of Computer and System Sciences*, 39(2):205 – 219, 1989. URL: http://www.sciencedirect.com/science/article/pii/0022000089900445, doi:https://doi.org/10.1016/0022-0000(89)90044-5.

[11] Michael Dennis, Ljubomir Perković, and Duru Türkoglu. The stretch factor of hexagon-Delaunay triangulations. *CoRR*, abs/1711.00068, 2017. URL: http://arxiv.org/abs/1711.00068, arXiv:1711.00068.

[12] David P. Dobkin, Steven J. Friedman, and Kenneth J. Supowit. Delaunay graphs are almost as good as complete graphs. *Discrete & Computational Geometry*, 5(1):399–407, 1990. URL: http://dx.doi.org/10.1007/BF02187801, doi:10.1007/BF02187801.

[13] J. Mark Keil and Carl A. Gutwin. Classes of graphs which approximate the complete euclidean graph. *Discrete & Computational Geometry*, 7(1):13–28, 1992. URL: http://dx.doi.org/10.1007/BF02187821, doi:10.1007/BF02187821.

[14] Giri Narasimhan and Michiel Smid. *Geometric Spanner Networks*. Cambridge University Press, New York, NY, USA, 2007.

[15] Ge Xia. Improved upper bound on the stretch factor of Delaunay triangulations. In *Proceedings of the Twenty-seventh Annual Symposium on Computational Geometry*, SoCG '11, pages 264–273, New York, NY, USA, 2011. ACM. URL: http://doi.acm.org/10.1145/1998196.1998235,

doi:10.1145/1998196.1998235.
[16] Ge Xia and Liang Zhang. Toward the tight bound of the stretch factor of Delaunay triangulations. In *Proceedings of the Canadian Conference on Computational Geometry*, CCCG '11, 2011.

Appendix A. A Trace of MixedChordArc and an Illustration of the Proof of Theorem 2.1.

In these figures we illustrate the proof of Theorem 2.1.

Figure A.1a illustrates the triangles and their respective circumcircles of the Delaunay triangulation intersected by st, as well as the path $\mathcal{P}\langle s,t\rangle$. In figure A.1b, recall that C_0^P is the circle centered at s with radius $r_0^P = 0$. We see that C_1^B is the circle through t_i that is balanced with respect to C_0^P, i.e., $|\mathcal{A}_1^B(p_0,t_1)| = |\mathcal{B}_1^B(b_1' = p_0, t_1)| = \pi r_1^B$.

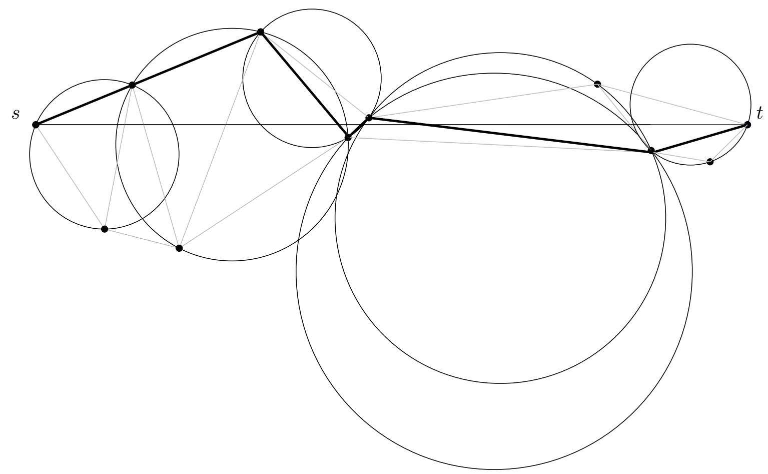

(a) $\mathcal{T}, \mathcal{C}$, and $\mathcal{P}\langle s,t\rangle$.

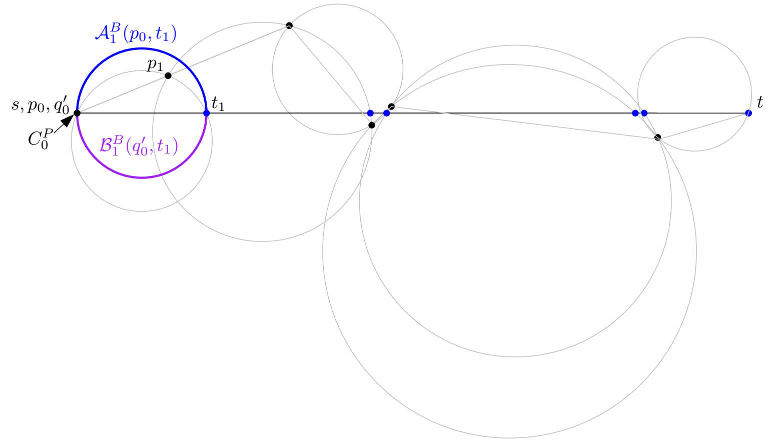

(b) C_0^P and C_1^B are balanced.

Figure A.1: Initial configuration and construction of C_1^B given C_0^P.

In Figure A.2a we see C_1^P through p_1 and t_1 with radius $r_1^P = r_1^B < r_1$. In this example it is clear that $|\mathcal{A}_1^B(p_0,t_1)| \geq |p_0p_1| + |\mathcal{A}_1^P(p_1,t_1)|$ since they are both convex and $\mathcal{A}_1^B(p_0,t_1)$ contains $p_0p_1 + \mathcal{A}_1^P(p_1,t_1)$.

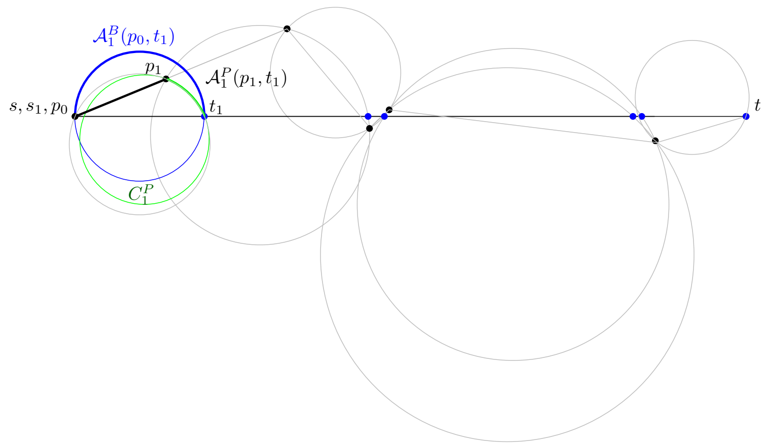

(a) C_1^P with radius $r_1^p = r_1^B$.

Figure A.2

In Figure A.3a, C_2^B is balanced with respect to C_1^P, that is, $|\mathcal{A}_2^B(p_1, t_2)| = |p_1 q_2'| + |\mathcal{B}_2^B(q_2', t_2)|$. If Figure A.3b we show the placement of C_2^P.

In Figure A.3c, C_3^B is balanced with C_2^P, but note that this time $r_3^B > r_3$. Thus in Figure A.4a, we note that $r_3^P = r_3 < r_3^B$, and therefore $C_3^P = C_3$.

In Figure A.4b, C_4^B is balanced with C_3^P, with p_3 is under st, thus $|\mathcal{B}_4^B(p_3, t_4)| = |p_4 q_4'| + |\mathcal{A}_4^B(q_4', t_4)|$. In Figure A.4c, $p_3 p_4$ and $\mathcal{A}_4^P(p_4, t_4)$ are not convex. Thus $|\mathcal{B}_4^B(p_3, t_4)| = |p_3 q_4'| + |\mathcal{A}_4^B(q_4', t_4)| \geq |p_3 p_4| + |\mathcal{A}_4^P(p_4, t_4)|$ is proven by other means. See Appendix B.

In Figures A.5a and A.5b, the path of $p_4 q_5'$ and $\mathcal{B}_5^B(q_5', t_5)$ does not contain the path of $p_4 p_5$ and $\mathcal{B}_5^P(p_5, t_5)$, thus we cannot use a simple proof to show $|\mathcal{A}_5^B(p_4, t_5)| = |p_4 q_5'| + |\mathcal{B}_5^B(q_5', t_5)| \geq |p_4 p_5| + |\mathcal{B}_5^P(p_5, t_5)|$. See Appendix B.

In Figure A.5c, note that $p_5 = q_6'$. Thus C_6^B being balanced with C_5^P implies that $|\mathcal{A}_6^B(p_5, t_6)| = |\mathcal{B}_6^B(p_5 = q_6', t_6)|$. Since $p_6 = t$, C_6^P is the circle centered at t with radius $r_6^P = 0$, and thus degenerate.

In Figure A.6a, we see the arcs in $\Phi(C_{i-1}^P, C_i^B)$, for all $0 < i \leq 6$. For example, $\Phi(C_1^P, C_2^B) = |\mathcal{A}_2^B(p_1, t_2)| - \mathscr{D}_1^P - \lambda |s_1^P s_2^B| - (\Phi - \lambda)|t_1 t_2|$.

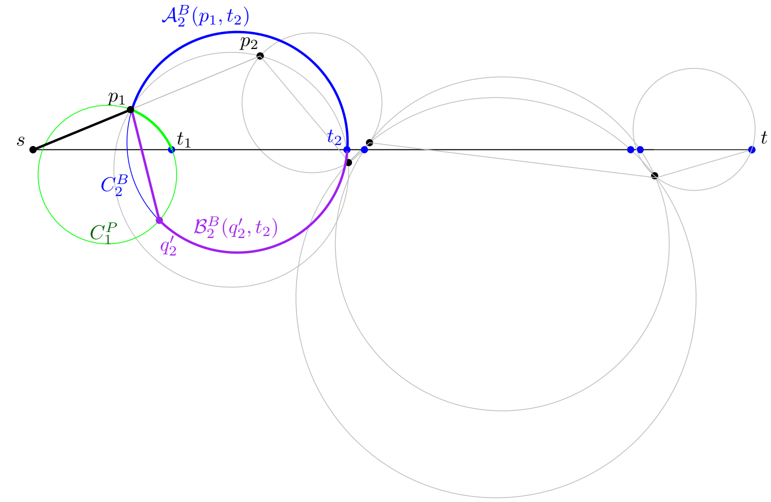

(a) C_2^B is balanced with C_1^P.

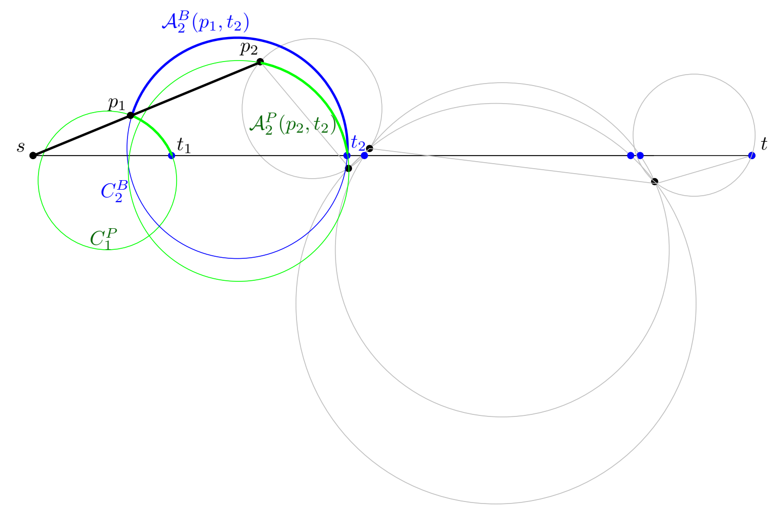

(b) C_2^P with radius $r_2^P = r_2^B$.

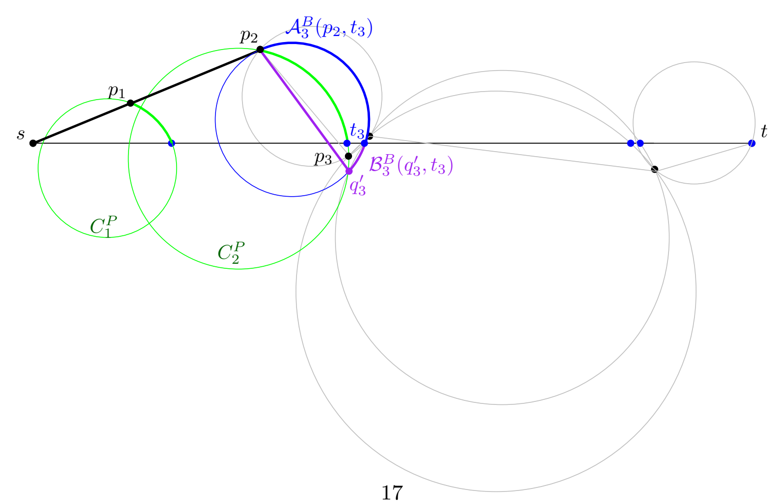

(c) C_3^B is balanced with C_2^P.

Figure A.3

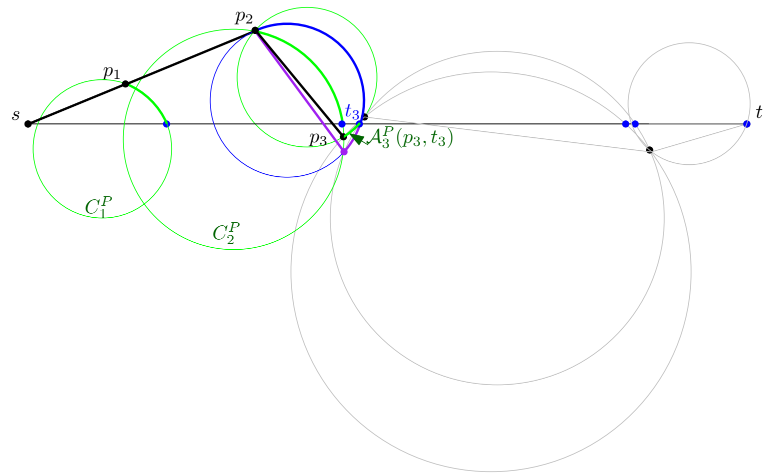

(a) Since $r_3 < r_3^B$, we set $r_3^P = r_3$, and thus $C_3^P = C_3$.

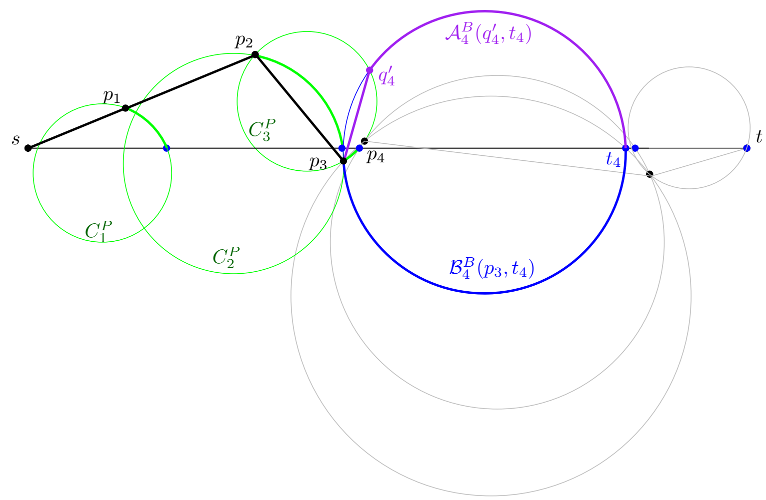

(b) C_4^B is balanced with C_3^P.

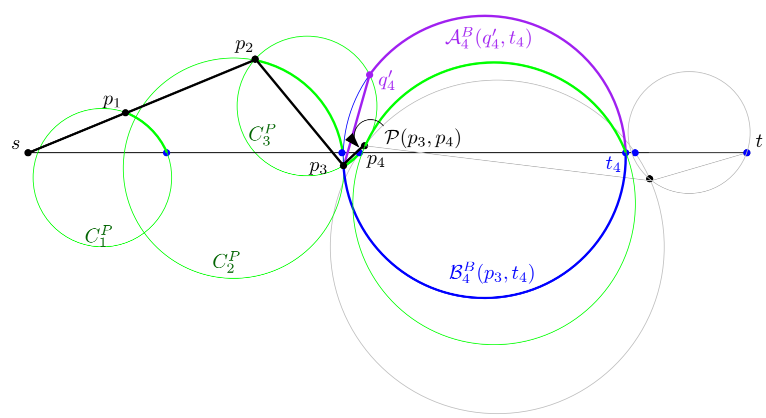

(c) C_4^P with radius $r_4^P = r_4^B$.

Figure A.4

Appendix B. Proof of Lemma 4.2.

We will prove part 1 of Lemma 4.2; the proof of part 2 is symmetric. Thus we assume that p_{i-1} is above st. Let C be any circle with p_{i-1} and t_{i-1} on its boundary. Let C' be any circle with p_{i-1} and t_i on its boundary. Let q be the lowest intersection point of C and C'.

Of the following two paths from p_{i-1} to t_i, $|p_{i-1}q| + |\mathcal{B}_{C'}(q, t_i)|$ and $|\mathcal{A}_{C'}(p_{i-1}, t_i)|$, let $\mathcal{P}_{\mathcal{S}}(C, C')$ be the shorter and let $\mathcal{P}_{\mathcal{L}}(C, C')$ be the longer. If the paths have equal length label both paths $\mathcal{P}_{\mathcal{S}}(C, C')$.

Lemma B.1. *Let C be a fixed circle with p_{i-1} and t_{i-1} on its boundary. Of all circles C' with p_{i-1} and t_i on its boundary, $|\mathcal{P}_{\mathcal{S}}(C, C')|$ is maximized when C and C' are balanced.*

Proof. Note that $\mathcal{P}_{\mathcal{S}}(C, C')$ and $\mathcal{P}_{\mathcal{L}}(C, C')$ are both convex. We prove the lemma by contradiction. Let C' be the circle through p_{i-1} and t_i such that C and C' are balanced. Let C'' be a circle through p_{i-1} and t_i such that $|\mathcal{P}_{\mathcal{S}}(C, C'')| > |\mathcal{P}_{\mathcal{S}}(C, C')|$. Since C' and C'' intersect in p_{i-1} and t_i, the part of C' on one side of $p_{i-1}t_i$ is contained in C'', and the part of C' to the other side of $p_{i-1}t_i$ contains C''. Consider the path $\mathcal{P}_{\mathcal{S}}(C, C')$ to the side of $p_{i-1}t_i$ where C' contains C''. Observe that $\mathcal{P}_{\mathcal{S}}(C, C')$ is convex and either contains $\mathcal{P}_{\mathcal{S}}(C, C'')$ or $\mathcal{P}_{\mathcal{L}}(C, C'')$. In either case, $|\mathcal{P}_{\mathcal{S}}(C, C')| > |\mathcal{P}_{\mathcal{S}}(C, C'')|$, a contradiction. See Fig. B.1. ∎

Recall that in this section, p_{i-1} is assumed to be above st. Therefore q_i denotes the lowest intersection point of C_{i-1} and C_i. Let $\widehat{q_i}$ be the lowest intersection point of C_{i-1}^P and C_i. Then we have the following lemma.

Lemma B.2. $|p_{i-1}q_i| + |\mathcal{B}_i(q_i, t_i)| \leq |p_{i-1}\widehat{q_i}| + |\mathcal{B}_i(\widehat{q_i}, t_i)|$.

Proof. Let l_i be the leftmost intersection of C_i with st. We know q_i is on the opposite side of st as p_{i-1}. If $\widehat{q_i}$ is on the same side of st as p_{i-1}, then it must be on the arc $\mathcal{B}_i(p_{i-1}, l_i)$ (by construction), thus q_i is on $\mathcal{B}_i(\widehat{q_i}, t_i)$, and the lemma is true by the triangle inequality.

Assume that $\widehat{q_i}$ is below st. If $r_{i-1}^P = r_{i-1}$, then $C_{i-1}^P = C_{i-1}$ and $\widehat{q_i} = q_i$, from which the inequality becomes trivial. Assume that $r_{i-1}^P = \min\{r_{i-1}, r_{i-1}^B\} = r_{i-1}^B < r_{i-1}$.

Since C_{i-1}^P and C_{i-1} intersect p_{i-1} and t_{i-1}, and since $r_{i-1}^P < r_{i-1}$, the convex hull of $\mathcal{A}_{i-1}^P(p_{i-1}, t_{i-1})$ contains the convex hull of $\mathcal{A}_{i-1}(p_{i-1}, t_{i-1})$. That means that the part of C_{i-1}^P to the left of $p_{i-1}t_{i-1}$ is contained in C_{i-1}. Therefore q_i is on $\mathcal{B}_i(\widehat{q_i}, t_i)$, and thus $|p_{i-1}q_i| < |p_{i-1}\widehat{q_i}| + |\mathcal{B}_i(\widehat{q_i}, q_i)|$ by the triangle inequality, which implies the lemma. ∎

Lemma B.3. $|p_{i-1}p_i| + |\mathscr{D}_i| \leq |\mathcal{P}_{\mathcal{S}}(C_{i-1}, C_i)| \leq |\mathcal{P}_{\mathcal{S}}(C_{i-1}^P, C_i)| \leq |\mathcal{A}_i^B(p_{i-1}, t_i)|$.

Proof. For the first inequality, we consider two cases: Either p_i is above st, or p_i is below st. If p_i is above st, then the path does not cross st, therefore $|p_{i-1}p_i| + |\mathscr{D}_i| = |p_{i-1}p_i| + |\mathcal{A}_i(p_i, t_i)| < |\mathcal{A}_i(p_{i-1}, t_i)| = |\mathcal{P}_{\mathcal{S}}(C_{i-1}, C_i)|$ by the triangle inequality. If p_i is below st, then the path does cross st, therefore $|p_{i-1}p_i| + |\mathscr{D}_i| = |p_{i-1}p_i| + |\mathcal{B}_i(p_i, t_i)| \leq \min\{|\mathcal{A}_i(p_{i-1}, t_i)|, |p_{i-1}q_i| + |\mathcal{B}_i(q_i, t_i)|\} = |\mathcal{P}_{\mathcal{S}}(C_{i-1}, C_i)|$ by the triangle inequality.

By Lemma B.2, we have

$$\begin{aligned}|\mathcal{P}_{\mathcal{S}}(C_{i-1}, C_i)| &= \min\{|\mathcal{A}_i(p_{i-1}, t_i)|, |p_{i-1}q_i| + |\mathcal{B}_i(q_i, t_i)|\}\\ &\le \min\{|\mathcal{A}_i(p_{i-1}, t_i)|, |p_{i-1}\widehat{q_i}| + |\mathcal{B}_i(\widehat{q_i}, t_i)|\}\\ &= |\mathcal{P}_{\mathcal{S}}(C^P_{i-1}, C_i)|.\end{aligned}$$

For the last inequality, $|\mathcal{P}_{\mathcal{S}}(C^P_{i-1}, C_i)|$ is equal to the smallest of $|p_{i-1}\widehat{q_i}|+|\mathcal{B}_i(\widehat{q_i}, t_i)|$ and $|\mathcal{A}_i(p_{i-1}, t_i)|$. Therefore, $|\mathcal{P}_{\mathcal{S}}(C^P_{i-1}, C_i)| \le |\mathcal{P}_{\mathcal{S}}(C^P_{i-1}, C^B_i)| = |\mathcal{A}^B_i(p_{i-1}, t_i)|$ by Lemma B.1, since C^P_{i-1} and C^B_i are balanced. This proves the lemma. ◻

Proof of Lemma 4.2. Assume that p_{i-1} is above st. We have to prove that

$$|\mathcal{A}^B_i(p_{i-1}, t_i)| \ge |p_{i-1}p_i| + |\mathscr{D}^P_i|. \tag{B.1}$$

If $r^P_i = r_i < r^B_i$, then $C^P_i = C_i$, and the right-hand side of (B.1) is equal to $|p_{i-1}p_i| + |\mathscr{D}_i|$. Lemma 4.2 then follows from Lemma B.3. Otherwise $r^P_i = \min\{r_i, r^B_i\} = r^B_i < r_i$. We consider two cases:

1. $|\mathcal{A}_i(p_{i-1}, t_i)| < \pi r_i$ and
2. $|\mathcal{A}_i(p_{i-1}, t_i)| > \pi r_i$.

Note that if $|\mathcal{A}_i(p_{i-1}, t_i)| = \pi r_i$, then r_i is the smallest radius of any circle through p_{i-1} and t_i, and thus $r^B_i \ge r_i$. Thus these two cases cover all possibilities.

Observation B.4. *We have the following two inequalities*

$$|p_{i-1}t_i| > |p_it_i| \ \textit{and} \tag{B.2}$$
$$|\mathcal{A}_i(p_{i-1}, t_i)| \ge |p_{i-1}p_i| + |\mathscr{D}_i|. \tag{B.3}$$

Given a circle C and two points u and v on C, let $\Gamma_C(u, v)$ be the shorter of the two arcs $\mathcal{A}_C(u, v)$ and $\mathcal{B}_C(u, v)$. For a given radius r, let

$$\mathcal{Z}(r) = |\Gamma_C(p_{i-1}, t_i)| - |p_{i-1}p_i| - |\Gamma_{C'}(p_i, t_i)|,$$

where C (respectively C') is any circle with radius r, and with p_{i-1} (respectively p_i) and t_i on its boundary[1]. Since $r^P_i = r^B_i$, we need to show that $\mathcal{Z}(r^P_i) \ge 0$.

Let us consider Case 1. Observe that in $\mathcal{Z}(r_i)$, $C = C' = C_i$ since p_{i-1}, p_i, and t_i all belong to C_i. Therefore, by (B.3) and the definition of $\mathscr{D}_i$, we have $\mathcal{Z}(r_i) \ge 0$. Thus, if we can prove that $\mathcal{Z}(r)$ never decreases as r goes from r_i down to $r^P_i = r^B_i$, we are done. Hence, we want to show that $\frac{d\mathcal{Z}(r)}{dr} \le 0$. In other words, we want to show

$$\frac{d|\Gamma_C(p_{i-1}, t_i)|}{dr} \le \frac{d|\Gamma_{C'}(p_i, t_i)|}{dr}. \tag{B.4}$$

Let α be the angle at the center of C subtended by $\Gamma_C(p_{i-1}, t_i)$, and let β be the angle at the center of C' subtended by $\Gamma_{C'}(p_i, t_i)$. By (B.2) we have $\alpha > \beta$. Note that $|\Gamma_C(p_{i-1}, t_i)| = \alpha r$, and $|\Gamma_{C'}(p_i, t_i)| = \beta r$. Since they are both linear in r, if we prove

$$\frac{d\alpha}{dr} \le \frac{d\beta}{dr}, \tag{B.5}$$

[1] Notice that $\mathcal{Z}(r)$ is defined for all $r \ge |p_{i-1}t_i|/2$.

we have proven (B.4). We have $\sin(\alpha/2) = \frac{|p_{i-1}t_i|}{2r}$, thus $\alpha = 2\arcsin\left(\frac{|p_{i-1}t_i|}{2r}\right)$. Therefore

$$\frac{d\alpha}{dr} = -\frac{|p_{i-1}t_i|}{2\sqrt{1-\left(\frac{|p_{i-1}t_i|}{2r}\right)^2}} \underset{by (B.2)}{\leq} -\frac{|p_i t_i|}{2\sqrt{1-\left(\frac{|p_i t_i|}{2r}\right)^2}} = \frac{d\beta}{dr},$$ ∎

which proves Case 1.

Let us consider Case 2. Since $|\mathcal{A}_i(p_{i-1}, t_i)| > \pi r_i$, it must be that $|p_{i-1}b_i| + |\mathcal{B}_i(b_i, t_i)| < |\mathcal{A}_i(p_{i-1}, t_i)|$, and the algorithm crossed st at p_{i-1} (and thus $p_i = b_i$). Note that $\pi r_i > |\mathcal{B}_i(p_{i-1}, t_i)| > |p_{i-1}b_i| + |\mathcal{B}_i(b_i, t_i)| = |p_{i-1}p_i| + |\mathscr{D}_i|$. Thus $|\mathcal{B}_i(p_{i-1}, t_i)| - |p_{i-1}p_i| - |\mathcal{B}_i(p_i, t_i)| = \mathcal{Z}(r_i) \geq 0$, and we apply the same argument as above to show that $\mathcal{Z}(r_i^P) \geq 0$.

Appendix C. Proofs of Lemmas 3.8 and 3.9 - Analyzing $\Phi(C_{i-1}, C_i)$.

In this section, we want to prove Lemmas 3.8 and 3.9. In other words, we wish to show $\Phi(C_{i-1}, C_i) \leq 0$, where

$$\Phi(C_{i-1}, C_i) = |\mathcal{A}_i(p_{i-1}, t_i)| - |\mathcal{A}_{i-1}(p_{i-1}, t_i)| - \lambda|s_{i-1}s_i| - (\mu - \lambda)|t_{i-1}t_i| \quad \text{when } p_{i-1} \text{ is above } st \text{, and} \tag{C.1}$$

$$\Phi(C_{i-1}, C_i) = |\mathcal{B}_i(p_{i-1}, t_i)| - |\mathcal{B}_{i-1}(p_{i-1}, t_i)| - \lambda|s_{i-1}s_i| - (\mu - \lambda)|t_{i-1}t_i| \quad \text{when } p_{i-1} \text{ is below } st. \tag{C.2}$$

Since these two cases are symmetric, for the remainder of the proof, we assume that p_{i-1} is above st, thus we focus on proving (C.1).

We can rewrite $-\lambda|s_{i-1}s_i|$ as

$$\begin{aligned} -\lambda|s_{i-1}s_i| &= -\lambda(x(s_i) - x(s_{i-1})) \\ &= -\lambda(x(t_i) - 2r_i - x(t_{i-1}) + 2r_{i-1}) \\ &= -\lambda|t_{i-1}t_i| - 2\lambda(r_{i-1} - r_i). \end{aligned}$$

Thus we can rewrite $\Phi(C_{i-1}, C_i)$ as

$$\Phi(C_{i-1}, C_i) = |\mathcal{A}_i(p_{i-1}, t_i)| - |\mathcal{A}_{i-1}(p_{i-1}, t_{i-1})| - 2\lambda(r_{i-1} - r_i) - \mu|t_{i-1}t_i|.$$

Recall that Lemmas 3.8 and 3.9 were introduced in Section 3.3, where we assumed that c_{i-1} and c_i lie on the x-axis, with $x(c_i) > x(c_{i-1})$, and p_{i-1} and q_i lie on the y-axis. Therefore $x(p_{i-1}) = x(q_i) = 0$.

The following lemma is a useful result.

Lemma C.1. *Let us fix C_{i-1}, C_i, p_{i-1} and t_i. Consider all line segments st such that t_i is on st, st intersects C_{i-1}, and c_{i-1} is on or above st. Among all such line segments st, $\Phi(C_{i-1}, C_i)$ is maximized when c_{i-1} is on st.*

Proof. Consider the case where c_{i-1} is above st. We rotate st until it contains c_{i-1} and observe the changes in $\Phi(C_{i-1}, C_i)$.

During the rotation of st, r_{i-1}, r_i, and t_i remain fixed, whereas t_{i-1} is changing. Note that $|t_{i-1}t_i|$ is minimized when st contains c_{i-1}. Thus $-\mu|t_{i-1}t_i|$ is increasing. We also note that $-|\mathcal{A}_{i-1}(p_{i-1}, t_{i-1})|$ is increasing, while $|\mathcal{A}_i(p_{i-1}, t_i)|$ remains constant. Thus, for all cases where c_{i-1} is on or above st, $\Phi(C_{i-1}, C_i)$ is maximized when c_{i-1} is on st. ∎

Thus, for the rest of the proof, we assume that c_{i-1} is either on or below st.

Let α (respectively β) be the angle (respectively the signed angle) defined by the line segment c_ip_{i-1} (respectively c_it_i) and the x-axis such that $|\mathcal{A}_i(p_{i-1}, t_i)| = (\alpha+\beta)r_i$ (refer to Fig. C.1). Thus $0 \le \alpha \le \pi$ and $-\alpha \le \beta \le \alpha$. Let γ be the signed angle between the x-axis and st such that $-\pi/2 < \gamma < \pi/2$. Observe that $-\pi/2 < \beta - \gamma < \pi/2$.

First, recall the definition of Transformation 3.10. As we apply Transformation 3.10, we update the values of α, β, and γ. Observe that, after we have completed Transformation 3.10, we have $C_i = C_{i-1}$ and thus $\Phi(C_{i-1}, C_i) = 0$. If we can show that $\Phi(C_{i-1}, C_i)$ was increasing while $x(c_i)$ decreased, then it must be that $\Phi(C_{i-1}, C_i) \le 0$ before Transformation 3.10. Thus we wish to find the change in $\Phi(C_{i-1}, C_i)$ with respect to the change in $x(c_i)$ during Transformation 3.10. Therefore we wish to calculate the derivative of $\Phi(C_{i-1}, C_i)$ with respect to $x(c_i)$.

We define a function $\tau(\alpha, \beta, \gamma) = \frac{d\Phi(C_{i-1}, C_i)}{dx(c_i)}$. Thus if we show $\tau(\alpha, \beta, \gamma) \le 0$, we can apply Lemma 3.11 and we are done.

However, this does not always work, as we sometimes encounter degenerate cases where $\frac{d\Phi(C_{i-1}, C_i)}{dx(c_i)} > 0$ at some point during Transformation 3.10. For the cases when this happens, we use a different argument to show that, before applying Transformation 3.10, when C_{i-1} and C_i are balanced, $\Phi(C_{i-1}, C_i) \le 0$.

Thus we use a combination of Lemma 3.11, intermediate circles, and geometric proofs to show that $\Phi(C_{i-1}, C_i) \le 0$ in all cases when C_{i-1} and C_i are balanced.

In Appendix C.1 we compute $\tau(\alpha, \beta, \gamma) = \frac{d\Phi(C_{i-1}, C_i)}{dx(c_i)}$. In Appendix C.2 we simplify and analyze this function. In Appendix C.3 we identify the different cases we need to consider to prove Lemmas 3.8 and 3.9, and then apply the appropriate techniques to prove them.

C.1. Analyzing $\frac{d\Phi(C_{i-1}, C_i)}{dx(c_i)}$. We compute $\frac{d\Phi(C_{i-1}, C_i)}{dx(c_i)}$ piece by piece. Note that $x(c_i) = -r_i \cos\alpha$ and $y(p_{i-1}) = r_i \sin\alpha$.

$$\text{(C.3)}\qquad \frac{dr_i}{dx(c_i)} = \frac{d\sqrt{x(c_i)^2 + y(p_{i-1})^2}}{dx(c_i)} = \frac{x(c_i)}{\sqrt{x(c_i)^2 + y(p_{i-1})^2}} = \frac{x(c_i)}{r_i} = -\cos\alpha$$

$$\frac{d\alpha}{dx(c_i)} = \frac{d(\pi/2 + \arctan(\frac{x(c_i)}{y(p_{i-1})}))}{dx(c_i)} = \frac{y(p_{i-1})}{x(c_i)^2 + y(p_{i-1})^2} = \frac{y(p_{i-1})}{r_i^2} = \frac{\sin\alpha}{r_i}$$

$$\frac{d(\alpha r_i)}{dx(c_i)} = \alpha\frac{dr_i}{dx(c_i)} + r_i\frac{d\alpha}{dx(c_i)} = \sin\alpha - \alpha\cos\alpha$$

To calculate $\frac{d|t_{i-1}t_i|}{dx(c_i)}$ and $\frac{d\beta}{dx(c_i)}$ we need the total chain rule, or total derivative. We consider $|t_{i-1}t_i|$ as a function of $x(c_i)$ and r_i. However, r_i is also a function of $x(c_i)$. Thus we can express the change in $|t_{i-1}t_i|$ with respect to the change in $x(c_i)$ as:

$$\frac{d|t_{i-1}t_i|}{dx(c_i)} = \frac{\partial|t_{i-1}t_i|}{\partial x(c_i)}\frac{dx(c_i)}{dx(c_i)} + \frac{\partial|t_{i-1}t_i|}{\partial r_i}\frac{dr_i}{dx(c_i)} = \frac{\partial|t_{i-1}t_i|}{\partial x(c_i)} + \frac{\partial|t_{i-1}t_i|}{\partial r_i}\frac{dr_i}{dx(c_i)}$$

Geometrically, $\partial x(c_i)$ represents translating c_i along the x-axis while fixing the radius r_i. ∂r_i represents changing the radius r_i of C_i, while keeping $x(c_i)$ fixed. See Fig. C.3. However, the change in r_i is dependent on $x(c_i)$, hence we multiply by $\frac{dr_i}{dx(c_i)}$.

The partial derivatives $\frac{\partial|t_{i-1}t_i|}{\partial x(c_i)}$ and $\frac{\partial|t_{i-1}t_i|}{\partial r_i}$ can be individually determined using simple geometry. We determine $\frac{d\beta}{dx(c_i)}$ using the same technique.

C.1.1. Calculating $\frac{d|t_{i-1}t_i|}{dx(c_i)}$. In Fig. C.5a we examine the geometry of $\frac{\partial|t_{i-1}t_i|}{\partial x(c_i)}$. Applying the sine rule yields

$$\frac{\sin(\pi/2+\beta-\gamma)}{\partial x(c_i)} = \frac{\sin(\pi/2-\beta)}{\partial|t_{i-1}t_i|}$$

$$\frac{\partial|t_{i-1}t_i|}{\partial x(c_i)} = \frac{\sin(\pi/2-\beta)}{\sin(\pi/2+\beta-\gamma)} = \frac{\cos\beta}{\cos(\beta-\gamma)}$$

In Fig. C.4b we examine the geometry of $\frac{\partial|t_{i-1}t_i|}{\partial r_i}$. Applying the sine rule yields

$$\frac{\sin(\pi/2-\beta+\gamma)}{\partial r_i} = \frac{\sin(\pi/2)}{\partial|t_{i-1}t_i|}$$

$$\frac{\partial|t_{i-1}t_i|}{\partial r_i} = \frac{1}{\sin(\pi/2+\beta-\gamma)} = \frac{1}{\cos(\beta-\gamma)}$$

.

From (C.3) we have $\frac{dr_i}{dx(c_i)} = -\cos\alpha$. Thus

$$\begin{aligned}\frac{d|t_{i-1}t_i|}{dx(c_i)} &= \frac{\partial|t_{i-1}t_i|}{\partial x(c_i)} + \frac{\partial|t_{i-1}t_i|}{\partial r_i}\frac{dr_i}{dx(c_i)}\\ &= \frac{\cos\beta}{\cos(\beta-\gamma)} - \frac{1}{\cos(\beta-\gamma)}\cos\alpha\\ &= \frac{\cos\beta-\cos\alpha}{\cos(\beta-\gamma)}.\end{aligned} \tag{C.4}$$

C.1.2. Calculating $\dfrac{d\beta}{dx(c_i)}$. The total derivative of $\frac{d\beta}{dx(c_i)}$ is

$$\frac{d\beta}{dx(c_i)} = \frac{\partial\beta}{\partial x(c_i)}\frac{dx(c_i)}{dx(c_i)} + \frac{\partial\beta}{\partial r_i}\frac{dr_i}{dx(c_i)} = \frac{\partial\beta}{\partial x(c_i)} + \frac{\partial\beta}{\partial r_i}\frac{dr_i}{dx(c_i)}$$

Fig. C.6a shows the geometry of $\frac{\partial\beta}{\partial x(c_i})$. Applying the sine rule yields

$$\text{(C.5)} \qquad \frac{(\partial\beta)r_i}{\sin\gamma} = \frac{\partial x(c_i)}{\sin(\pi/2+\beta-\gamma)}$$

$$\text{(C.6)} \qquad \frac{\partial\beta}{\partial x(c_i)} = \frac{\sin\gamma}{r_i\cos(\beta-\gamma)}.$$

Fig. C.6b shows the geometry of $\frac{\partial\beta}{\partial x(r_i)}$. Applying the sine rule yields

$$\frac{\sin(\pi/2-\beta+\gamma)}{\partial x(r_i)} = \frac{\sin(\beta-\gamma)}{-(\partial\beta)r_i}$$

$$\frac{(\partial\beta)r_i}{\partial x(r_i)} = -\frac{\sin(\beta-\gamma)}{\sin(\pi/2+\beta-\gamma)}$$

$$\text{(C.7)} \qquad \frac{\partial\beta}{\partial x(r_i)} = -\frac{\sin(\beta-\gamma)}{\cos(\beta-\gamma)r_i}.$$

Thus the total derivative is:

$$\begin{aligned}\frac{d\beta}{dx(c_i)} &= \frac{\partial\beta}{\partial x(c_i)} + \frac{\partial\beta}{\partial x(r_i)}\frac{dr_i}{dx(c_i)} \\ &= \frac{\sin\gamma}{\cos(\beta-\gamma)r_i} - \frac{\sin(\beta-\gamma)}{\cos(\beta-\gamma)r_i}(-\cos\alpha) \\ &= \frac{\sin\gamma+\cos\alpha\sin(\beta-\gamma)}{\cos(\beta-\gamma)r_i}\end{aligned}$$

The change in βr_i with $x(c_i)$ is

$$\begin{aligned}\frac{d(\beta r_i)}{dx(c_i)} &= \frac{\sin\gamma+\cos\alpha\sin(\beta-\gamma)}{\cos(\beta-\gamma)r_i}r_i - \beta\cos\alpha \\ &= \frac{\sin\gamma+\cos\alpha\sin(\beta-\gamma)}{\cos(\beta-\gamma)} - \beta\cos\alpha.\end{aligned}$$

Thus

$$\begin{aligned}\frac{d|\mathcal{A}_i(p_{i-1},t_i)|}{dx(c_i)} &= \frac{d(\alpha+\beta)r_i}{dx(c_i)} \\ &= \sin\alpha - \alpha\cos\alpha + \frac{\cos\alpha\sin(\beta-\gamma)+\sin\gamma}{\cos(\beta-\gamma)} - \beta\cos\alpha \\ &= \sin\alpha - (\alpha+\beta)\cos\alpha + \frac{\cos\alpha\sin(\beta-\gamma)+\sin\gamma}{\cos(\beta-\gamma)}.\end{aligned}$$

The change in $(r_{i-1}-r_i)$ with respect to $x(c_i)$ is

$$\text{(C.8)} \qquad \frac{d(r_{i-1}-r_i)}{dx(c_i)} = \frac{dr_{i-1}}{dx(c_i)} - \frac{dr_i}{dx(c_i)}$$

$$\text{(C.9)} \qquad = \cos\alpha.$$

Thus the change in $\Phi(C_{i-1}, C_i)$ with respect to the change in $x(c_i)$ is given by

$$\begin{aligned}
&\frac{d\Phi(C_{i-1}, C_i)}{dx(c_i)} \\
&= \frac{d(|\mathcal{A}_i(p_{i-1}, t_i)| - |\mathcal{A}_{i-1}(p_{i-1}, t_{i-1})| - 2\lambda(r_{i-1} - r_i) - \mu|t_{i-1}t_i|)}{dx(c_i)} \\
&= \frac{d(\alpha+\beta)r_i}{dx(c_i)} - \frac{d2\lambda(r_{i-1} - r_i)}{dx(c_i)} - \frac{d\mu|t_{i-1}t_i|}{dx(c_i)} \\
&= \sin\alpha - (\alpha+\beta)\cos\alpha + \frac{\cos\alpha\sin(\beta-\gamma)+\sin\gamma}{\cos(\beta-\gamma)} - 2\lambda\cos\alpha - \mu\left(\frac{\cos\beta-\cos\alpha}{\cos(\beta-\gamma)}\right) \\
&= \sin\alpha - (\alpha+\beta+2\lambda)\cos\alpha + \frac{\cos\alpha\sin(\beta-\gamma)+\sin\gamma}{\cos(\beta-\gamma)} - \mu\left(\frac{\cos\beta-\cos\alpha}{\cos(\beta-\gamma)}\right)
\end{aligned}$$

C.2. Simplifying $\frac{d\Phi(C_{i-1},C_i)}{dx(c_i)}$. Define a function:

$$\tau(\alpha,\beta,\gamma) = \sin\alpha - (\alpha+\beta+2\lambda)\cos\alpha + \frac{\cos\alpha\sin(\beta-\gamma)+\sin\gamma}{\cos(\beta-\gamma)} - \mu\left(\frac{\cos\beta-\cos\alpha}{\cos(\beta-\gamma)}\right)$$

In this section our goal is to find values of α, β, and γ for which $\tau(\alpha,\beta,\gamma) \le 0$. We study each parameter separately, and then conclude. In Section C.2.1 we analyze $\tau(\alpha,\beta,\gamma)$ with respect to γ. In Section C.2.2 we analyze $\tau(\alpha,\beta,\gamma)$ with respect to β. Finally, in Section C.2.3 we analyze $\tau(\alpha,\beta,\gamma)$ with respect to α.

C.2.1. Maximizing $\tau(\alpha,\beta,\gamma)$ With Respect to γ. To find the value of γ that maximizes $\tau(\alpha,\beta,\gamma)$, we find $\frac{d\tau(\alpha,\beta,\gamma)}{d\gamma}$.

$$\begin{aligned}
\frac{d\tau(\alpha,\beta,\gamma)}{d\gamma} &= \\
&\frac{-\cos\alpha + \cos\gamma\cos(\beta-\gamma) - \sin\gamma\sin(\beta-\gamma) + \mu\sin(\beta-\gamma)(\cos\beta-\cos\alpha)}{\cos^2(\beta-\gamma)} \\
&= \frac{\cos\beta - \cos\alpha + \mu\sin(\beta-\gamma)(\cos\beta-\cos\alpha)}{\cos^2(\beta-\gamma)} \\
&= \frac{(1+\mu\sin(\beta-\gamma))(\cos\beta-\cos\alpha)}{\cos^2(\beta-\gamma)}
\end{aligned}$$

To maximize $\tau(\alpha,\beta,\gamma)$, let γ^* be the value for which $(1+\mu\sin(\beta-\gamma^*)) = 0$, in other words, $\gamma^* = \beta - \arcsin(-1/\mu)$. The ranges of α, β, and γ give us that $\frac{\cos\beta-\cos\alpha}{\cos^2(\beta-\gamma)} \ge 0$. Therefore $\frac{d\tau(\alpha,\beta,\gamma)}{d\gamma} = 0$ when $\gamma = \gamma^*$, and it is positive when $\gamma < \gamma^*$ and it is negative when $\gamma > \gamma^*$. Thus $\tau(\alpha,\beta,\gamma) \le \tau(\alpha,\beta,\gamma^*)$ for all $0 \le \alpha \le \pi$ and $-\alpha \le \beta \le \alpha$.

We can rewrite $\tau(\alpha,\beta,\gamma^*)$ as:

$\tau(\alpha,\beta,\gamma^*) = \cos(\beta-\gamma^*)(\sin\alpha - (\alpha+\beta+2\lambda)\cos\alpha) + \cos\alpha\sin(\beta-\gamma^*) + \sin\gamma^* - \mu(\cos\beta-\cos\alpha)$

$= \sqrt{1-(1/\mu)^2}(\sin\alpha - (\alpha+\beta+2\lambda)\cos\alpha) - \dfrac{\cos\alpha}{\mu} + \sin\left(\beta - \arcsin\left(\frac{-1}{\mu}\right)\right) - \mu(\cos\beta - \cos\alpha)$

$= \sqrt{1-(1/\mu)^2}(\sin\alpha - (\alpha+\beta+2\lambda)\cos\alpha) - \dfrac{\cos\alpha}{\mu} + \sin\beta\sqrt{1-(1/\mu)^2} + \dfrac{\cos\beta}{\mu} - \mu(\cos\beta - \cos\alpha)$

$= \sqrt{1-(1/\mu)^2}(\sin\alpha + \sin\beta - (\alpha+\beta+2\lambda)\cos\alpha) - \left(\mu - \dfrac{1}{\mu}\right)(\cos\beta - \cos\alpha).$

Let $A = \sqrt{1-(1/\mu)^2} = \dfrac{\sqrt{1+\sin(1)}}{\sqrt{2}}$ and let $B = \left(\mu - \dfrac{1}{\mu}\right) = A\left(\dfrac{1+\sin(1)}{\cos(1)}\right)$. Then we have

$$\tau(\alpha,\beta,\gamma^*) = A(\sin\alpha + \sin\beta - (\alpha+\beta+2\lambda)\cos\alpha) - B(\cos\beta - \cos\alpha).$$

C.2.2. Maximizing $\tau(\alpha,\beta,\gamma^*)$ With Respect to β.. To see how $\tau(\alpha,\beta,\gamma^*)$ behaves with respect to β, we calculate:

$$\frac{d\tau(\alpha,\beta,\gamma^*)}{d\beta} = A(\cos\beta - \cos\alpha) + B(\sin\beta).$$

We can now prove the following lemma.

LEMMA C.2. *For a fixed α, $\tau(\alpha,\beta,\gamma^*)$, as a function of β, is unimodal and $\tau(\alpha,\beta,\gamma^*) \le \max\{\tau(\alpha,-\alpha,\gamma^*), \tau(\alpha,\alpha,\gamma^*)\}$.*

Proof. The expression $A(\cos\beta - \cos\alpha)$ is always positive, since $|\beta| \le \alpha$. Moreover $B(\sin\beta)$ has the same sign as β. Thus $\dfrac{d\tau(\alpha,\beta,\gamma^*)}{d\beta}$ is convex in β, which means it is maximized at the lowest and highest values of β, i.e., $\tau(\alpha,\beta,\gamma^*) \le \max\{\tau(\alpha,-\alpha,\gamma^*), \tau(\alpha,\alpha,\gamma^*)\}$. ∎

C.2.3. $\tau(\alpha,\sin\alpha,\gamma^*) \le 0$. In this section we prove the following lemma.

LEMMA C.3. *$\tau(\alpha,\sin\alpha,\gamma^*) \le \tau(\pi/2,\sin(\pi/2),\gamma^*) = 0$, for all $0 \le \alpha \le \pi$.*

First we prove the equality. When $\alpha = \pi/2$, we have

$$\tau(\pi/2,\sin(\pi/2),\gamma^*) = A(1+\sin(1)) - B\cos(1) = 0. \tag{C.10}$$

Note that we obtain the value μ by letting $A = \sqrt{1-(1/\mu)^2}$ and $B = \left(\mu - \frac{1}{\mu}\right)$ and then solving (C.10) for μ.

Now we show that $\tau(\alpha,\sin\alpha,\gamma^*) \le \tau(\pi/2,\sin(\pi/2),\gamma^*)$. Observe that $\tau(\alpha,\sin\alpha,\gamma^*)$ is a function of a single variable α. We find the derivative of $\tau(\alpha,\sin\alpha,\gamma^*)$ with respect to α. Let $\eta = \dfrac{d\tau(\alpha,\sin\alpha,\gamma^*)}{d\alpha}$. Then

$$\begin{aligned}\eta =& \frac{d}{d\alpha}A(\sin\alpha + \sin(\sin\alpha) - (\alpha+\sin\alpha+2\lambda)\cos\alpha) - B(\cos(\sin\alpha) - \cos\alpha)\\ =& A(\cos(\sin\alpha)\cos\alpha - \cos^2\alpha + (\alpha+\sin\alpha+2\lambda)\sin\alpha) + B(\sin(\sin\alpha)\cos\alpha - \sin\alpha).\end{aligned}$$

Let $\eta_1 = \cos\alpha(A(\cos(\sin\alpha) - \cos\alpha))$ and let $\eta_2 = A(\alpha + \sin\alpha + 2\lambda)\sin\alpha + B\sin(\sin\alpha)\cos\alpha - B\sin\alpha$. Thus $\eta = \eta_1 + \eta_2$. Note that $\eta_1 > 0$ when $0 \le \alpha < \pi/2$, $\eta_1 = 0$ when $\alpha = \pi/2$, and $\eta_1 < 0$ when $\pi/2 < \alpha \le \pi$. We wish to show that η_2 exhibits the same behaviour. To this end, we define the function:

$$\eta_2' = A(\alpha + \sin\alpha + 2\lambda)\sin\alpha + B\sin(1)\sin\alpha\cos\alpha - B\sin\alpha.$$

Lemma C.4. *The function $\eta_2' > 0$ for $0 \le \alpha < \pi/2$, $\eta_2' = 0$ when $\alpha = \pi/2$, and $\eta_2' < 0$ when $\pi/2 < \alpha \le \pi$.*

Proof. Let $\eta_3 = \dfrac{\eta_2'}{\sin\alpha} = A(\alpha + \sin\alpha + 2\lambda) + B\sin(1)\cos\alpha - B$. We take the second derivative of η_3 with respect to α.

$$\begin{aligned}\frac{d^2\eta_3}{d\alpha^2} &= \frac{d^2}{d\alpha^2}A(\alpha + \sin\alpha + 2\lambda) + B\sin(1)\cos\alpha - B\\ &= \frac{d}{d\alpha}A(1 + \cos\alpha) - B\sin(1)\sin\alpha)\\ &= -A\sin\alpha - B\sin(1)\cos\alpha.\end{aligned}$$

For $0 \le \alpha \le \pi/2$, $\dfrac{d^2\eta_3}{d\alpha^2} < 0$. For $\pi/2 < \alpha \le \pi$, the first term is increasing until it reaches 0 at $\alpha = \pi$. The second term becomes positive and increases until it's maximized at $\alpha = \pi$. Thus $\dfrac{d^2\eta_3}{d\alpha^2}$ is negative followed by positive, which implies that η_3 is concave followed by convex. At $\alpha = 0$ we have $A(\alpha + \sin\alpha + 2\lambda) + B\sin(1)\cos\alpha - B = 2A\lambda + B(\sin(1) - 1) > 0.28$ which is positive. At $\alpha = \pi$ we have $A(\pi + 2\lambda) - B(\sin(1) + 1) < -2.20$ which is negative. This, together with the fact that $\dfrac{d^2\eta_3}{d\alpha^2}$ is concave followed by convex implies that η_3 intersects the x-axis in only one place. We know $\sin\alpha = 0$ when $\alpha = 0$ and when $\alpha = \pi$, and $\sin\alpha > 0$ when $0 < \alpha < \pi$. Since $\eta_2' = \eta_3\sin\alpha$, $\eta_2' = 0$ when $\alpha = 0$ or π. Thus η_2' intersects the x-axis at 0, π, and one other place.

When $\alpha = \pi/2$, we have

$$\begin{aligned}\eta_2' &= A(\alpha + \sin\alpha + 2\lambda)\sin\alpha + B\sin(1)\sin\alpha\cos\alpha - B\sin\alpha\\ &= A(\pi/2 + 1 + 2\lambda) - B \qquad \text{(C.11)}\\ &= A\left(\pi/2 + 1 + 2\left(\frac{1+\sin(1)}{\cos(1)} - \pi/2 - 1\right)/2\right) - A\left(\frac{1+\sin(1)}{\cos(1)}\right)\\ &= A\left(\frac{1+\sin(1)}{\cos(1)}\right) - A\left(\frac{1+\sin(1)}{\cos(1)}\right)\\ &= 0.\end{aligned}$$

∎

Note that (C.11) is where we obtain the value for λ.

The function η_2' is η_2 with the term $\cos\alpha\sin(\sin\alpha)$ replaced by $\cos\alpha\sin(1)\sin\alpha$. To relate η_2' to η_2 we show the following:

Lemma C.5. $\cos\alpha\sin(1)\sin\alpha \le \cos\alpha\sin(\sin\alpha)$ *for* $0 \le \alpha \le \pi/2$, *and* $\cos\alpha\sin(1)\sin\alpha \ge \cos\alpha\sin(\sin\alpha)$ *for all* $\pi/2 < \alpha \le \pi$.

Proof. To prove the claim, let $\theta = \sin\alpha$. Since $\cos\alpha$ is positive for $0 \le \alpha < \pi/2$, and negative for $\pi/2 < \alpha \le \pi$, proving Lemma C.5 is equivalent to proving $\theta\sin(1) \le \sin\theta$, for all $0 \le \theta \le 1$. We note that $\theta\sin(1)$ is a linear function with a slope of $\sin(1)$, while $\sin\theta$ is a convex function in the given interval. They intersect at $\theta = 0$ and $\theta = 1$, and $\sin\theta$ contains $\theta\sin(1)$ from $0 \le \theta \le 1$. Thus $\theta\sin(1) \le \sin\theta$, for all $0 \le \theta \le 1$. ◻

As a consequence we get the following corollaries:

COROLLARY C.6. *$\eta_2' \le \eta_2$ for all $0 \le \alpha < \pi/2$ and $\eta_2' \ge \eta_2$ for all $\pi/2 < \alpha \le \pi$, and $\eta_2' = \eta_2$ for all $\alpha = \pi/2$*

which leads to

COROLLARY C.7. *The function $\eta_2 > 0$ when $0 \le \alpha < \pi/2$, $\eta_2 = 0$ when $\alpha = \pi/2$, and $\eta_2 < 0$ when $\pi/2 < \alpha \le \pi$.*

Note that $\eta_1 = 0$ when $\alpha = 0$ and $\pi/2$, is positive when $0 < \alpha < \pi/2$, and negative for $\pi/2 < \alpha \le \pi$. This implies that $\eta = 0$ when $\alpha = 0$ and $\pi/2$, is positive for $0 < \alpha < \pi/2$, and negative for $\pi/2 < \alpha \le \pi$. This implies that $\tau(\alpha, \sin\alpha, \gamma^*)$ is maximized when $\alpha = \pi/2$.

We can now prove Lemma C.3.

Proof of Lemma C.3. Corollary C.7 implies that $\tau(\alpha, \sin\alpha, \gamma^*)$ is maximized when $\alpha = \pi/2$. Thus

$$\tau(\alpha, \sin\alpha, \gamma^*) \le \tau(\pi/2, 1, \gamma^*) = \sqrt{1 - (1/\mu)^2}(1 + \sin(1)) - \left(\mu - \frac{1}{\mu}\right)\cos(1) \le 0 \tag{C.12}$$

for $\lambda = \left(\frac{1+\sin(1)}{\cos(1)} - \pi/2 - 1\right)/2 \approx 0.42$ and $\mu = \sqrt{\frac{2}{1-\sin(1)}} < 3.56$. ◻

C.3. Proofs of Lemmas 3.8 and 3.9. Recall that $\tau(\alpha, \beta, \gamma^*)$ is unimodal with respect to β (refer to Lemma C.2). We now simplify it further.

LEMMA C.8. *For $0 \le \beta \le \sin\alpha$, $\tau(\alpha, \beta, \gamma^*) \le \tau(\alpha, \sin\alpha, \gamma^*)$.*

Proof. Recall that

$$\frac{d\tau(\alpha, \beta, \gamma^*)}{d\beta} = A(\cos\beta - \cos\alpha) + B(\sin\beta). \tag{C.13}$$

◻

Note that $\dfrac{d\tau(\alpha, \beta, \gamma^*)}{d\beta} > 0$ when β is positive. Thus we have that $\tau(\alpha, \beta, \gamma) \le \tau(\alpha, \sin\alpha, \gamma^*)$.

In order to enumerate all the cases we need to consider to prove $\Phi(C_{i-1}, C_i) \le 0$, we distinguish between *starting conditions* and *events*. Given circles C_{i-1} and C_i, starting conditions refer to the locations of C_{i-1}, C_i, and *st* before applying Transformation 3.10. By extension, this includes the value of $y(t_{i-1})$ and the angles α, β, and γ. Recall that as we apply Transformation 3.10, we update α, β, γ, as well as the lengths of the arcs of C_{i-1} and the position of t_i. Thus an event refers to an angle entering, exiting, or staying within some range, or any other condition that occurs during the transformation.

C.3.1. Proof of Lemma 3.8. Lemma 3.8 assumes that $y(t_{i-1}) \leq 0$. Proving Lemma 3.8 is equivalent to proving the following two lemmas.

LEMMA C.9. *Consider any starting condition where C_{i-1} and C_i are such that $y(t_{i-1}) \leq 0$ and $0 \leq \alpha \leq \pi/2$. Then $\Phi(C_{i-1}, C_i) \leq 0$.*

LEMMA C.10. *Consider any starting condition where C_{i-1} and C_i are such that $y(t_{i-1}) \leq 0$ and $\pi/2 < \alpha \leq \pi$. Then $\Phi(C_{i-1}, C_i) \leq 0$.*

Observe that C_i and C_{i-1} being balanced implies the starting condition $y(t_i) < 0$, which implies that during Transformation 3.10, the event $\beta < 0$ does not occur. We need the following lemma to prove Lemma C.9.

LEMMA C.11. *Consider any starting condition where C_{i-1} and C_i are such that $\alpha \leq \pi/2$ and $\beta \leq \sin\alpha$. Then, during Transformation 3.10, $\beta \leq \sin\alpha$.*

Proof. Let v_i be the point on C_i where $|\mathcal{A}_i(p_{i-1}, v_i)| = |p_{i-1}q_i| + |\mathcal{B}_i(q_i, v_i)|$. We show that v_i does not go above st during Transformation 3.10, which implies the lemma.

Since c_{i-1} is on or below st, the slope of st is negative. Let e_i be the rightmost (East-most) point of C_i. Let $\beta' = \angle(v_i c_i e_i)$. During Transformation 3.10, since $\beta' r_i = |\mathcal{A}_i(e_i, v_i)| = |p_{i-1}q_i|/2$ is constant, but r_i is increasing and β' is decreasing ($\mathcal{A}_i(e_i, v_i)$ is getting flatter), v_i moves downwards. Since v_i is below c_i, v_i moves left as c_i moves left. Thus the path of v_i (from left to right) maintains a positive slope. Since st has a negative slope, and v_i intersects st initially (that is, $v_i = t_i$), this implies that v_i cannot go above st during Transformation 3.10. See Fig. C.7. $\square$

We can now prove Lemma C.9.

Proof of Lemma C.9. The proof follows from Lemmas C.11, C.3 and 3.11. $\square$

Note that, given the starting conditions of Lemma C.10, if the event $\beta > \sin\alpha$ does not occur, then Lemmas C.3 and 3.11 imply Lemma C.10. In the following lemma, we identify a starting condition for which $\beta > \sin\alpha$ never occurs during Transformation 3.10.

LEMMA C.12. *Let w_i be the leftmost (West-most) point of C_i. Consider any starting condition where C_{i-1} and C_i are such that $\alpha > \pi/2$, $\beta \leq \sin\alpha$ and st is on or above w_i. Then during Transformation 3.10, $\beta \leq \sin\alpha$.*

Proof. Note that $\beta = \sin\alpha$ if and only if $\beta r_i = r_i \sin\alpha = |p_{i-1}q_i|/2$. Since $|p_{i-1}q_i|/2$ stays constant during Transformation 3.10, and $\beta r_i \leq r_i \sin\alpha = |p_{i-1}q_i|/2$ before Transformation 3.10, it is enough to show that βr_i is decreasing during Transformation 3.10 while $\alpha > \pi/2$. If $\alpha \leq \pi/2$ during the transformation, we apply Lemma C.11. Let C_K be any intermediate circle through p_{i-1} and q_i during Transformation 3.10. Fixing t_i, if we increase γ, β on C_K will decrease. Thus the greatest value for β on C_K is when γ is minimized. Since we assume that w_i is on or below st, it is enough to show that βr_i is increasing during Transformation 3.10 when st is on w_i. Recall that

$$\frac{d\beta r_i}{dx(c_i)} = \frac{\cos\alpha \sin(\beta - \gamma) + \sin\gamma}{\cos(\beta - \gamma)} - \beta\cos\alpha. \tag{C.14}$$

Since $\alpha > \pi/2$ and $\beta > 0$, we have $-\beta\cos\alpha > 0$. Also recall that $-\pi/2 \leq \beta - \gamma \leq$

$\pi/2$, thus $\cos(\beta-\gamma) > 0$. Therefore to show that $\dfrac{d\beta r_i}{dx(c_i)}$ is non-negative, it is sufficient to show that $\sin\gamma \geq \sin(\beta-\gamma)$, or $\gamma \geq \beta/2$ (since $\gamma \leq \pi/2$). This is true when w_i is on or below st, as required. ∎

This leads to the following Corollary.

COROLLARY C.13. *Consider any starting condition where C_{i-1} and C_i are such that $\alpha > \pi/2$ and c_{i-1} is inside C_i. Then during Transformation 3.10, $\beta \leq \sin\alpha$.*

It remains to prove Lemma C.10 when the event $\beta > \sin\alpha$ occurs. Since C_{i-1} and C_i are balanced, one of the starting conditions is $\beta = \sin\alpha$. Recall that c_{i-1} is assumed to be on or below st. Corollary C.13 tells us we can assume c_{i-1} is outside of C_i. We look at two cases with the following starting conditions.

$\alpha > \pi/2, c_{i-1}$ is outside of C_i and $r_i \geq r_{i-1}$ (refer to Lemma C.14).

$\alpha > \pi/2, c_{i-1}$ is outside of C_i and $r_i < r_{i-1}$ (refer to Lemma C.15).

LEMMA C.14. *Consider any starting condition where C_{i-1} and C_i are such that $\alpha > \pi/2$, c_{i-1} is outside of C_i, and $r_i \geq r_{i-1}$. Then $\Phi(C_{i-1}, C_i) \leq 0$.*

Proof. See Fig. C.8. Let C_Q be a circle through p_{i-1} and q_i with radius $r_Q = |p_{i-1}q_i|/2$. First we show that s_Q is between s_{i-1} and s_i on st. Let u_i be the intersection of C_i and the line through t_i and c_i, where $u_i \neq t_i$. Lemma 3.7 tells us that s_Q is between s_{i-1} and s_i on st, if u_k and u_i are left of $p_{i-1}q_i$, which is true if $|y(t_Q)| \leq y(p_{i-1})$ and $|y(t_i)| \leq y(p_{i-1})$. Since c_{i-1} is on or below st, the slope of st is negative, and since $y(t_{i-1}) \leq 0$, we have $|y(t_Q)| < |y(t_i)|$. We have $y(p_{i-1}) = r_i \sin\alpha$, and $|y(t_i)| = r_i \sin(\sin\alpha) \leq r_i \sin\alpha = y(p_{i-1})$ when $\alpha \leq \pi/2$, and thus s_Q is between s_{i-1} and s_i on st.

Thus we have $\Phi(C_{i-1}, C_i) = \Phi(C_{i-1}, C_Q) + \Phi(C_Q, C_i)$, and it is sufficient to prove that $\Phi(C_{i-1}, C_Q) \leq 0$ and $\Phi(C_Q, C_i) \leq 0$.

If st is below c_Q, then $\Phi(C_Q, C_i)$ is increased when st goes through c_Q, so we assume that c_Q is on or below st. We apply Transformation 3.10 to C_i and C_Q. Since $y(t_{i-1}) \leq 0$, and $y(t_i) \leq 0$, we have $y(t_Q) \leq 0$, and thus $\beta \geq 0$ during Transformation 3.10. Since c_Q is inside C_i, Corollary C.13 tells us that $\beta \leq \sin\alpha$ during Transformation 3.10. Together with the fact that $\tau(\alpha, \beta, \gamma) \leq 0$ when $0 \leq \beta \leq \sin\alpha$, this implies that $\Phi(C_Q, C_i) \leq 0$ by Lemma 3.11.

We now apply Transformation 3.10 to C_{i-1} and C_Q. Since $\alpha = \pi/2$ before Transformation 3.10, Lemma C.11 tells us that $\beta \leq \sin\alpha$ during Transformation 3.10 if $\beta \leq \sin\alpha$ initially. Proving that initially we have $\beta \leq \sin\alpha$ is equivalent to proving that t_Q is above v_Q, or equivalently, that v_Q is below st.

Let C_K be a circle through p_{i-1} and q_i such that t_K is between t_{i-1} and t_i. Notice that C_K is any intermediate circle encountered during Transformation 3.10. If we fix t_i, then β is maximized on C_K when γ is minimized. Since we assume c_{i-1} is on or below st, we conclude γ is minimized when st intersects c_{i-1}. To minimize γ further we move c_{i-1} as far left as it can go, i.e., to the point where $r_i = r_{i-1}$. Thus it is sufficient to show v_Q is below st when $r_i = r_{i-1}$.

Let p'_{i-1} and q'_i be the points on C_i that mirror p_{i-1} and q_i in the vertical line through c_i. Note that the line segment $c_{i-1}q'_i$ is below the line segment $c_{i-1}t_i$, which is part of st. Thus, showing that v_Q is below $c_{i-1}q'_i$ shows that v_Q is below st.

We begin by showing that if v_Q is below $c_{i-1}q'_i$ when $r_i = r_{i-1}$ and c_{i-1} intersects C_i, then v_Q is below $c_{i-1}q'_i$ for any c_{i-1} outside of C_i where $r_i = r_{i-1}$.

See Fig. C.9. Note that $x(q_i) - x(c_{i-1}) = x(c_i) - x(q_i) = x(q'_i) - x(c_i)$, thus $2(x(q_i) - x(c_{i-1})) = x(q'_i) - x(q_i)$. Thus one third of $c_{i-1}q'_i$ is to the left of $p_{i-1}q_i$, while two thirds of $c_{i-1}q'_i$ is to the right. Since $y(c_{i-1})$ and $y(q'_i)$ are constant, this implies that as $c_{i-1}q'_i$ grows it pivots at the intersection of itself and $p_{i-1}q_i$. Thus v_Q being under $c_{i-1}q'_i$ when c_{i-1} and C_i intersect implies that it is always under $c_{i-1}q'_i$. Thus it is enough to show that v_Q is under $c_{i-1}q'_i$ when c_{i-1} intersects C_i.

See Figs. C.10 and C.11. Assume that $r_i = r_{i-1} = 1$, which implies that $r_Q = \sin(\pi/3)$, and $|c_{i-1}c_Q| = 1/2$. Note that when Transformation 3.10 gets to [2]C_Q, we have $\alpha = \pi/2$, thus we need to prove that $\beta \leq \sin\alpha = 1$. Let t'_Q be the intersection of $c_{i-1}q'_i$ and C_Q. Since $c_{i-1}q'_i$ lies under st, and $\angle(t'_Q c_Q c_i) > \beta$, it is sufficient to show that $\angle(t'_Q c_Q c_i) < 1$.

Let $\theta = \angle(c_Q t'_Q c_{i-1})$, and note that $\angle(q'_i c_{i-1} c_Q) = \pi/6$. We can find θ using the sine rule. Thus $\sin\theta = \dfrac{\sin(\pi/6)}{2\sin(\pi/3)}$, and $\theta < 0.3$. We see that $\angle(t'_Q c_Q c_i) = \theta + \pi/6 < 0.82 < 1$, as required.

LEMMA C.15. *If $r_i < r_{i-1}$, $\alpha > \pi/2$ and c_{i-1} is outside of C_i, then $\Phi(C_{i-1}, C_i) \leq 0$.*

Proof. Let C_P be the circle with radius r_i through p_{i-1} and q_i such that $C_P \neq C_i$. Notice that C_P is one of the intermediate circles encountered during Transformation 3.10. See Fig. C.12. We have $\Phi(C_{i-1}, C_i) = \Phi(C_{i-1}, C_P) + \Phi(C_P, C_i)$, and thus it is sufficient to prove that $\Phi(C_{i-1}, C_P) \leq 0$ and $\Phi(C_P, C_i) \leq 0$. We do this by applying Transformation 3.10 to C_i and C_P, and then to C_P and C_{i-1}.

Since $r_P = r_i$, we have $\Phi(C_P, C_i) \leq 0$ by Lemma C.14. Since we assumed that c_{i-1} is on or below st, we know that st has a negative slope. Thus $y(t_P) > y(t_i)$, which implies that [2]β as defined by C_P is less than β as defined by C_i. Thus when applying Transformation 3.10 to C_P and C_{i-1}, we know that $0 \leq \beta < \sin\alpha$ by Lemma C.11, and thus $\Phi(C_{i-1}, C_P) \leq 0$ by Lemma 3.11. ∎

Proof of Lemma C.10. The proof follows from Lemmas C.14 and C.15. ∎

C.3.2. Proof of Lemma 3.9. First observe the following.

LEMMA C.16. *For $0 \leq \alpha \leq \pi/2$, $\tau(\alpha, -\alpha, \gamma^*) \leq 0$.*

Proof.

$$\begin{aligned}\tau(\alpha, -\alpha, \gamma^*) &= A(\sin\alpha + \sin(-\alpha) - (\alpha - \alpha + 2\lambda)\cos\alpha) - B(\cos(-\alpha) - \cos\alpha) \\ &= -2\lambda\cos\alpha \\ &\leq 0.\end{aligned}$$
∎

We now break Lemma 3.9 into the two lemmas.

LEMMA C.17. *Consider any starting condition where C_{i-1} and C_i are such that $y(t_{i-1}) > 0$ and $0 \leq \alpha \leq \pi/2$. Then $\Phi(C_{i-1}, C_i) \leq 0$.*

[2]Recall that, as we apply Transformation 3.10, we update the values of α, β, and γ.

Proof. We know $\tau(\alpha, \beta, \gamma^*)$ is unimodal with respect to β by Lemma C.2. The starting condition $0 \le \alpha \le \pi/2$ together with Lemma C.11 imply that $-\alpha \le \beta \le \sin\alpha$. Thus the proof follows from Lemmas C.16, C.3, and 3.11. ∎

We are thus left to prove the following lemma in order to prove Lemma C.10. Note that in this case, instead of working on $\tau(\alpha, \beta, \gamma^*)$, we use a geometric proof.

LEMMA C.18. *Consider any starting condition where C_{i-1} and C_i are such that $y(t_{i-1}) > 0$ and $\pi/2 < \alpha \le \pi$. Then $\Phi(C_{i-1}, C_i) \le 0$.*

Proof. If c_{i-1} is left of $p_{i-1}q_i$, then let C_Q be a circle through p_{i-1} and q_i with diameter $|p_{i-1}b_i|$. Otherwise let $C_Q = C_{i-1}$. We will show that $\Phi(C_{i-1}, C_i) \le \Phi(C_{i-1}, C_Q) + \Phi(C_Q, C_i) \le 0$.

Note that since t_{i-1} is inside C_i, and $y(t_{i-1}) > 0$, Lemma C.12 implies that β as defined by C_Q[3] is less than $\sin\alpha$, where α as defined by C_Q is $\pi/2$. Lemma C.12 implies the event $\beta \le \sin\alpha$. This implies that $\Phi(C_{i-1}, C_Q) \le 0$ by Lemmas C.3, C.16 and 3.11. Thus we need only show that $\Phi(C_Q, C_i) \le 0$. Note that if $y(t_Q) \le 0$, then $\Phi(C_Q, C_i) \le 0$ by Lemma 3.8. Thus we assume that $y(t_Q) > 0$.

To show $\Phi(C_Q, C_i) \le 0$ in this case we will show three inequalities.

$$|\mathcal{A}_i(p_{i-1}, t_i)| \le \pi/2|p_{i-1}t_i|, \tag{C.15}$$

$$|\mathcal{A}_Q(p_{i-1}, t_Q)| + \mu|t_Q t_i| \ge \frac{\mu\sin(1) + 1}{\sin(1) + 1}|p_{i-1}t_i|, \tag{C.16}$$

$$2(r_i - r_Q) \le |p_{i-1}t_i|. \tag{C.17}$$

See Fig. C.13. Assuming (C.15), (C.16), and (C.17) are true, we substitute these values into $\Phi(C_Q, C_i)$ and get

$$\begin{aligned}
\Phi(C_Q, C_i) &= |\mathcal{A}_i(p_{i-1}, t_i)| - |\mathcal{A}_Q(p_{i-1}, t_Q)| - 2\lambda(r_Q - r_i) - \mu|t_Q t_i| \\
&\le \left(\pi/2 + 1 + \lambda - \frac{(\mu - 1)\sin(1)}{\sin(1) + 1}\right)|p_{i-1}t_i| \\
&\le \left(\pi/2 + \lambda - \frac{\mu\sin(1) + 1}{\sin(1) + 1}\right)|p_{i-1}t_i| \\
&\le (2 - 2.16)|p_{i-1}t_i| \\
&\le 0.
\end{aligned}$$

Inequality (C.15) is satisfied whenever $|\mathcal{A}_i(p_{i-1}, t_i)| = |p_{i-1}q_i| + |\mathcal{B}_i(q_i, t_i)|$, which is always the case initially when C_{i-1} and C_i are balanced.

For inequality (C.16), note that $|\mathcal{A}_Q(p_{i-1}, t_Q)| \ge |p_{i-1}t_Q|$, and $|p_{i-1}t_Q| + |t_Q t_i| \ge |p_{i-1}t_i|$ by the triangle inequality. Thus it remains to show that $|t_Q t_i| \ge |p_{i-1}t_i|\frac{sin(1)}{sin(1)+1}$.

Recall that $y(t_Q) > 0$. If we increase $y(t_Q)$, observe that $|t_Q t_i|$ also increases. Notice that the minimum value of $|t_Q t_i|$ is when t_Q corresponds to the intersection of st and the x-axis. Thus for the minimum value of $|t_Q t_i|$, we will assume that $y(t_Q) = 0$.

Recall that l_i is the leftmost intersection of C_i and st, and e_i is the rightmost point of C_i. If $|y(t_i)| \ge |y(l_i)|$, then $y(t_Q) = 0$ implies that $|t_Q t_i| \ge r_i \ge |p_{i-1}t_i|/2 \ge$

[3] Recall that, as we apply Transformation 3.10, we update the values of α, β, and γ.

$|p_{i-1}t_i|\frac{sin(1)}{sin(1)+1}$ as required. So assume that $|y(t_i)| < |y(l_i)|$, which implies that c_i is below st, and thus below l_it_i, which is a segment of st. Observe that since p_{i-1} is a vertex, it is above st. Since c_i is below l_it_i, but $p_{i-1}t_i$ is above l_it_i, this implies that $|l_it_i| \geq |p_{i-1}t_i|$. This means that it is sufficient to prove $|t_Qt_i| \geq |l_it_i|\frac{sin(1)}{sin(1)+1}$. Note that $|t_Qt_i|$ is the part of $|l_it_i|$ below the x-axis. Thus $|t_Qt_i|/|l_it_i| = |y(t_i)|/(|y(l_i)| + |y(t_i)|)$. This expression is minimized when $|y(t_i)|/|y(l_i)|$ is smallest. Also $|y(l_i)|$ is largest when $l_i = p_{i-1}$. Note that $|y(p_{i-1})| = r_i \sin\alpha$, and that $|y(t_i)| = r_i \sin(\sin\alpha)$. Thus $|y(t_i)|/|y(l_i)| = \sin(\sin\alpha)/\sin\alpha$, which is minimized when $\alpha = \pi/2$. This implies that $|y(t_i)|/(|y(l_i)| + |y(t_i)|) = |t_Qt_i|/|l_it_i| \geq \sin(1)/(\sin(\pi/2) + \sin(1)) = \sin(1)/(\sin(1) + 1)$. Thus $|t_Qt_i| \geq |l_it_i|\frac{\sin(1)}{\sin(1)+1} \geq |p_{i-1}t_i|\frac{\sin(1)}{\sin(1)+1}$ as required.

Let us now prove (C.17). Observe that c_i is right of $|p_{i-1}q_i|$, which is right of $|p_{i-1}w_i|$. Together with the fact that $|p_{i-1}q_i|$ and $|p_{i-1}w_i|$ are both chords of C_i, then $|p_{i-1}w_i| < |p_{i-1}q_i|$. Moreover, c_i is below $p_{i-1}t_i$, which is below $p_{i-1}e_i$. Together with the fact that $|p_{i-1}t_i|$ and $|p_{i-1}e_i|$ are both chords of C_i, then $|p_{i-1}e_i| \leq |p_{i-1}t_i|$. Finally, since p_{i-1} and q_i both lie on C_Q, then $|p_{i-1}q_i| \leq 2r_Q$. Thus we have

$$\begin{aligned}
2r_i &= |w_ie_i| \\
&\leq |p_{i-1}e_i| + |p_{i-1}w_i| && \text{by the triangle inequality,} \\
&\leq |p_{i-1}e_i| + |p_{i-1}q_i| \\
&\leq |p_{i-1}t_i| + 2r_Q, && \square
\end{aligned}$$

from which we have $2(r_i - r_Q) \leq |p_{i-1}t_i|$, as required.

Appendix D. Analysis of $MinArc$ algorithm.

THEOREM D.1. *MinArc routing algorithm on the Delaunay triangulation has a routing ratio of at most* $(\delta + \pi) \approx 3.952$*, with* $\delta = 0.8105$.

The bound on the routing ratio is close to the actual bound, as we show in Section D.3 and illustrate in Fig. D.1, our algorithm has a routing ratio of at least 3.2 in the worst case.

We devote this section to the proof of Theorem D.1. We start by introducing additional definitions, notations, and structural results. Some of the notations are illustrated in Figure D.3.

Given a path $\mathcal{P}$ from p to q and a path $\mathcal{Q}$ from q to r, $\mathcal{P} + \mathcal{Q}$ denotes the concatenation of $\mathcal{P}$ and $\mathcal{Q}$. We say that the path $\mathcal{P}$ from p to q is *inside* a path $\mathcal{Q}$ that also goes from p to q if the path $\mathcal{P}$ is inside the bounded region delimited by $\mathcal{Q} + qp$. Given a path $\mathcal{P}$ and two points p and q on $\mathcal{P}$, we denote by $\mathcal{P}(p, q)$ the sub-path of $\mathcal{P}$ that goes from p to q.

In order to bound the length of $\mathcal{P}\langle s, t\rangle$, we need to define the *potential paths* and and *snail curve* as follows.

Given two points p and q such that $x(p) < x(q)$ and $y(p) = y(q)$, we define the path $\mathcal{S}_{p,q}$ as follows. Let C_a be the circle of center q that goes through p and let p' be the top point of C_a. Let C_b be the circle of diameter qp'. The path $\mathcal{S}_{p,q}$ consists of the clockwise arc of C_a from p to p' together with the clockwise arc of C_2 from p' to q. We call $\mathcal{S}_{p,q}$ the *snail curve* from p to q (see Figure D.2). Note that $|\mathcal{S}_{p,q}| = \pi(x(q) - x(p))$. Let $\overline{\mathcal{S}}_{p,q}$ be the symmetric of $\mathcal{S}_{p,q}$ with respect to the line pq.

The *potential path* $\mathcal{D'}_i$, for $i = 0, 1, \ldots, n-1$, is defined as follows. Given t_i the rightmost point on st of C_{i+1}, there is a unique point of st s_i such that p_i is on the snail curve $\mathcal{S}_{s_i,t_{i+1}}$ or $\overline{\mathcal{S}}_{s_i,t_{i+1}}$ (depending on whether or not p_i lies above st). The *potential path* $\mathcal{D'}_i$ is the sub-path of this curve from s_i to p_i.

Let f_i be the first point p_j after p_i such that p_ip_j intersects st. Notice that $f_{n-1} = t$. We also set $f_n = t$. In Fig. D.3, $f_0 = p_1$, $f_1 = p_2$, $f_2 = p_3$ and $f_3 = f_4 = f_5 = t$.

LEMMA D.2. *For all* $0 < i \leq n$*:*

$$x(s) \leq x(t_{i-1}) \leq x(t_i) \leq x(t), \tag{D.1}$$

$$x(s_{i-1}) \leq x(s_i) \leq x(f_{i-1}) \leq x(f_i). \tag{D.2}$$

Proof. The proof of Lemma 3.5 extends to our case since we consider the rightmost triangle intersecting st and thus proves (D.1).

Now let us prove Equation (D.2). The point s_i only depends on p_i and t_{i+1}. For a fix p_i, moving t_{i+1} leftward will also move s_i leftward: if $x(p_i) \geq x(t_{i+1})$, moving slightly the snail curve leftward will leave p_i outside the snail shape so the snail curve needs to be larger to go through p_i; if $x(p_i) < x(t_{i+1})$, s_i and p_i are on the same circle centered at t_{i+1} and moving slightly this center leftward will also move the intersection of the corresponding circle with st, which is s_i leftward. So, to prove that $x(s_{i-1}) \leq x(s_i)$, we only need to prove it in the extreme case where $t_{i+1} = t_i$. So now let us consider this case in which $C_i = C_{i+1}$.

Let the closed curve $\mathcal{D}$ be $\mathcal{S}_{s_i,t_{i+1}} \cup \overline{\mathcal{S}}_{s_i,t_{i+1}}$. By definition, C_{i+1} intersects $\mathcal{D}$ at p_i. This implies that its diameter is larger than $|s_it_{i+1}|$. Moreover as t_{i+1} is the rightmost intersection of C_i with st, the center c_i of C_i is such that $x(c_i) \leq x(t_{i+1})$. Altogether this implies that C_i intersects $\mathcal{D}$ twice and the point $\overline{r}_i$ that is diametrically opposed to t_{i+1} on C_i is outside $\mathcal{D}$ (see Figure D.4). Since the points $\overline{r}_i, p_{i-1}, p_i, t_{i+1}$ appear in that order moving clockwise or counterclockwise around C_i, the point p_{i-1} lies outside the bounded region delimited by $\mathcal{D}$. Hence the snail curve going through $t_i = t_{i+1}$ and p_{i-1} must be bigger than then one going through p_i. Hence $x(s_{i-1}) < x(s_i)$.

We now prove the second inequality in (D.2). We first observe that $f_{i-1} = p_j$ and $f_i = p_{j'}$ for some $i \leq j \leq j'$. Using the first inequality, we have that $x(t_{i+1}) \leq x(t_{j+1}) \leq x(p_j) = x(f_{i-1})$, so the second inequality in (D.2) holds.

The third inequality in (D.2) trivially holds when $j = j'$, so we assume otherwise. In that case, $i = j$, $p_j, p_{j+1}, \ldots, p_{j'-1}$ are all on the same side of st, and p_{j-1} and $p_{j'}$ are on the other side. Without loss of generality, we assume that $p_{j'}$ lies above st.

This implies that p_j lies below st and on $\mathcal{D'}_{j-1}$, which is also of type B, and

$$x(p_j) \leq x(t_j) \leq x(t_{j+1}). \tag{D.3}$$

Observe that if for some i, $x(p_i) \leq x(p_{i-1})$, then $x(t_i) \leq x(p_i)$. Hence for any i, $x(p_i) \geq \min(x(t_i), x(p_{i-1}))$. Applying iteratively this last inequality, we get

$$\min(x(p_j), x(t_{j+1})) \leq x(p_{j'-1}). \tag{D.4}$$

Since, $p_{j'-1}p_{j'}$ crosses st, $\mathcal{D'}_{j'-1}$ is of type B and $p_{j'-1}p_{j'}$ has positive slope, hence

$$x(p_{j'-1}) \leq x(p_{j'}). \tag{D.5}$$

□

Combining (D.3), (D.4) and (D.5) we get $x(f_{i-1}) = x(p_j) < x(p_{j'-1}) < x(p_{j'}) = x(f_i)$ and (D.2) holds.

D.1. Proof of Theorem D.1. In this section, we introduce a key lemma and use it to prove our main theorem.

Let $\overline{f}_i = (x(f_i), 0)$ be the orthogonal projections of points f_i onto st. Finally, we define the path $\mathcal{D}'_i$ to be the arc of $\mathcal{S}_{s_i,t_{i+1}}$ from s_i to p_i, for $0 \le i \le n-1$ (see Fig. D.3).

We start with a simple lemma on the last step of the routing algorithm to motivate these definitions.

Lemma D.3. $|p_{n-1}t| \le |\mathcal{S}_{s_{n-1},t}| - |\mathcal{D}'_{n-1}|$.

Proof. This follows from the fact that path $\mathcal{D}'_{n-1} + p_{n-1}t$ from s_{n-1} to t is convex and inside $\mathcal{S}_{s_{n-1},t}$. ∎

Let $\overline{p}_i$ the projection of p_i on the x-axis.

The following lemma is the key to proving Theorem D.1.

Lemma D.4. *For all* $0 < i < n$ *and* $\delta = 0.8105$,

$$\text{(D.6)} \quad |p_{i-1}, p_i| \le |\mathcal{D}'_i| - |\mathcal{D}'_{i-1}| + |\mathcal{S}_{s_{i-1},s_i}| + |y(f_i)| + \max(0, |y(f_i)| - \delta|\overline{p}_i\overline{f}_i|) - |y(f_{i-1})| - \max(0, |y(f_{i-1})| - \delta|\overline{p}_{i-1}\overline{f}_{i-1}|) + \delta|\overline{f}_{i-1}\overline{f}_i|.$$

This lemma is illustrated in Fig. D.3. We first show how to use Lemma D.4 to prove Theorem D.1, and then we prove Lemma D.4.

Proof of Theorem D.1. By Lemma D.2, $\sum_{i=1}^{n-1} |\overline{f}_{i-1}\overline{f}_i| < |st|$ and $\sum_{i=1}^{n} |\mathcal{S}_{s_{i-1},s_i}| = |\mathcal{S}_{s,t}|$. Therefore, by summing the $n-1$ inequalities from Lemma D.4 and the inequality from Lemma D.3, we get

$$\begin{aligned} |\mathcal{P}\langle s,t\rangle| &\le \sum_{i=1}^{n} |p_{i-1}p_i| \\ &< -|\mathcal{D}'_0| + |\mathcal{S}_{s,t}| + |y(f_{n-1})| + \max(0, |y(f_{n-1})| - \delta|\overline{p}_{n-1}\overline{f}_{n-1}|) \\ &\quad -|y(f_0)| - \max(0, |y(f_0)| - \delta|\overline{p}_0\overline{f}_0|) + \delta|st|. \end{aligned}$$

Since $f_0 = s$ and $f_{n-1} = t$, we have $y(f_0) = y(f_{n-1}) = 0$ and it follows that

$$|\mathcal{P}\langle s,t\rangle| < |\mathcal{S}_{s,t}| + \delta|st| \le (\pi + \delta)|st|,$$

which completes the proof. ∎

D.2. Proof of the Key Lemma. We categorize the potential paths $\mathcal{D}'_i$ into two types:

- Type A: p_ip_{i+1} does not cross st.
- Type B: p_ip_{i+1} crosses st.

Proof of Lemma D.4. We consider three cases depending on the types of potential $\mathcal{D}'_{i-1}$ and $\mathcal{D}'_i$. Note that if $\mathcal{D}'_{i-1}$ is of type A, then $f_{i-1} = f_i$. Hence, in this case, it is sufficient to prove

$$|p_{i-1}p_i| \le |\mathcal{D}'_i| - |\mathcal{D}'_{i-1}| + |\mathcal{S}_{s_{i-1},s_i}|$$

or equivalently

$$|\mathcal{D}'_{i-1} + p_{i-1}p_i| \leq |\mathcal{S}_{s_{i-1},s_i} + \mathcal{D}'_i|. \tag{D.7}$$

In Figure D.7, the left-hand side of Equation (D.7) is represented by a blue curve and the right-hand side by a green curve. Before proving the different cases, we will show that $|\mathcal{S}_{s_{i-1},s_i} + \mathcal{D}'_i|$ is minimized when $t_{i+1} = t_i$ (as represented by the green curves in Figs. D.7 and D.8). To prove this we require the following geometric lemma.

Lemma D.5. *Let C be a circle with center c and points p and t on the boundary. If p, t and c lie on a line we perturb p slightly so that they do not. Let $\mathcal{A}\langle p, t\rangle$ be the arc from p to t on C with central angle $2\alpha < \pi$. Then $|\mathcal{A}\langle p, t\rangle| = |pt|\frac{\alpha}{\sin\alpha}$.*

Proof. Let r be the radius of C. Then $|\mathcal{A}\langle p, t\rangle| = r2\alpha$. Observe that $|pt| = r2\sin\alpha$, thus $r = \frac{|pt|}{2\sin\alpha}$. Substituting for r we have $|\mathcal{A}\langle p, t\rangle| = |pt|\frac{\alpha}{\sin\alpha}$, as required. ∎

Lemma D.6. *$|\mathcal{S}_{s_{i-1},s_i} + \mathcal{D}'_i|$ is minimized when $t_{i+1} = t_i$.*

Proof. We will fix s, t, t_i, and p_i, and allow t_{i+1} to move along st between t_i and t while observing the changes in $|\mathcal{S}_{s_{i-1},s_i} + \mathcal{D}'_i|$. Let $\beta = tt_ip_i$ and $\alpha = \angle tt_{i+1}p_i$. Since t, t_i and p_i are fixed, β remains constant. Observe that as we move t_{i+1} to the right, α increases. Thus $\beta \leq \alpha \leq \pi$. We will express $|\mathcal{S}_{s_{i-1},s_i} + \mathcal{D}'_i|$ in terms of β and α and find the derivative with respect to α.

Observe that $|\mathcal{S}_{s_{i-1},s_i} + \mathcal{D}'_i| = |\mathcal{S}_{s_{i-1},s_i} + \mathcal{S}_{s_i,t_{i+1}} - \mathcal{S}_{s_i,t_{i+1}}(p_i, t_{i+1})| = |\mathcal{S}_{s_{i-1},t_{i+1}}| - |\mathcal{S}_{s_i,t_{i+1}}(p_i, t_{i+1})|$, where $\mathcal{S}_{s_i,t_{i+1}}(p_i, t_{i+1})$ is the arc of $\mathcal{S}_{s_i,t_{i+1}}$ from p_i to t_{i+1}. We will first develop an expression for $|\mathcal{S}_{s_{i-1},t_{i+1}}|$. Let $\overline{p}_i$ be the orthogonal projection of p_i onto st.

$$\begin{aligned}
|\mathcal{S}_{s_{i-1},t_{i+1}}| &= \pi|s_{i-1}, t_{i+1}| \\
&= \pi\left(|s_{i-1}t_i| + |t_i\overline{p}_i| - |t_{i+1}\overline{p}_i|\right) \\
&= \pi\left(|s_{i-1}t_i| + \frac{y(p_i)}{\tan\beta} - \frac{y(p_i)}{\tan\alpha}\right).
\end{aligned}$$

Since $\mathcal{S}_{s_i,t_{i+1}}$ is composed of two arcs with different radii, we will have two expressions for $|\mathcal{S}_{s_i,t_{i+1}}(p_i, t_{i+1})|$, one for when $0 \leq \alpha \leq \pi/2$ and one for when $\pi/2 < \alpha \leq \pi$. Using Lemma D.5 and the fact that $|p_it_i| = \frac{y(p_i)}{\sin\alpha}$, when $0 \leq \alpha \leq \pi/2$ we have

$$\begin{aligned}
|\mathcal{S}_{s_i,t_{i+1}}(p_i, t_{i+1})| &= |p_it_i|\frac{\alpha}{\sin\alpha} \\
&= y(p_i)\frac{\alpha}{\sin^2\alpha}.
\end{aligned}$$

Let $M(\alpha)$ be $|\mathcal{S}_{s_i,t_i}| + |\mathcal{S}_{t_i,\overline{p_i}}| - |\mathcal{S}_{t_{i+1},\overline{p}_i}| - |\mathcal{S}_{s_i,t_{i+1}}(p_i, t_{i+1})|$ expressed in terms of α. Since s, t, and p_i are fixed, let $y(p_i) = 1$. Then for $0 \leq \alpha \leq \pi/2$, we have

$$\begin{aligned}
M(\alpha) &= |\mathcal{S}_{s_i,t_i}| + |\mathcal{S}_{t_i,\overline{p_i}}| - |\mathcal{S}_{t_{i+1},\overline{p}_i}| - |\mathcal{S}_{s_i,t_{i+1}}(p_i, t_{i+1})| \\
&= \pi|s_it_i| + \frac{\pi}{\tan\beta} - \frac{\pi}{\tan\alpha} - \frac{\alpha}{\sin^2\alpha}.
\end{aligned}$$

When $\pi/2 < \alpha \le \pi$ observe that $|\mathcal{S}_{s_i,t_{i+1}}(p_i,t_{i+1})| = \alpha|p_i t_{i+1}|$, and $|p_i t_{i+1}| = \frac{y(p_i)}{\sin\alpha} = \frac{1}{\sin\alpha}$. Thus $|\mathcal{S}_{s_i,t_{i+1}}(p_i,t_{i+1})| = \frac{\alpha}{\sin\alpha}$, and we have

$$\begin{aligned} M(\alpha) &= |\mathcal{S}_{s_i,t_i}| + |\mathcal{S}_{t_i,\overline{p_i}}| - |\mathcal{S}_{t_{i+1},\overline{p}_i}| - |\mathcal{S}_{s_i,t_{i+1}}(p_i,t_{i+1})| \\ &= \pi|s_i t_i| + \frac{\pi}{\tan\beta} - \frac{\pi}{\tan\alpha} - \frac{\alpha}{\sin\alpha}. \end{aligned}$$

We now wish to calculate $\frac{dM(\alpha)}{d\alpha}$. For $0 \le \alpha \le \pi/2$ we have

$$\frac{dM(\alpha)}{d\alpha} = \frac{(\pi-1)\sin\alpha + 2\alpha\cos\alpha}{\sin^3\alpha}$$

which is positive in the range $0 \le \alpha \le \pi/2$. When $\pi/2 < \alpha \le \pi$ we have

$$\begin{aligned} \frac{dM(\alpha)}{d\alpha} &= \frac{d}{d\alpha}\left(-\frac{\pi}{\tan\alpha} - \frac{\alpha}{\sin\alpha}\right) \\ &= \frac{\pi - \sin\alpha + \alpha\cos\alpha}{\sin^2\alpha}. \end{aligned} \tag{D.8}$$

We wish to show that (D.8) is non-negative for $\pi/2 < \alpha \le \pi$. Since $\sin^2\alpha$ is clearly non-negative, we are left to determine the sign of $\pi - \sin\alpha + \alpha\cos\alpha$. Observe that

$$\begin{aligned} &\frac{d}{d\alpha}\pi - \sin\alpha + \alpha\cos\alpha \\ =& -\cos\alpha + \cos\alpha - \alpha\sin\alpha \\ =& -\alpha\sin\alpha \\ \le& 0. \end{aligned}$$

This implies that (D.8) is minimized when $\alpha = \pi$, at which point $\frac{\pi-\sin\alpha+\alpha\cos\alpha}{\sin^2\alpha} = 0$. Thus $\frac{dM(\alpha)}{d\alpha}$ is non-negative, meaning that $M(\alpha)$ increases with α, implying that it is minimized when $\alpha = \beta$, or when $t_i = t_{i+1}$, as required. ∎

Case 1: $\mathcal{D}'_{i-1}$ is of type A. To show that Equation (D.7) holds, Lemma D.6 implies we only need to consider the case where $t_{i+1} = t_i$ (see Figure D.8). We will show this inequality for $t_{i+1} = t_i$ in the first two cases of the proof.

Adding $\mathcal{Q} := \mathcal{S}_{s_i,t_{i+1}}(p_i,t_{i+1})$ on both sides of inequality (D.7) becomes:

$$|\mathcal{D}'_{i-1} + p_{i-1}p_i + \mathcal{Q}| \le |\mathcal{S}_{s_{i-1},s_i} + \mathcal{S}_{s_i,t_{i+1}}| = |\mathcal{S}_{s_{i-1},t_{i+1}}|. \tag{D.9}$$

Observe that $p_{i-1}p_i$ is inside $p_iA + \mathcal{S}_{s_{i-1},t_{i+1}}(A,p_i)$, hence

$$|p_{i-1}p_i| \le |p_iA + \mathcal{S}_{s_{i-1},t_{i+1}}(A,p_i)|. \tag{D.10}$$

By Observing that $\mathcal{Q}$ and $\mathcal{S}_{s_{i-1},t_{i+1}}(t_{i+1},A)$ are homothetic and that p_iA is shorter than an curve homothetic to $\mathcal{Q}$ going from p_i to A we get

$$|\mathcal{Q} + p_iA| < |\mathcal{S}_{s_{i-1},t_{i+1}}(t_{i+1},A)|. \tag{D.11}$$

From (D.10) we get:

$$|\mathcal{D}'_{i-1} + p_{i-1}p_i + \mathcal{Q}| \leq |\mathcal{D}'_{i-1} + p_iA| + \mathcal{S}_{s_{i-1},t_{i+1}}(A,p_i) + \mathcal{Q}|.$$

From (D.11) we get: $|\mathcal{Q} + p_iA + \mathcal{S}_{s_{i-1},t_{i+1}}(A,p_i) + \mathcal{D}'_{i-1}| \leq |\mathcal{S}_{s_{i-1},t_{i+1}}(t_{i+1},A) + \mathcal{S}_{s_{i-1},t_{i+1}}(A,p_i) + \mathcal{D}'_{i-1}| = |\mathcal{S}_{s_{i-1},t_{i+1}}|$.

The combination of the two last inequality proves (D.9) and thus this lemma for Case 1.

Case 2: $\mathcal{D}'_{i-1}$ is of type B and $\mathcal{D}'_i$ is of type A or B.

In this case, the "potential" may not be enough to cope with zig-zags. As in the [2], the δ coefficient of Equation (D.6) is introduced in order to repair this case.

In this context, let us rewrite Equation (D.6) as follows:

$$\text{(D.12)}\quad |\mathcal{D}'_{i-1}| + |p_{i-1}p_i| + |y(p_i)| + \max(0, |y(p_i)| - \delta|\overline{p}_{i-1}\overline{p}_i|) \leq |\mathcal{D}'_i| + |\mathcal{S}_{s_{i-1},s_i}| + |y(f_i)| + \max(0, |y(f_i)| - \delta|\overline{p}_i\overline{f}_i|) + \delta|\overline{p}_i\overline{f}_i|.$$

Fig D.9 illustrates this inequality: the left hand side is represented in blue and the right hand side is represented in green. The dashed line represents the contribution of $\delta|\overline{p}_i\overline{f}_i|$.

If the points p_i, t_i, f_i and the distance $|p_{i-1}t_i|$ are fixed, one can observe that moving p_{i-1} counterclockwise on the circle of center t_i is increasing the LHS of (D.12) without changing its RHS. Moreover, as long as the upper arc remains shorter than the lower arc, the part below $[st]$ of the circle C_{i-1} generated by this move is included in the former circle C_i hence, f_i remains outside the new C_i and the new configuration remains valid. So, the extreme case is such that $p_{i-1}t_i$ is a diameter of C_i (going further violates the hypothesis that the route goes through p_i after p_{i-1}). So assume now that C_i is of diameter t_i, p_{i-1}.

Since the RHS is decreasing with the distance $|c_if_i|$, we can simply consider the cases where f_i is on C_i. Without loss of generality, we set st as the "x" axis, $t_i = (1,0)$ and $x(c_i) = 0$. Then we define an angle β such that f_i has coordinates: $(x(c_i) + |c_it_i|\cos(\beta), y(c_i) + |c_it_i|\sin(\beta))$. β has values between β_0 and β_1, where β_0 corresponds to the case $y(f_i) = 0$ and β_1 corresponds to the case $x(f_i) = x(p_i)$. We first need to decide what part of $\max(0, |y(f_i)| - \delta|\overline{p}_i\overline{f}_i|)$ is used w.r.t. the position of f_i. Let M be the function defined by

$$\begin{aligned}
M(\beta) &= \frac{|y(f_i)| - \delta|\overline{p}_i\overline{f}_i|}{|c_it_i|}\\
&= -y(c_i) + \sin(\beta) - \delta(\cos(\beta) - \frac{x(p_i)}{|c_it_i|})\\
&= \sin(\beta) - \delta\cos(\beta) - y(c_i) + \frac{\delta x(p_i)}{|c_it_i|}\\
&= \sqrt{1+\delta^2}(\frac{1}{\sqrt{1+\delta^2}}\sin(\beta) - \frac{\delta}{\sqrt{1+\delta^2}}\cos(\beta)) + c_1\\
&= \sqrt{1+\delta^2}(\sin(\arccos(\frac{\delta}{\sqrt{1+\delta^2}}))\sin(\beta) - \cos(\arccos(\frac{\delta}{\sqrt{1+\delta^2}}))\cos(\beta)) + c_1\\
&= \sqrt{1+\delta^2}\cdot\cos(\beta + (\pi + \arccos(\frac{\delta}{\sqrt{1+\delta^2}}))) + c_1,
\end{aligned}$$

where $c_1 = -y(c_i) + \frac{\delta x(p_i)}{|c_i t_i|}$. In addition, $M(\beta_0) = -\delta(x(f_i) - x(p_i)) < 0$ and $M(\beta_1) = y(p_i) > 0$. So, the behavior of $\max(0, |y(f_i)| - \delta|\overline{p}_i\overline{f}_i|)$ for β from β_0 to β_1 is as follows: it is null up to $\beta = \beta_{crit}$ (where $|y(f_i)| - \delta|\overline{p}_i\overline{f}_i| = 0$) and then it is first increasing and then decreasing from β_{crit} to β_1.

Let Δ be the difference between the RHS and the LHS of Equation (D.12). We are first interested in the variations of Δ w.r.t. β. We thus can drop some parts of Δ. It remains $\Delta' = |y(f_i)| + \max(0, |y(f_i)| - \delta|\overline{p}_i\overline{f}_i|) + \delta|\overline{f}_{i-1}\overline{f}_i| + c_2$. Let us look what happens on $[\beta_{crit}, \beta_1]$. On this interval, $\Delta' = 2|y(f_i)| - \delta|\overline{p}_i\overline{f}_i|) + \delta|\overline{f}_{i-1}\overline{f}_i| + c_2$. We obtain $\frac{\partial\Delta}{\partial\beta} = 2\cos(\beta) + \delta\sin(\beta) - \delta sin(\beta) = 2\cos(\beta)$. So Δ has two potential critical values that are β_1 and β_{crit}. Let us now look what happens on $[\beta_0, \beta_{crit}]$. Here, $\Delta' = |y(f_i)| + \delta|\overline{f}_{i-1}\overline{f}_i| + c_2 = \sin(\beta) + \delta\cos(\beta) + c_3 = \sqrt{1+\delta^2} \cdot \cos(\beta - \arccos(\frac{\delta}{\sqrt{1+\delta^2}})) + c_3$, for some constant c_3. Let $\beta_{\max}$ be $\arccos(\frac{\delta}{\sqrt{1+\delta^2}})$. We have $\Delta'(\beta_{\max} + \beta) = \Delta'(\beta_{\max} - \beta)$. We have $\beta_{\max} > \frac{\pi}{4}$ and $\beta_0 \leq 0$. Since Δ' is increasing from β_0 to $\beta_{\max}$ we have $\Delta'(\beta_0) < \Delta'(\beta_{crit}) < \Delta'(\beta_{\max})$. Thus, it is not useful to consider β_{crit} as a critical value.

Let α be the angle (c_i, p_i) with the left half horizontal line (see Figure D.9). Let θ be the angle (t_i, c_i) with the left half horizontal line (or, alternatively, the angle between (p_{i-1}, c_i) with the left half horizontal line). We also set $t_i = (1, 0)$.

Case 2.1: $\beta = \beta_0$

We wish to show (D.12). Since $\beta = \beta_0$, we have $|y(f_i)| = 0$. Thus it is sufficient to show

$$|\mathcal{D}'_{i-1}| + |p_{i-1}p_i| + |y(p_i)| + \max(0, |y(p_i)| - \delta|\overline{p}_{i-1}\overline{p}_i|) \leq |\mathcal{D}'_i| + |\mathcal{S}_{s_{i-1},s_i}| + \delta|\overline{p}_i\overline{f}_i|. \tag{D.13}$$

See Fig. D.11. We will use a geometric transformation to find a version of this expression that maximizes the LHS and minimizes the RHS of (D.13). Lemma D.6 implies that we can assume that $t_{i+1} = t_i$, since this will minimize $|\mathcal{D}'_i| + |\mathcal{S}_{s_{i-1},s_i}|$ on the RHS. Observe that since $\mathcal{D}'_{i-1}$ is type B, that $x(p_{i-1}) \leq x(p_i) \leq x(t_i)$. That means p_i is on the large arc of $\mathcal{S}_{s_i,t_{i+1}}$, and p_{i-1} is on the large arc of $\mathcal{S}_{s_{i-1},t_i}$. That means $\mathcal{D}'_{i-1}$ and $\mathcal{D}'_i$ are arcs of concentric circles centered at $t_{i+1} = t_i$ that go through p_{i-1} and p_i respectively. Call these circles O_{i-1} and O_i respectively. Thus we can fix p_{i-1}, p_i and t_i and rotate st around t_i and observe the changes in (D.13). We will show that (D.13) is maximized when p_i lies on st.

First observe that, since O_{i-1} and O_i are fixed and concentric, that $|\mathcal{S}_{s_{i-1},s_i}|$ stays constant. Let γ be the angle between t_ip_i and st as st rotates around t_i. Observe that $y(p_i) = |p_it_i|\sin\gamma$ and $|\overline{p}_{i-1}\overline{p}_i| = |p_{i-1}p_i|\sin\gamma$. Thus $|y(p_i)| - \delta|\overline{p}_{i-1}\overline{p}_i|$ has the same sign as $|p_it_i| - \delta|p_{i-1}p_i|$, which, since these points are fixed, does not change sign throughout the transformation. This gives us two cases to consider. If $|p_it_i| - \delta|p_{i-1}p_i| \leq 0$, then

$$|\mathcal{D}'_{i-1}| + |p_{i-1}p_i| + |y(p_i)| \leq |\mathcal{D}'_i| + |\mathcal{S}_{s_{i-1},s_i}| + \delta|\overline{p}_i\overline{f}_i|. \tag{D.14}$$

Let $M = |\mathcal{D}'_{i-1}| + |p_{i-1}p_i| + |y(p_i)| - |\mathcal{D}'_i| - |\mathcal{S}_{s_{i-1},s_i}| - \delta|\overline{p}_i\overline{f}_i|$. Thus if $M \leq 0$, (D.14) is true. Let β be the angle $\angle p_i t_i p_{i-1}$, and let γ be the angle $\angle p_i t_i s$, and note that $\gamma \le \beta$. We express M as a function of γ:

$$M(\gamma) = (\beta - \gamma)|p_{i-1}t_i| + |p_{i-1}p_i| + |p_i t_i| \sin\gamma - |p_i t_i|\gamma - |\mathcal{S}_{s_{i-1},s_i}| - \delta|p_i t_i| \cos\gamma.$$

We examine $\frac{dM(\gamma)}{d\gamma}$.

$$\begin{aligned}\frac{dM(\gamma)}{d\gamma} &= -|p_{i-1}t_i| + |p_i t_i|(\cos\gamma - 1 + \delta\sin\gamma)\\ &\le |p_i t_i|(\cos\gamma + \delta\sin\gamma - 2).\end{aligned}$$

Since $\delta < 1$, $\frac{dM(\gamma)}{d\gamma} < 0$, and thus $M(\gamma)$ is decreasing in γ and maximized when $\gamma = 0$, which is when p_i is on st.

Otherwise $|p_i t_i| - \delta|p_{i-1}p_i| > 0$, then

$$|\mathcal{D}'_{i-1}| + |p_{i-1}p_i| + 2|y(p_i)| \le |\mathcal{D}'_i| + |\mathcal{S}_{s_{i-1},s_i}| + \delta|\overline{p}_{i-1}\overline{f}_i|.$$

Let $M' = |\mathcal{D}'_{i-1}| + |p_{i-1}p_i| + 2|y(p_i)| - |\mathcal{D}'_i| - |\mathcal{S}_{s_{i-1},s_i}| - \delta|\overline{p}_{i-1}\overline{f}_i|$, which, expressed as a function of γ is

$$M'(\gamma) = (\beta - \gamma)|p_{i-1}t_i| + |p_{i-1}p_i| + 2|p_i t_i| \sin\gamma - |p_i t_i|\gamma - |\mathcal{S}_{s_{i-1},s_i}| - \delta|p_{i-1}t_i| \cos\gamma.$$

Then $\frac{dM'(\gamma)}{d\gamma}$ is

$$\begin{aligned}\frac{dM'(\gamma)}{d\gamma} &= |p_{i-1}t_i|(\delta\sin\gamma - 1) + |p_i t_i|(2\cos\gamma - 1)\\ &= \sin\gamma(|p_{i-1}t_i|\delta - |p_i t_i|) - |p_{i-1}t_i| + |p_i t_i|(2\cos\gamma - \frac{1}{\sin\gamma}).\end{aligned}$$

We know $|p_{i-1}t_i|\delta - |p_i t_i| \le 0$ by our assumption in this case, thus all three terms are negative for $0 \le \gamma \le \pi/2$, thus $M'(\gamma)$ is decreasing in γ and is maximized when p_i lies on st, at which point $M(\gamma) = M'(\gamma)$. So we set $\gamma = 0$ and examine M as it varies in β. When $\gamma = 0$,

$$\begin{aligned}M(\beta) &= \beta|p_{i-1}t_i| + |p_{i-1}p_i| - |\mathcal{S}_{s_{i-1},p_i}| - \delta|p_i t_i|\\ &\le (\beta + \sin\beta - \pi(1 - \cos\beta) - \delta\cos\beta)|p_{i-1}t_i|\end{aligned}$$

Let $N(\beta) = \beta + \sin\beta - \pi(1 - \cos\beta) - \delta\cos\beta$. We will find the minimum value of δ for which $N(\beta) \le 0$, $0 \le \beta \le \pi/2$.

$$\frac{dN(\beta)}{d\beta} = 1 + \cos\beta - \pi\sin\beta + \delta\sin\beta. \tag{D.15}$$

Since $0 \leq \beta \leq \pi/2$, $\sin\beta$ is strictly increasing in this range and $\cos\beta$ is decreasing, for a given value of δ, (D.15) has one value β for which (D.15) is 0. Let θ^* be the value for which $\theta^* = \pi - \cot(\theta^*/2)$. Let $\delta = \beta^*$, and observe (D.15) when $\beta = \beta^*$.

$$\begin{aligned}
&1 + \cos\beta - \pi\sin\beta + \delta\sin\beta \\
=&1 + \cos\beta^* - \pi\sin\beta^* + (\pi - \cot(\beta^*/2))\sin\beta^* \\
=&1 + \cos\beta^* - \frac{\sin\beta^*\cos(\beta^*/2)}{\sin(\beta^*/2)} \\
=&1 + \cos^2(\beta^*/2) - \sin^2(\beta^*/2) - 2\cos^2(\beta^*/2) \\
=&1 - \sin^2(\beta^*/2) - \cos^2(\beta^*/2) \\
=&0.
\end{aligned}$$

Observe that $M(\beta)$ is negative when $\beta = 0$ and when $\beta = \pi/2$. And when $\beta = \beta^*$

$$\begin{aligned}
&M(\beta^*) = (\beta^* + \sin\beta^* - \pi(1 - \cos\beta^*) - \delta\cos\beta^*)|p_{i-1}t_i| \\
&\leq (\pi - \cot(\beta^*/2) + \sin\beta^* - \pi + \pi\cos\beta^* - \pi\cos\beta^* + \frac{\cos\beta^*\cos(\beta^*/2)}{\sin(\beta^*/2)})|p_{i-1}t_i| \\
&\leq \left(\sin\beta^* - \frac{(1-\cos\beta^*)\cos(\beta^*/2)}{\sin(\beta^*/2)}\right)|p_{i-1}t_i| \\
&\leq \sin\beta^* - 2\sin(\beta^*/2)\cos(\beta^*/2) \\
&= 0.
\end{aligned}$$

Thus $M(\beta) \leq 0$ for $0 \leq \beta \leq \pi/2$ and $\delta = \theta^* < 0.8105$ leading to a routing ratio smaller than 3.96.

Case 2.2: $\beta = \beta_1$**,** $x(f_i) = x(p_i)$

Observe first that the LHS of (D.12) is upper bounded by $2|y(p_{i-1})| + 3y(p_i) + x(p_i) - x(s_{i-1})$ and the RHS is lower bounded by $y(p_i) + x(p_i) - x(s_{i-1}) + 2|y(f_i)|$. Hence it is enough to prove that:

$$|y(p_{i-1})| + y(p_i) \leq |y(f_i)|.$$

In fact this inequality is an equality since $|y(p_{i-1}| = 2R\sin(\theta), y(p_i) = R\sin(\alpha) - R\sin(\theta)$ and $|y(f_i)| = R(\sin(\theta)\sin(\alpha))$, where R is the radius of circle C_i. This proves (D.12) and thus this lemma for this last case. ◻

D.3. Lower Bounds.

THEOREM D.7. *The routing ratio of MinArc algorithm on a Delaunay triangulation is at least* 3.2 *in the worst case.*

Proof. We construct a point set using a sequence of circles C_i defined as follows. The coordinates of points s, t and c_1 are respectively $(-1, 0), (1, -\epsilon)$ and $(-0.7652277146, 0)$. The point p_1 is on C_1 such that the angle (sc_1p_1) is $17.349883181°$. Let C_2 be the circle of center and radius $(0, -0.0320133045)$ and 1, respectively and let t' be the point such that p_1t' is a diameter of C_2.

For $i = 3, 4 \ldots$, we define circle C_i to be the circle of diameter $p_{i-1}t'$. Then we set p_i to be a point on C_i lying above p_{i-1} so that $|p_{i-1}p_i| < \epsilon$ for some $\epsilon > 0$. We continue to place circles and points in this way until t' is the lowest point of C_j for some j. Then, we add points $p_j, ..., p_n$ on the clockwise arc of C_j from p_j to t' so that $|p_l p_{l+1}| < \epsilon$ for $l = j, \ldots, k$, where $p_{n+1} = t'$ (as shown in Fig. D.1). We then construct the Delaunay triangulation of the point set so that s, p_1, and p_2 form a triangle and p_i, p_{i+1} and t' form a triangle for $i = 1, \ldots, n-1$. Finally, we set t to be p_n.

Next, we perturb the configuration so that c_0 lies slightly below x-axis and the upper arc of C_i is slightly smaller than the lower arc for $i = 2, \ldots, j$ while preserving the edges of the triangulation. This perturbation ensures that the path computed by MinArc algorithm is $s, p_1, p_2, \ldots, p_n = t$. We observe that when ϵ approaches 0, the routing path computed tends to $\mathcal{S}_{s,t}$ whose length adds up to 6.4. Since the distance between s and t' is 2, the routing ratio of MinArc algorithm is therefore at least 3.2.□

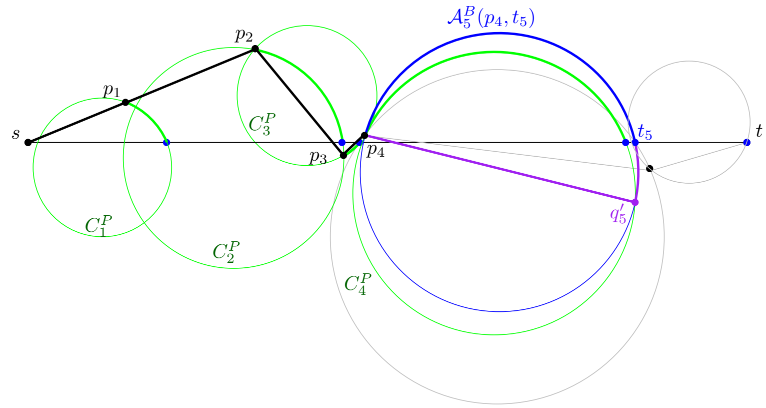

(a) C_5^B is balanced with C_4^P.

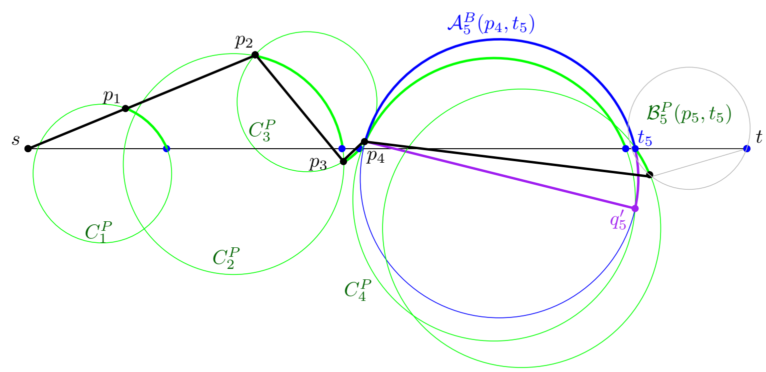

(b) C_5^P with radius $r_5^P = r_5^B$.

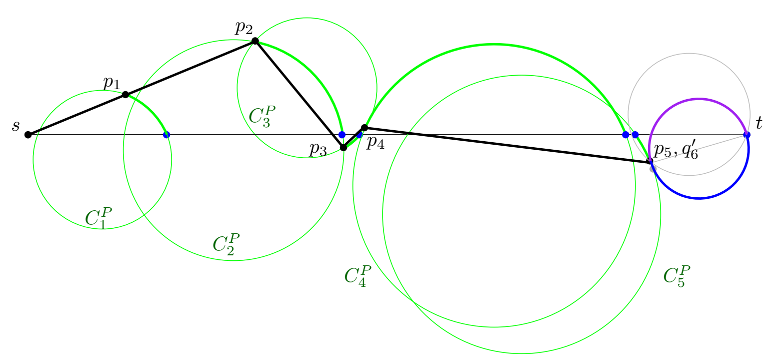

(c) C_6^B is balanced with C_5^P. Note that $q_6' = p_5$.

Figure A.5

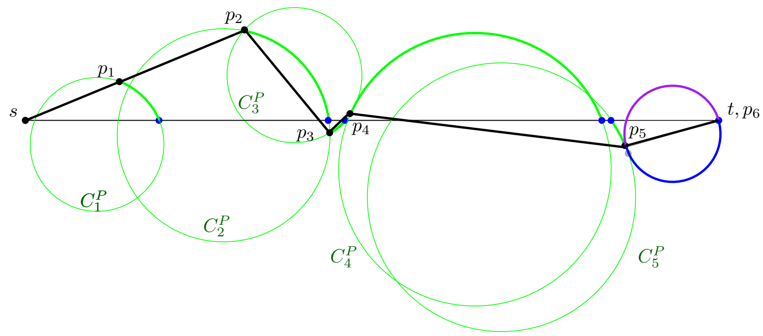

(a) C_6^P is centered at t with radius $r_6^P = 0$.

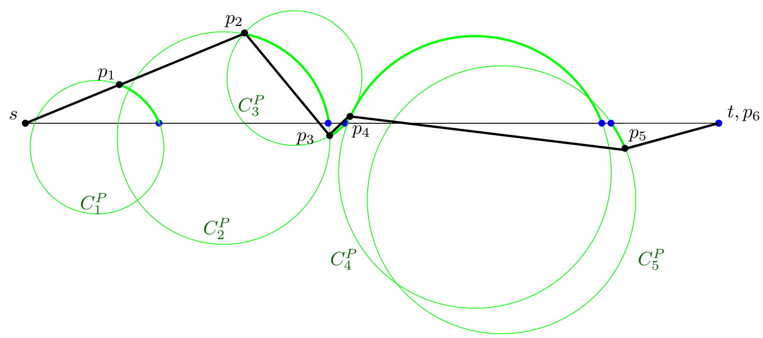

(b) $\mathcal{P}\langle s, t\rangle$ and all the potential circles.

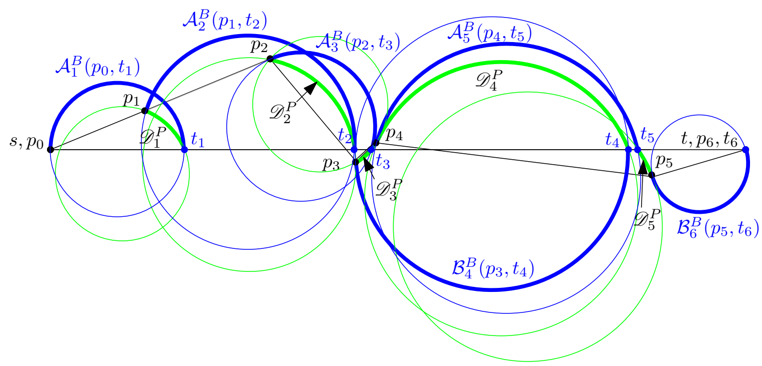

(c) The thick blue and green arcs are all the arcs considered when summing over $\Phi(C_{i-1}^P, C_i^B)$, for $1 \leq i \leq n$.

Figure A.6

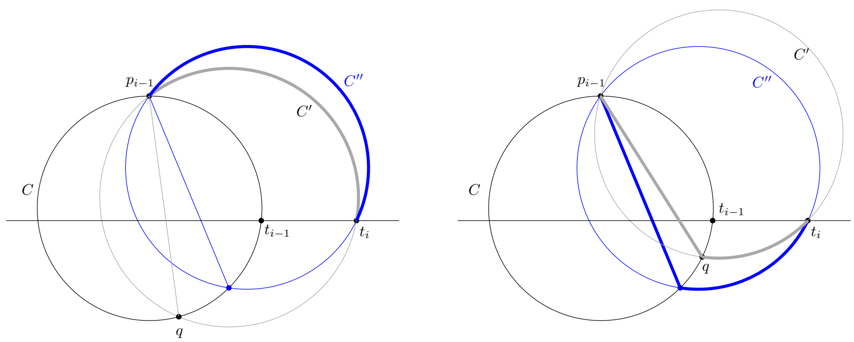

Figure B.1: Lemma B.1. $\mathcal{P}_{\mathcal{S}}(C_{i-1}, C_i)$ is longest when $C_i = C_i'$, that is C_{i-1} and C_i are balanced.

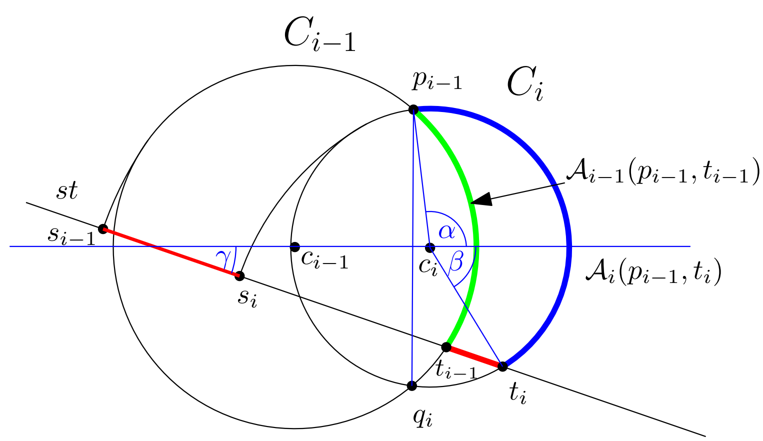

Figure C.1: c_{i-1} and c_i lie on the x-axis, and (p_{i-1}, q_i) lies along the y-axis.

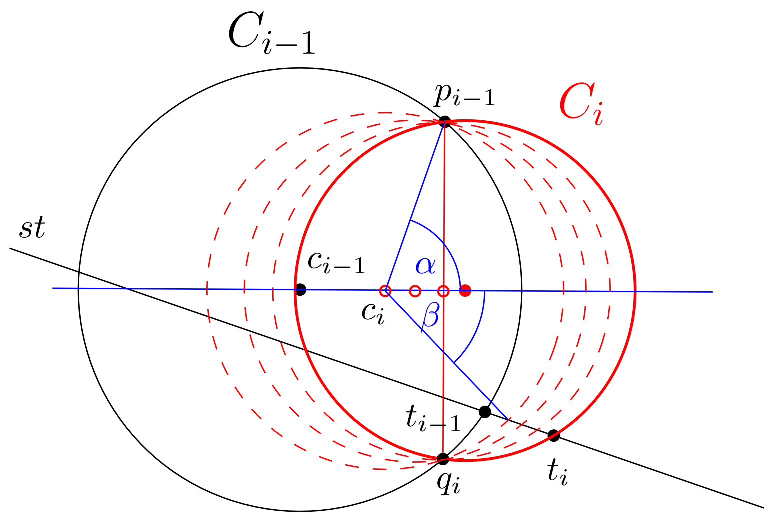

Figure C.2: Transformation 3.10. We fix p_{i-1} and q_i and translate c_i towards c_{i-1}.

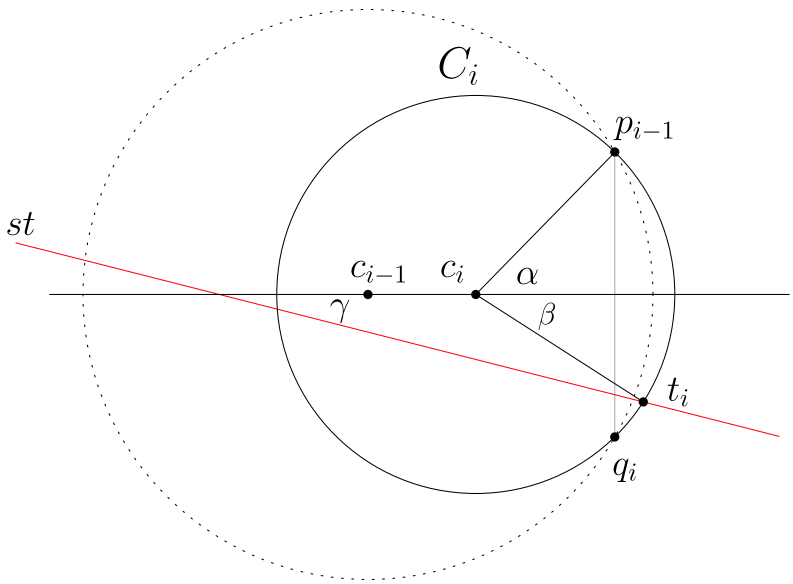

(a) Initial orientation of C_{i-1} and C_i.

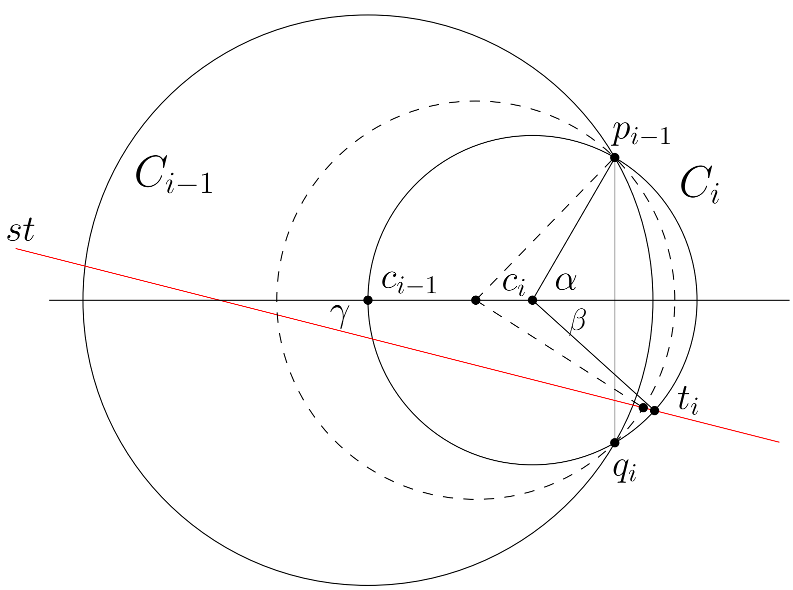

(b) The change in $x(c_i)$ represents moving c_i while fixing p_{i-1} and q_i.

Figure C.3

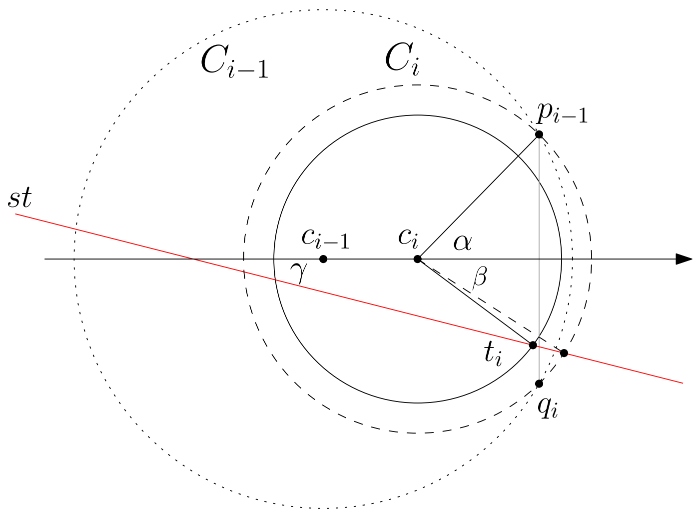

(a) In this case, $\frac{\partial |t_{i-1}t_i|}{\partial r_i}$ is obtained by fixing $x(c_i)$ and decreasing r_i.

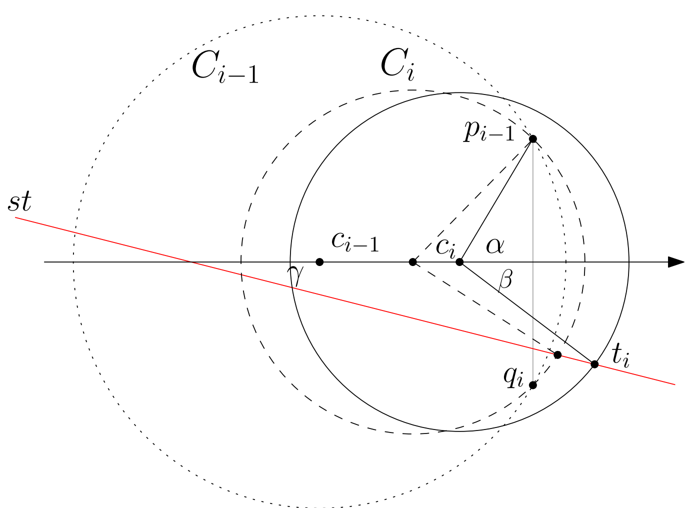

(b) $\frac{\partial |t_{i-1}t_i|}{\partial x(c_i)}$ is found by moving c_i while fixing r_i.

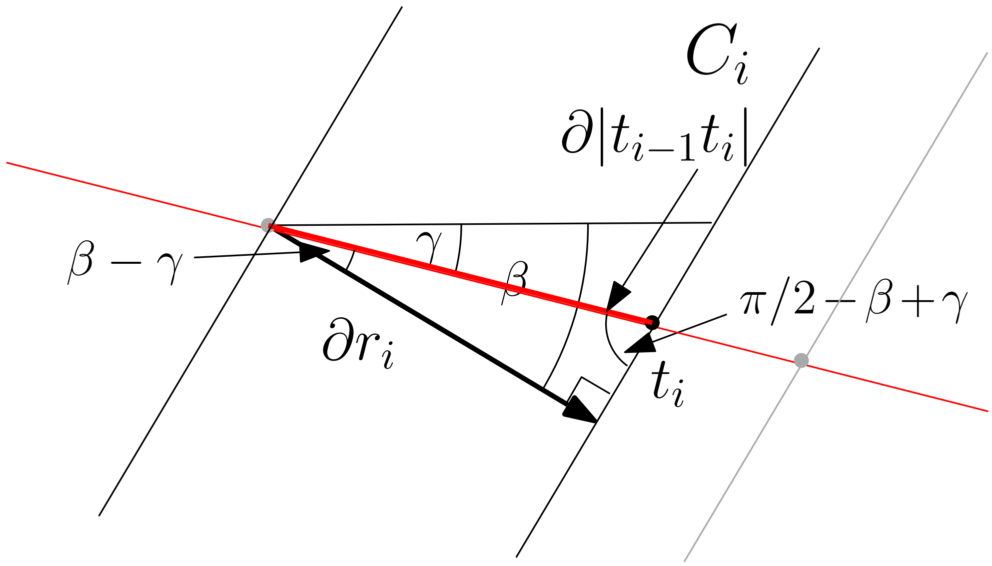

(a) $\frac{\partial|t_{i-1}t_i|}{\partial r_i}$.

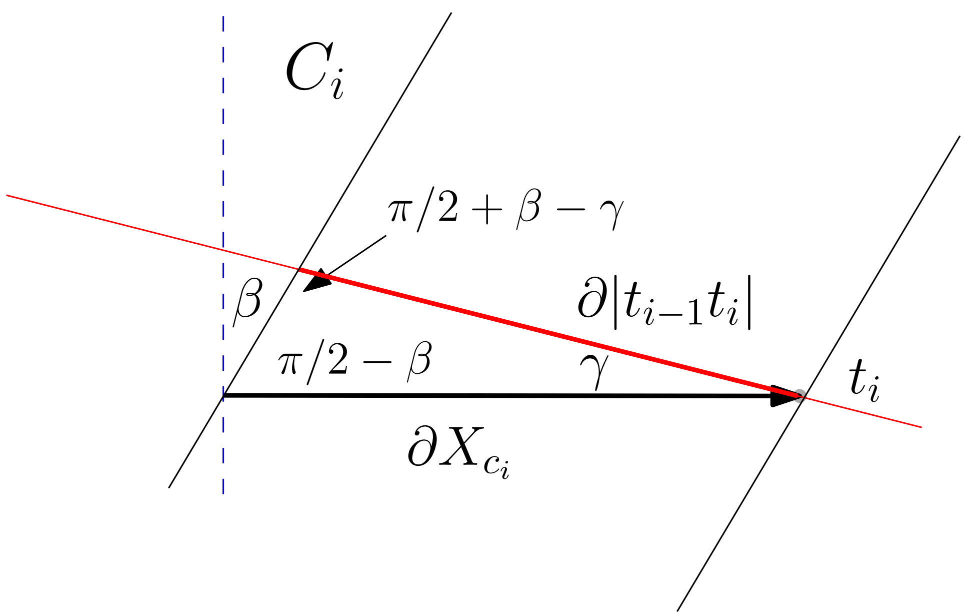

(b) $\frac{\partial|t_{i-1}t_i|}{\partial x(c_i)}$.

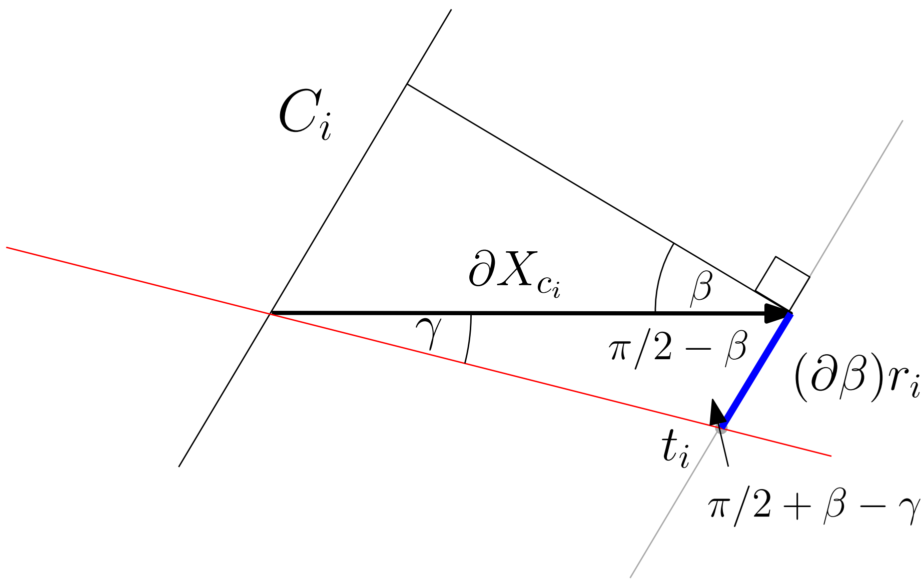

(a) The change in βr_i with $x(c_i)$. Note when $\gamma < \beta$, the change in βr_i with respect to $x(c_i)$ is positive.

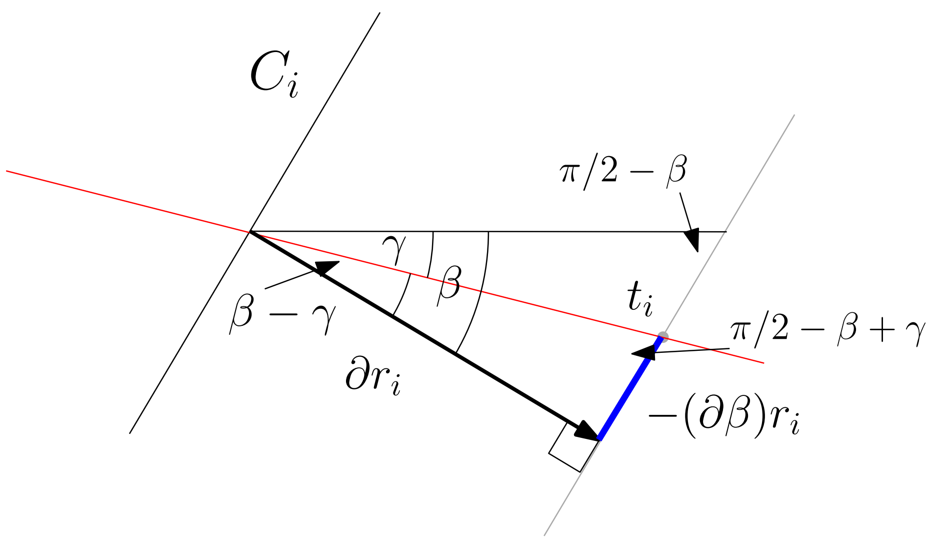

(b) The change in βr_i with r_i. Note when $\gamma < \beta$, the change in βr_i with respect to r_i is negative.

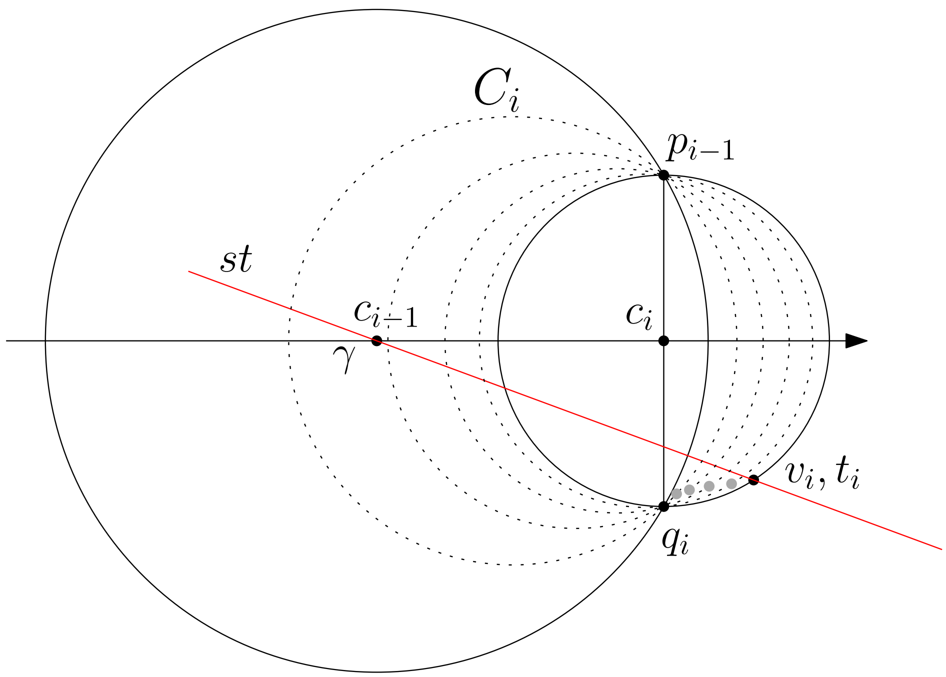

Figure C.7: The gray dots represent the path of v_i.

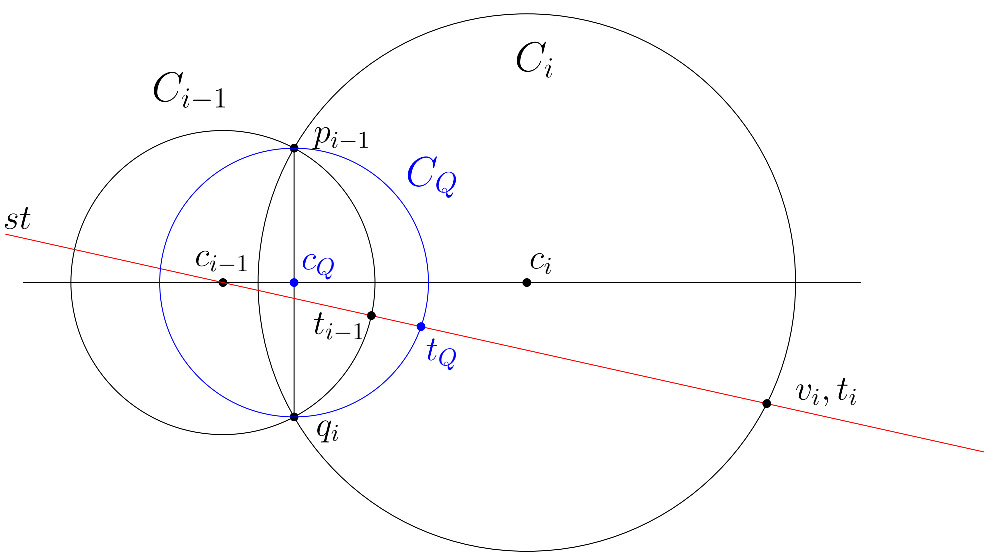

Figure C.8: Lemma C.14

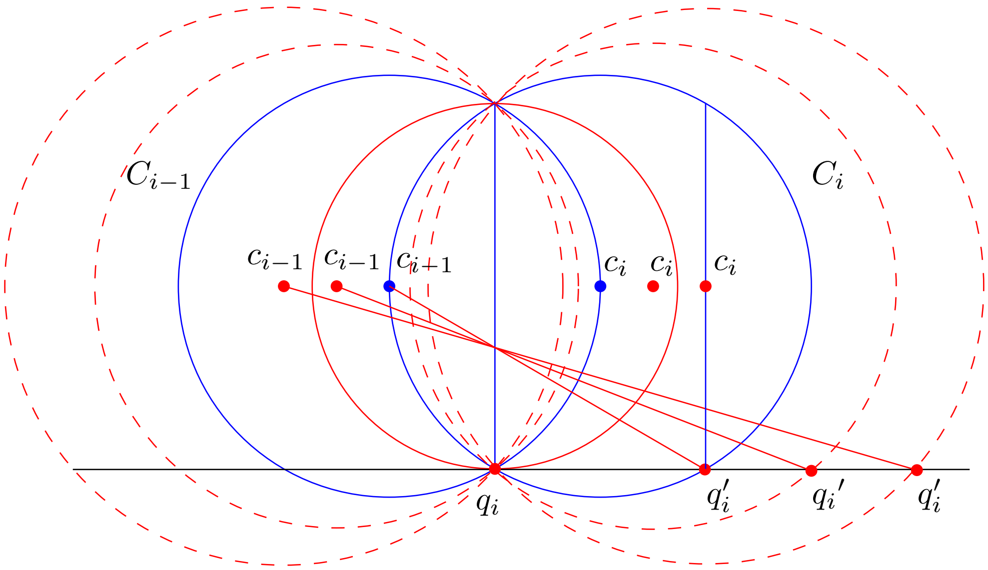

Figure C.9: Line segment $c_{i-1}q_i'$ as we increase r_i and r_{i-1}.

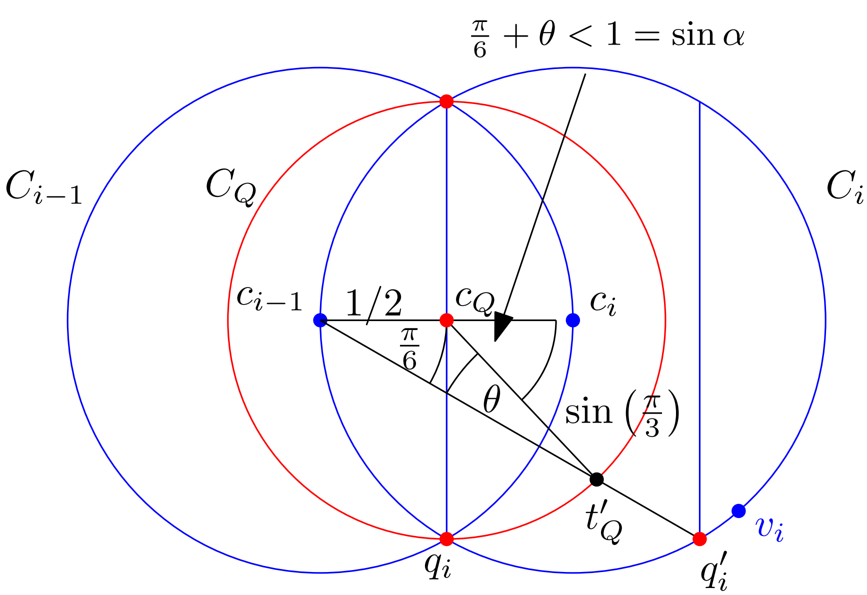

Figure C.10: Computing an upper bound on β on C_Q.

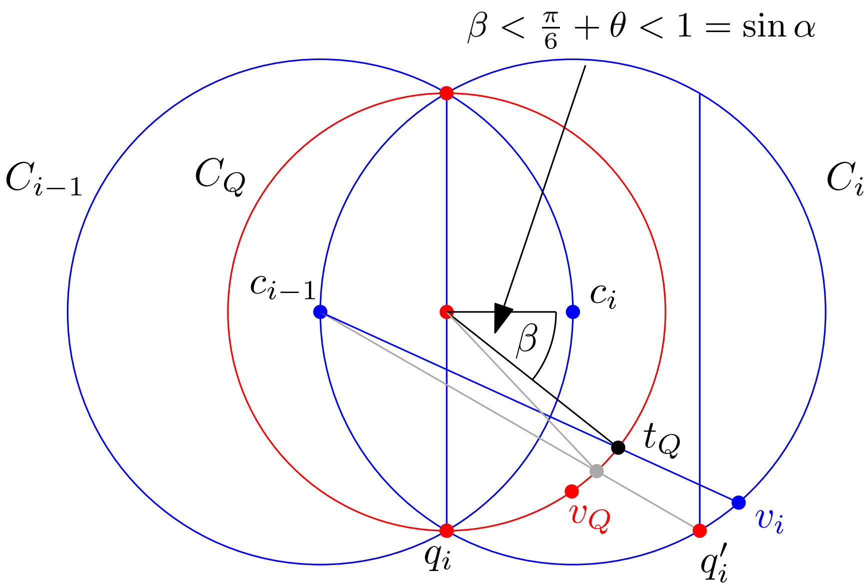

Figure C.11: Since $\beta < 1 = \sin\alpha$ on circle C_Q, v_Q is below st.

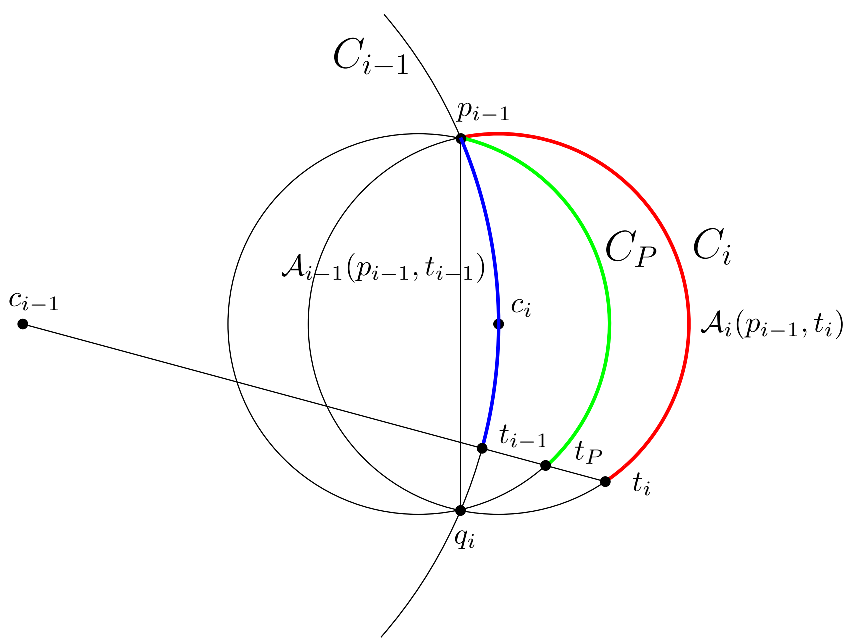

Figure C.12: The case where $\alpha > \pi/2$ and $r_{i-1} > r_i$.

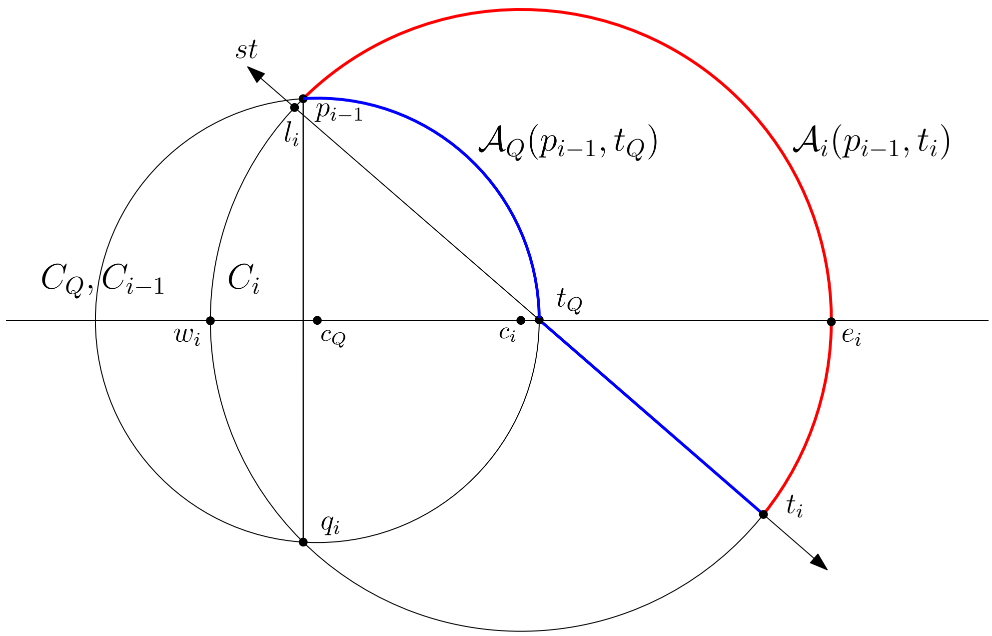

Figure C.13: $\Phi(C_Q, C_i) \leq 0$ when $y(t_Q) > 0$.

Figure D.1: On the right is a Delaunay triangulation that illustrates the lower bound on the routing ratio of MinArc algorithm. The path obtained by the algorithm is shown in bold; it has length $3.2|st|$. The left image zooms in on what happens close to point s.

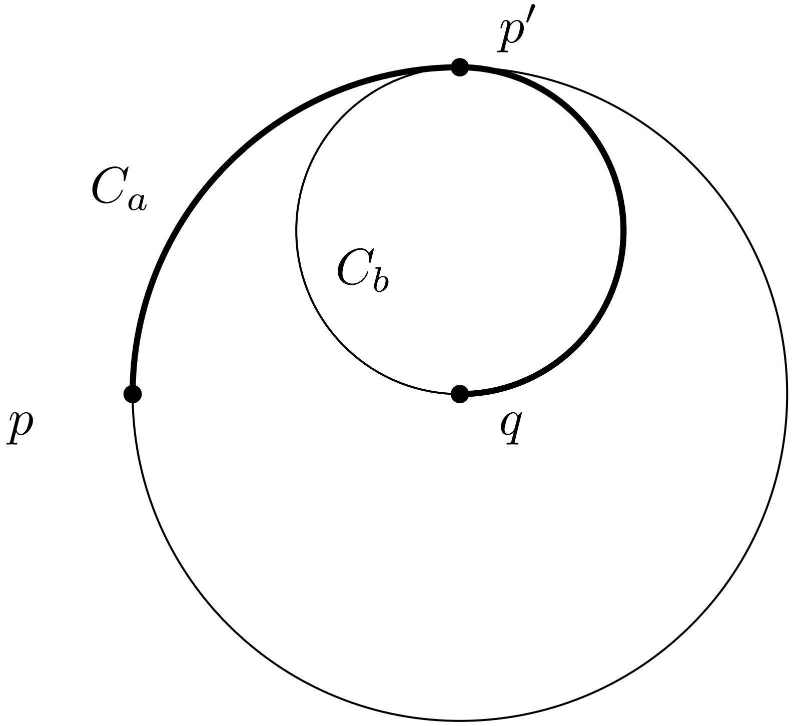

Figure D.2: Illustration of the definition of $\mathcal{S}_{p,q}$.

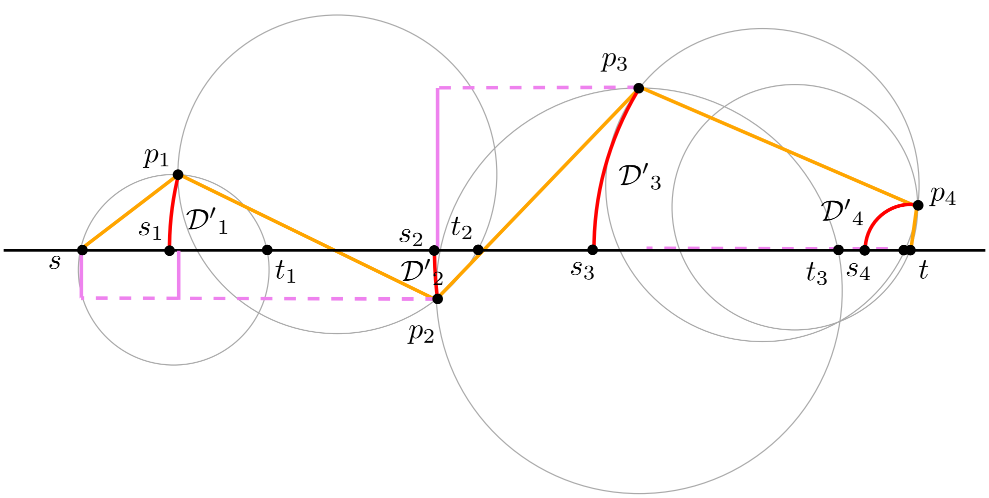

Figure D.3: Illustration of notations. The potential curve is displayed in red. To deal with *zig-zags* we also need another potential component displayed in purple.

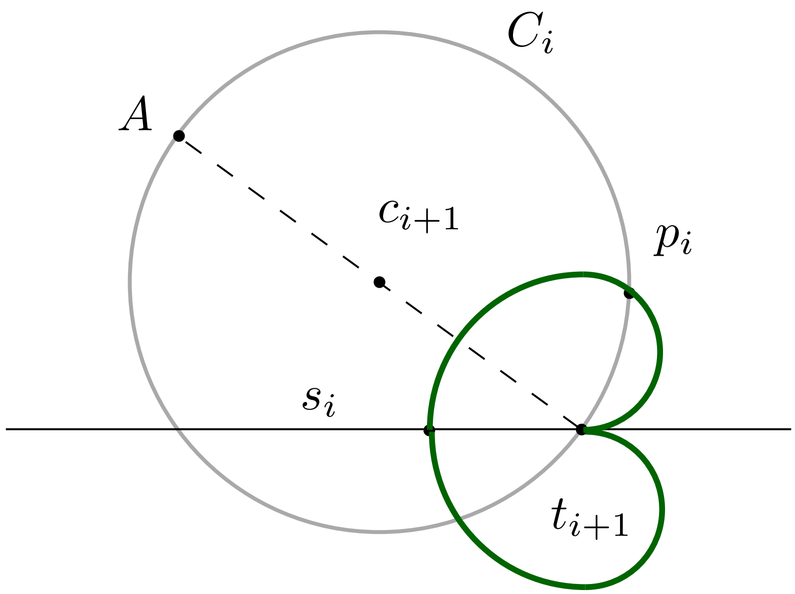

Figure D.4: Illustration of the proof of Lemma D.2.

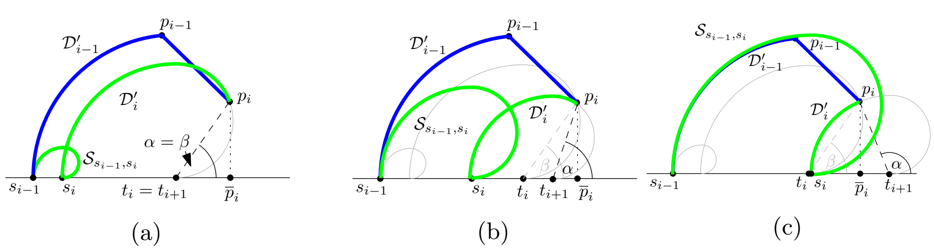

Figure D.5: We start with $t_i = t_{i+1}$, then translate t_{i+1} to the right while observing the changes in $|\mathcal{S}_{s_{i-1},s_i} + \mathcal{D}'{}_i|$, shown in green. For (c), $M(\alpha)$ in green for $\pi/2 < \alpha \leq \pi$. Observe that this is not a feasible arrangement of vertices, rather, it is an illustration of the behaviour of $M(\alpha)$.

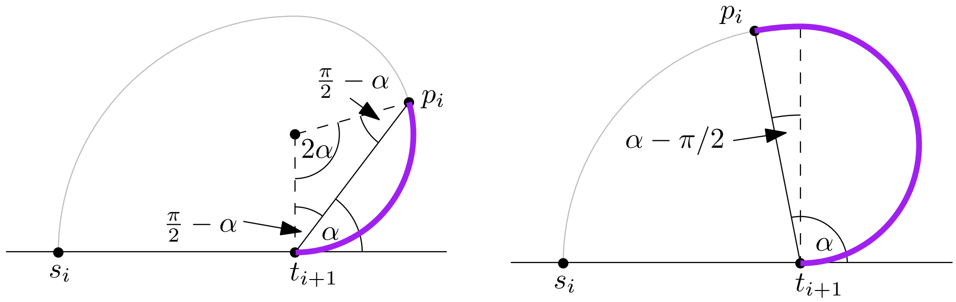

(a) $0 \leq \alpha \leq \pi/2$.

(b) $\pi/2 < \alpha \leq \pi$.

Figure D.6: Calculating $|\mathcal{S}_{s_i,t_{i+1}}(p_i, t_{i+1})|$ (purple) for different values of α.

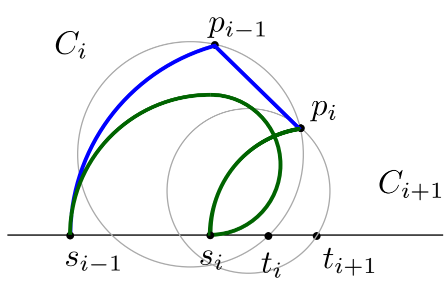

Figure D.7: the generic configuration for the case $\mathcal{D}'_{i-1}$ of type A.

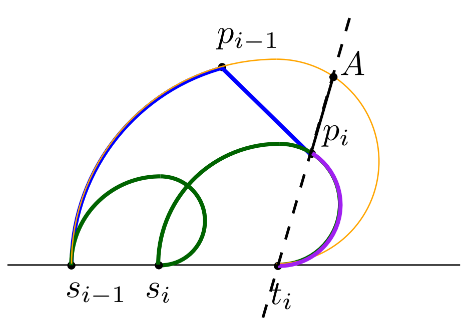

Figure D.8: Extreme case when $t_{i+1} = t_i$. In purple $\mathcal{S}_{s_{i-1},s_i}(p_i, t_{i+1})$ and in yellow $\mathcal{S}_{s_{i-1},t_{i+1}}$.

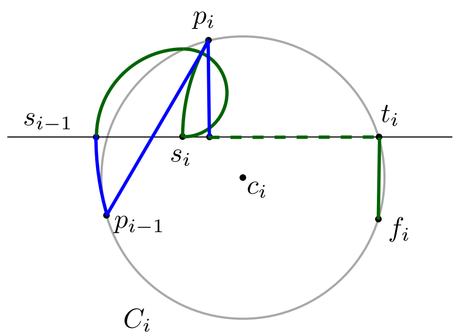

Figure D.9: Case 2

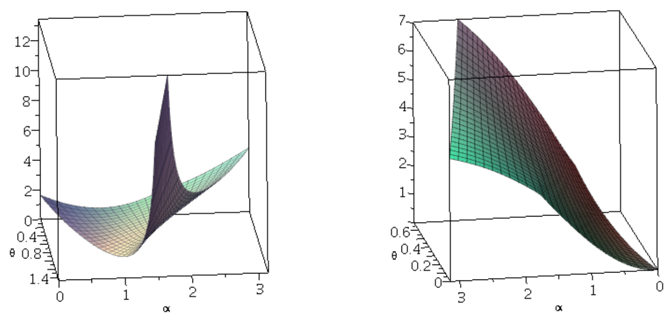

Figure D.10: $\Delta(\alpha, \theta, \beta)$ with $\beta = \beta_0$ on the left and $\beta = \beta_1$ on the right.

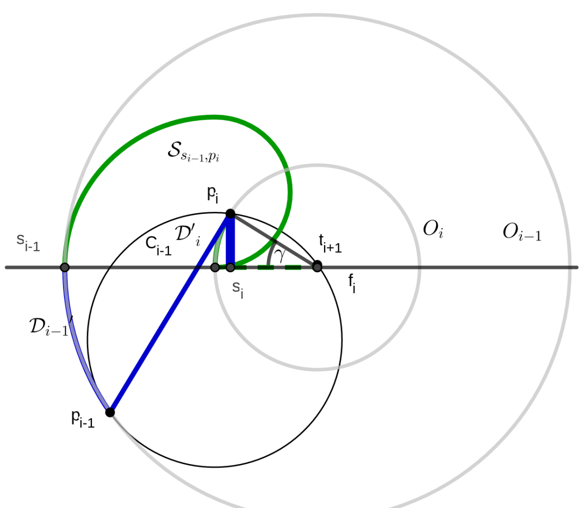

Figure D.11: When $\beta = \beta_0$.

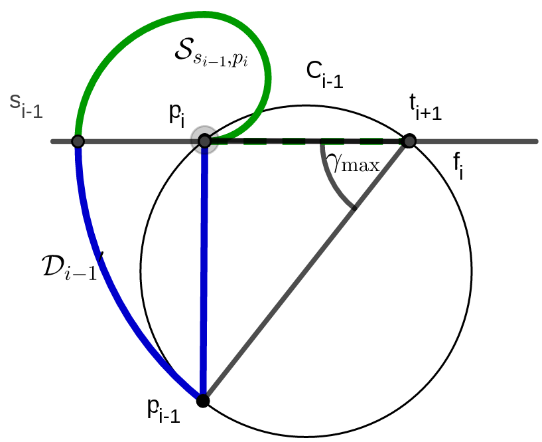

Figure D.12: When $\beta = \beta_0$ and p_i is on st.